TUM School of Life Sciences

Genetically Engineered Pigs for Xenotransplantation

Andrea Margareta Fischer

Vollständiger Abdruck der von der Fakultät TUM School of Life Sciences der Technischen Universität München zur Erlangung des akademischen Grades einer

Doktorin der Naturwissenschaften

genehmigten Dissertation.

Vorsitzender: Prof. Dr. Harald Luksch

Prüfer/-in der Dissertation:

1. Prof. Angelika Schnieke, Ph.D.
2. Prof. Dr. Eckhard Wolf

Die Dissertation wurde am 22.09.2021 bei der Technischen Universität München eingereicht und durch die Fakultät TUM School of Life Sciences am 03.12.2021 angenommen.

1. ABSTRACT

Xenotransplantation of porcine grafts is a promising option to overcome the shortage of donor organs in clinical transplantation. Availability of nuclear transfer technologies and modern gene-editing tools allow fast and efficient inactivation of defined genes and precise introduction of xenoprotective transgenes into the pig genome to resolve cross-species incompatibilities and immunological barriers.

The usage of multi-modified pigs has significantly prolonged xenograft survival in experimental pig-to-nonhuman primate models over the last decade. However, cellular rejection processes including xenogeneic T cell responses still preclude long-term xenograft acceptance. Transgenic expression of powerful T cell-regulatory proteins such as CTLA4-Ig and its high-affinity derivate LEA29Y provide substantial protection against xenoreactive T cells. Constitutive expression at high levels, however, impairs the immune competence of the donor pig and may also compromise the health status of the xenograft recipient. Therefore, a novel 'Smart Graft' approach was established to enable dynamic expression of e.g. CTLA4-Ig/LEA29Y in response to incipient rejection which is characterized by inflammation and tissue injury. A series of NF-κB-regulated candidate promoters was analyzed for basal promoter levels and inducibility by human pro-inflammatory cytokines in cultured porcine cells. These were modified to increase responsiveness to human TNF and IL-1β by adding clusters of SP-1 and/or NF-κB binding sites or removing regulatory elements. *In vivo* inducibility of the most promising promoters was evaluated based on a murine xenotransplantation model, resulting in an upregulation by a factor to 1.7 to 9.7 for five out of six promoters tested. To further assess the principle of dynamic transgene expression in porcine tissues and organs relevant for xenotransplantation, two gene-targeting vectors were generated for the placement of LEA29Y and PD-L1 at the porcine *ROSA26* locus.

Besides addition of human transgenes, the knockout of endogenous porcine genes is also essential for improving xenograft acceptance: Antibody-mediated rejection is reduced by inactivation of *GGTA1*, *CMAH* and *B4GALNT2*, the knockout of *ASGR1* reduces hepatic phagocytosis of human platelets, inactivation of *ULBP1* provides protection against NK cells and the removal of functional SLA class I molecules by knocking out *SLA-1*, *SLA-2*, *SLA-3* and/or *B2M* inhibits activation of xenoreactive cytotoxic T cells. Combining all desired gene knockouts

in a single animal is a labour and time-consuming challenge. The second part of this work therefore describes the development of a CRISPR/Cas9-based approach for an efficient fast-track inactivation of up to seven porcine genes or gene clusters.

2. KURZFASSUNG

Die Xenotransplantation porziner Zellen, Gewebe und Organe (sog. Xenografts) stellt eine vielversprechende Strategie dar, Engpässe an Spendermaterial für die klinische Transplantation zu beseitigen. Die Verfügbarkeit moderner Geneditierungs-Werkzeuge und etablierter Kerntransfer-Technologien erlaubt es, definierte Gene schnell und effizient zu inaktivieren und xeno-protektive Transgene präzise in das Schweine-Genom einzubringen, um immunologische Hürden und weitere Inkompatibilitäten zwischen den Spezies zu überwinden.

Durch die Verwendung multi-modifizierter Schweine als Organquelle konnte innerhalb der letzten Dekade das Überleben der Xenotransplantate in experimentellen Versuchen mit nicht-humanen Primaten signifikant verlängert werden. Allerdings verhindern zelluläre Abstoßungsprozesse, zu denen auch xenogene T-Zell-Antworten gehören, die langfristige Akzeptanz des Xenografts. Einen umfangreichen Schutz gegen xeno-reaktive T-Zellen bietet die transgene Expression starker T-Zell-regulatorischer Proteine wie CTLA4-Ig und dessen hochaffines Derivat LEA29Y. Jedoch kann deren dauerhafte Expression auf hohem Niveau die Immunkompetenz des Spendertiers massiv beeinträchtigen und sich zudem negativ auf die Gesundheit des Xenograft-Empfängers auswirken. Aus diesem Grund wurde als Teil dieser Arbeit der neuartige "Smart Graft"-Ansatz etabliert, der die dynamische Expression von beispielsweise CTLA4-Ig/LEA29Y als Reaktion auf eine beginnende Abstoßung erlaubt, die wiederum durch Entzündung und Gewebeschädigung gekennzeichnet ist. Es wurde eine Reihe von NF-κB-regulierten Promoter-Kandidaten hinsichtlich ihrer Grundaktivität und Induzierbarkeit durch humane pro-inflammatorische Zytokine in kultivierten porzinen Zellen analysiert. Anschließend wurden sie durch das Einfügen verschiedener Cluster von SP-1- und NK-κB-Bindestellen oder durch die Entfernung regulatorischer Elemente weiter modifiziert. Die *in-vivo*-Induzierbarkeit der vielversprechendsten Promotoren wurde dann in einem murinen Xenotransplantations-Modell evaluiert, wodurch bei fünf der sechs getesteten Promotoren eine Hochregulation um den Faktor 1.7 bis 9.7 nachgewiesen werden konnte. Um das Prinzip der Zytokin-abhängigen Transgen-Expression zukünftig in porzinen Geweben und Organen untersuchen zu können, wurden abschließend zwei Gen-*Targeting*-Vektoren

generiert, welche die Platzierung von *LEA29Y* und *PD-L1* an den porzinen *ROSA26*-Lokus ermöglichen.

Neben der Integration zusätzlicher Transgene ist auch der Knockout bestimmter Gene essenziell für die Verbesserung der Akzeptanz des Xenografts: Durch die Inaktivierung von *GGTA1*, *CMAH* und *B4GALNT2* wird die Antikörper-vermittelte Abstoßung gemindert, ein *ASGR1*-Knockout reduziert hepatische Phagozytose humaner Thrombozyten und die Inaktivierung von *ULBP1* bietet Schutz vor NK-Zellen. Zudem hemmt die Entfernung funktioneller SLA-Klasse-I-Proteinkomplexe durch das Ausschalten von *SLA-1*, *SLA-2*, *SLA-3* bzw. *B2M* die Aktivierung zytotoxischer xeno-reaktiver T-Zellen. Die Kombination aller gewünschter Genknockouts in einem einzigen Tier stellt allerdings eine arbeits- und zeitintensive Herausforderung dar. Daher wird im zweiten Teil dieser Arbeit die Entwicklung eines auf CRISPR/Cas9 basierenden Ansatzes beschrieben, der die simultane Inaktivierung von bis zu sieben porzinen Genen bzw. Gen-Clustern ermöglicht.

3. TABLE OF CONTENTS

4. INTRODUCTION

4.1 The organ shortage crisis

Organ transplantation is often the only treatment option for patients suffering from severe organ dysfunction and failure. However, the number of available donor organs has far exceeded the number of required grafts for years (see Figure 1)[1]. More than 7,500 patients were waiting for a kidney graft in Germany by the end of 2018, while only 2,309 persons received kidney transplantation in the same year [2]. In the same period, there was a demand for 719 donor hearts, but only 44% received the life-preserving organ [2]. As a result, 13% of patients either died or became unfit for transplantation while waiting for a graft in 2018 emphasizing the great need for donor organ [1, 2].

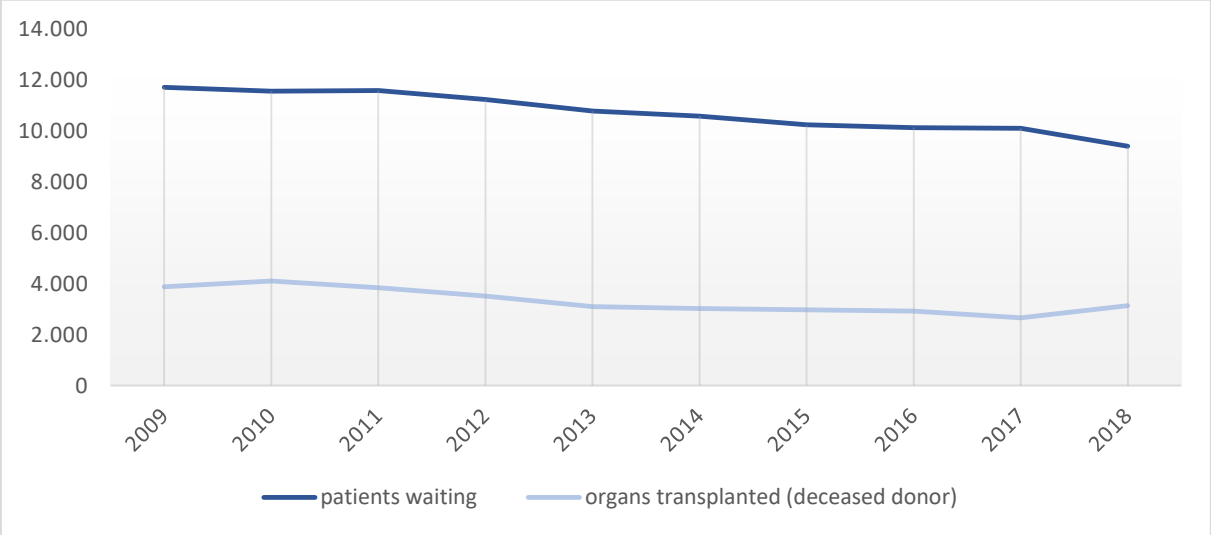

Figure 1 – Number of patients on the waiting list and of organs transplanted at year-end (Germany, 2009-2018) There is a huge discrepancy between patients waiting for a donor organ and organs transplanted. Data obtained from Eurotransplant International Foundation, Yearly Statistics Overview 2009-2018 [1].

The reasons for shortage of donor organs, not only in Germany but also worldwide, are diverse. Besides medical contraindications such as multi-organ failure and infectious diseases of the deceased patient, a large number of potential donors omitted to indicate their willingness to donate their organs after death. Moreover, the high refusal rate when next of kin is asked about donation further reduces the amount of available grafts for transplantation [3-8]. Improving public awareness and general knowledge of organ donation to reduce

reservations about the topic may indeed mitigate the imbalance between organ demand and supply to a certain extent [9-11]. However, searching for alternatives to classical organ transplantation may be inevitable in the medium to long term as increasing the pool of donors may still be insufficient to meet the demand.

4.2 Alternatives to human organ transplantation

There are several approaches to reduce dependency on human donor organs: among others, support by mechanical assist systems, the advent of bioengineered grafts and the usage of humanized organs of animal origin.

Mechanical devices designed to substitute certain organ functions have been in use for decades. A well-known example of extracorporeal support is the dialysis treatment of patients with impaired kidney function, which has been used regularly since the 1960s [12]. Despite the steady technological progress, the expected remaining lifetime of a dialysis patient aged 20-44 is about 18 years shorter than of a renal transplant recipient of the same age [13]. Long-term dialysis treatment also means an enormous reduction in the quality of life. For these reasons, kidney transplantation is preferable to permanent dialysis. Also, implantable mechanical devices to support or entirely replace native heart function have been widely used. According to the International Society for Heart and Lung Transplantation, 36% of patients receiving heart transplantations were bridged with cardiac assist devices between 2006 and 2013 [14]. However, all currently available devices have significant limitations in long-term therapy. Infections caused by percutaneous drivelines represent one of the leading causes of mortality in this context. Another severe problem is blood clot formation at the blood-device interface, leading to pump thrombi and thromboembolisms [15-17]. Further technological development is needed to satisfactorily replace human heart transplantation by implantable cardiac support systems.

Tissue Engineering is a further approach to regenerate or completely replace functionally impaired tissues and organs. This technology typically uses combinations of scaffold structures with biochemical molecules and specific cells, e.g. stem cells, autologous or allogenic cells, to artificially generate tissues and organs under laboratory conditions [18, 19]. One way of organ bioengineering is using scaffolds obtained by whole organ decellularization for subsequent re-

cultivation with the desired cell type. A major advantage of this method is the minimized immunogenicity of the graft when patient's own cells are used for recellularization. Nevertheless, donor organs are still needed for scaffold preparation. This disadvantage may be avoided by 3-dimentional (3D) bioprinting of the organ itself: precise layer-by-layer positioning of biological material, including liquefied extracellular-matrix-like components, growth factors and living cells, allows fabrication of 3D tissue structures, even with heterogeneous cell populations [19-23]. But there still is a long way to go until large-scale fabrication and transplantation of engineered solid organs becomes reality. A lot of issues must be addressed for future research, e.g. choosing the perfect composition of biomaterials and cell types, establishing perfusable vascular networks to ensure constant blood supply and enable functional innervation of the engineered organ [19, 20, 24].

Despite all efforts, it is reasonable to assume that neither mechanical devices nor bio-artificial grafts will mimic the entire functional spectrum of a solid organ. Another alternative to human donor organs is therefore using grafts of animal origin. This cross-species transplantation of organs, tissues or cells is referred to as xenotransplantation. The prospect of an unlimited source of fully functional 'donor' organs, which can be accessed whenever required, makes the concept of xenotransplantation so attractive. The chances, obstacles and the current state of xenotransplantation research is subject of the following chapters.

4.3 Xenotransplantation

4.3.1 The early days of cross-species transplantation

The idea of xenotransplantation is not a modern concept. Already several hundred years ago, efforts were made to cure patients suffering from certain diseases by transplantation of animal material. Early documentations of xenogeneic tissue transplantation date from the beginning of the 16th century, when a bone from a dog was used to replace a sick bone fragment of a human skull [25]. In the course of the 19th century, numerous experiments have been made with skin transplantations of diverse donor species, including sheep, dogs, cats, chicken and frogs [26]. However, none of these treatments resulted in permanent skin-engraftment [27]. Clinical attempts to transplant whole organs of animal origin came up during the 20th century. While initial efforts with pig, goat and lamb kidneys led to the death

of the recipient within a few days after transplantation, patient survivals of 98 and 270 days were achieved in the 1960s by using baboons and chimpanzees as kidney sources [28-30]. Other experiments with cardiac and liver transplants have also shown the biggest success when grafts from chimpanzees and baboons were used [28].

4.3.2 The pig as organ donor

Despite their phylogenetic proximity to humans and the associated reduced rejection reactions, the use of primates as donor has meanwhile been abandoned. Instead, the domestic pig (*Sus scrofa domesticus*) has become the focus of modern xenotransplantation research. It is similar to human in organ size and anatomy and can be kept under specific-pathogen-free (SPF) conditions at acceptable costs. In contrast to nonhuman primates (NHPs), the pig has ideal breeding characteristics because of its early sexual maturity, short gestation period and large litter size [27, 31]. Additionally, the risk of transmitting zoonoses from pigs to humans is estimated to be considerably lower than from apes or monkeys, even though some porcine pathogens might be relevant in pig-to-human xenotransplantation (see section 4.3.3.1) [27, 32, 33]. Nevertheless, immunosuppressive treatment alone is not sufficient to completely inhibit xenogeneic rejection processes due to the evolutionary distance between swine and human. However, the availability of well-established genetic engineering and cloning methods (see chapter 4.4) now allows to gradually reduce immunological and physiological barriers of pig-to-human transplantation (see chapter 4.3.3.2) and thereby improving xenograft compatibility.

4.3.3 Overcoming the obstacles to xenotransplantation

4.3.3.1 Microbiological safety of porcine grafts

The risk of pathogen transmission causing infection of the immunosuppressed recipient is already known from allotransplantation. Zoonoses are an additional risk potentially relevant for xenotransplantation. The ability to screen donor animals at regular intervals for potential pathogens, including bacteria, viruses and fungi, is a great advantage of xenotransplantation. Moreover, most infectious agents found in pigs to be used may be excluded from the herd

using SPF breeding methods. The potential donor pigs can be additionally treated with vaccines, antibiotics and chemotherapeutics to obtain animals free of transmittable pathogens [32]. Nevertheless, certain microorganisms are thought to pose a special risk for xenograft safety, including hepatitis E virus (HEV), porcine cytomegalovirus (PCMV) and porcine endogenous retroviruses (PERVs) [34-38].

HEV-E infection in humans typically causes self-limiting acute hepatitis but can develop to chronic hepatitis in immunocompromised patients including transplant recipients [39-41]. Swine HEV is very common in pig herds and was reported to cross the species barrier by direct animal contact or consumption of contaminated pork products, causing a zoonotic disease in rare cases [39, 42-44]. Within the herd, HEV is assumed to be transmitted via the faecal-oral route [45]. There are also indications that HEV can be transferred transplacentally from the sow to its unborn piglets [32, 46]. For this reason, special husbandry or caesarean delivery may not prevent vertical HEV transmission to the next generation. Proposals to eliminate the risk of zoonotic HEV infections after xenotransplantation are therefore vaccination of the donor animals or the treatment with anti-retroviral drugs [47].

Another pathogen that might be of concern in pig-to-human xenotransplantation is PCMV. This virus is highly prevalent throughout the world, causes lifelong latent infections and has the potential to infect human cells *in vitro* [32, 48, 49]. It is the first virus with proven pathogenicity in preclinical xenotransplantation experiments as significantly reduced survival times have been repeatedly observed after transplantation of PCMV-positive porcine grafts into NHPs [37, 50, 51]. Since PCMV is mainly transmitted by exposure to nasal secretion and urine of latently-infected animals, caesarean section or early weaning of the piglets with subsequent SPF breeding allows easy eradication of the virus from the herd [32, 49, 52]

Unlike exogenous pathogens, PERVs are an integral component of the porcine genome and can thus not be removed by medical treatment and special breeding methods. For this reason, they pose a special challenge in xenotransplantation research. There are three PERV subtypes differing in the structure of their envelope proteins [53]. PERV-A and -B are present in all pig strains at different copy numbers and were shown to infect human cells *in vitro*, whereas PERV-C is restricted to porcine cells [31, 53-56]. However, recombination between PERV-C and the *env* gene of PERV-A results in PERV-A/C variants that have a much higher capability to infect human cells compared to the parental PERV-A [54]. *In vivo* transmission of PERVs by

xenotransplantation has not been observed so far, neither in first clinical trials involving more than 200 patients nor in numerous pig-to-NHP studies [31, 38, 57]. Nevertheless, the risk of inducing tumors by insertional mutagenesis and immunodeficiencies, as it is already known from other retroviruses, cannot be completely excluded [58]. It is therefore advisable to select the potential donor animals for a low number of PERV-A and -B copies and low expression rates to minimize the probability of PERV transmission to the xenograft recipient. As PERV-C is present in many but not in all pigs, pigs not carrying PERV-C proviruses in the genome should be considered for xenotransplantation to prevent recombination to the highly infectious PERV-A/C variant [32]. Genetic manipulation of the donor is another chance to lower the risk of PERV transmission. Pigs transgenic for small interfering RNA (siRNA) molecules have been generated that specifically knock down expression of PERV proviruses [59-61]. The genome-wide knockout of all PERV loci, however, is considered as a major challenge due to the high number of copies in the genome. Nonetheless, Luhan Yang and colleagues successfully disrupted all of the 62 PERV copies in a porcine kidney cell line using the CRISPR/Cas9 technology (see section 4.4.1) [62]. Two years later, the same group published the generation of viable piglets with inactivation of all 25 PERV copies [63]. Since feasibility was demonstrated, the CRISPR/Cas9-mediated knockout represents a very promising way to reduce the risk of PERV transmission.

4.3.3.2 Xenograft rejection by immunological and physiological incompatibilities

The genetical distance between man and swine entails immunological and physiological incompatibilities. Xenotransplantation of porcine wildtype organs therefore leads to diverse rejection processes in the human recipient that have been intensively studied in preclinical pig-to-NHP experiments. Xenograft rejection is mainly divided in antibody-mediated rejection mechanisms, including hyperacute (HAR) and acute vascular xenograft rejection (AVXR), and immune cell-mediated rejection processes. The following chapters will describe the different molecular causes of xenograft rejection and present strategies to overcome them.

4.3.3.2.1 Hyperacute rejection (HAR)

HAR arises within minutes to hours after pig-to-NHP transplantation and leads to the early loss of the wildtype graft. Reason for the rapid immune response is binding of preformed, natural antibodies to xenogeneic epitopes at the porcine vessel endothelium inducing complement activation via the classical pathway [64, 65]. Subsequent complement-dependent inflammation, interstitial haemorrhage and endothelial necrosis cause serious injury to the porcine organ. Vascular thromboses and edema within the graft are further characteristics of HAR [66-68].

The most investigated antigen involved in HAR is the Galα1-3Galβ1-(3)4GlcNAc-R epitope (see Figure 2), called αGal in the following [69]. This carbohydrate residue is present at the surface of porcine and other mammalian cells and was also found on different bacteria [70-73]. Humans, apes and Old World monkeys, in contrast, do not express αGal due to inactivation of the gene encoding α1,3-galactosyltransferase 1 (gene name: *GGTA1*) during evolution [70, 74]. This enzyme catalyses the transfer of UDP-galactose to N-acetyllactosamine and is therefore required for αGal synthesis [70]. Humans possess a natural titer of anti-αGal immunoglobulins as a probable result of αGal expressing bacteria in the human intestinal flora, triggering HAR of porcine grafts after xenotransplantation [73, 75]. A major advance in overcoming this immunological obstacle was the development of *GGTA1*-deficient animals in 2002 [76-78]. It was shown that *GGTA1*-knockout grafts were protected from HAR after pig-to-baboon xenotransplantation [79, 80].

Apart from removing αGal epitopes to prevent HAR, expression of (human) complement regulatory proteins is a supplemental strategy to minimize complement activation by immune complexes. Several groups have already demonstrated the increased protection of porcine grafts expressing CD46, CD55 and/or CD59 against HAR in NHPs [81-85].

4.3.3.2.2 Acute vascular xenograft rejection (AVXR)

After overcoming HAR, AVXR is the next challenging hurdle. It develops within several days to weeks after xenotransplantation and is characterized by activation of donor endothelial cells (ECs), induction of complement and coagulation systems and leads to inflammation, apoptosis, platelet aggregation and thrombosis in the porcine graft [86-89]. Infiltration of

monocytes, natural killer (NK) cells and neutrophils is also observed [90]. AVXR involves a variety of mechanisms that are incompletely understood, but xenoreactive antibodies play an initiating role [91].

So called non-Gal antigens have drawn more attention since αGal epitopes can be removed by inactivating porcine GGTA1 (see section 4.3.3.2.1). The majority of preformed anti-non-Gal-antibodies in human sera recognizes CMP-N-glycolylneuraminic acid (Neu5Gc, see Figure 2), a sialic acid epitope on epithelial surfaces of pigs, NHPs and other mammals [92-95]. It derives from CMP-N-acetylneuraminic acid (Neu5Ac) hydroxylated by the enzyme CMP-N-acetylneuraminic acid hydroxylase (CMAH), which is defective in humans [96]. The first *GGTA1*/*CMAH*-double knockout pigs were published in 2013. Immune recognition studies showed that inactivating both *GGTA1* and *CMAH* reduces the xenoantigenicity of porcine cells, further than the knockout of *GGTA1* alone [97].

Another group of xenorelevant non-Gal-antigens is produced by the enzyme β1,4 N-acetyl-galactosaminyl transferase 2 (B4GALNT2). It catalyses the transfer of N-acetylgalactosamine (GalNAc) to a sialic acid modified lactosamine and is known to synthesize the Sda blood group antigen in humans and mice [98]. Also, porcine B4GALNT2 seems to generate different Sda-bearing epitopes, even though the structure of these molecules has not been clarified yet in pigs [99]. The majority of human sera tested by Estrada *et al.* was found to contain immunoglobulins that specifically bind antigens synthetized by porcine B4GALNT2. *In vitro* studies with PBMCs and erythrocytes from GGTA1/CMAH/B4GALNT2-deficient pigs revealed significantly reduced binding of human serum antibodies compared to cells lacking both *GGTA1* and *CMAH* gene function [100]. Further investigations showed that some, but not all, of the organs of those triple-knockout animals exhibited reduced xenoantigenicity compared to wildtype pigs [101]. These findings indicate that, at least in some organs, there may be further immunoreactive xenoantigens in addition to αGal, Neu5Gc and Sda participating in antibody-mediated rejection.

It is known from allotransplantation that antibodies against human major histocompatibility complex (MHC) molecules, induced by previous pregnancies, blood transfusions or transplantations, dramatically increase the risk of graft rejection [102]. The highly polymorphic MHC class I molecules are encoded by multiple genes, each having many alleles, and are expressed on the cell surfaces of most types of nucleated mammalian cells. Primary role of

these proteins is the presentation intracellular antigens to cytotoxic $CD8^+$ T lymphocytes and regulation of NK cell activity [103-105]. Human serum antibodies against human MHC class I proteins, termed human leukocyte antigen (HLA), were shown to cross-react with the porcine variant, called swine leukocyte antigen (SLA) [106]. This observation suggests the relevance to inactivate SLA class I proteins for improved xenograft survival. Functional porcine class I molecules are composed of a heavy α-chain (encoded by *SLA-1*, *SLA-2* and *SLA-3*) with highly variable domains, a light β-chain termed beta-2-microglobulin (B2M) and short peptides (see Figure 2) [107-109]. Pigs lacking functional SLA class I molecules on cell surface have been generated by knocking out either *SLA-1*, *SLA-2* and *SLA-3* or *B2M* [108, 109]. Recently, our group has succeeded in engineering animals neither expressing functional SLA class I molecules nor the carbohydrate xenoantigens αGal, Neu5Gc and Sda. [110]. Cells from these *GGTA1*/*CMAH*/*B4GALNT2*/*B2M* four-fold knockout pigs showed the strongest reduction of human IgG and IgM binding in an artificial microvessel perfusion setup when compared to *CMAH* single and *GGTA1*/*CMAH* double-knockout cells. It is likely that new antigens will be discovered with every further knockout performed. Future research will show whether these will be relevant for successful xenotransplantation.

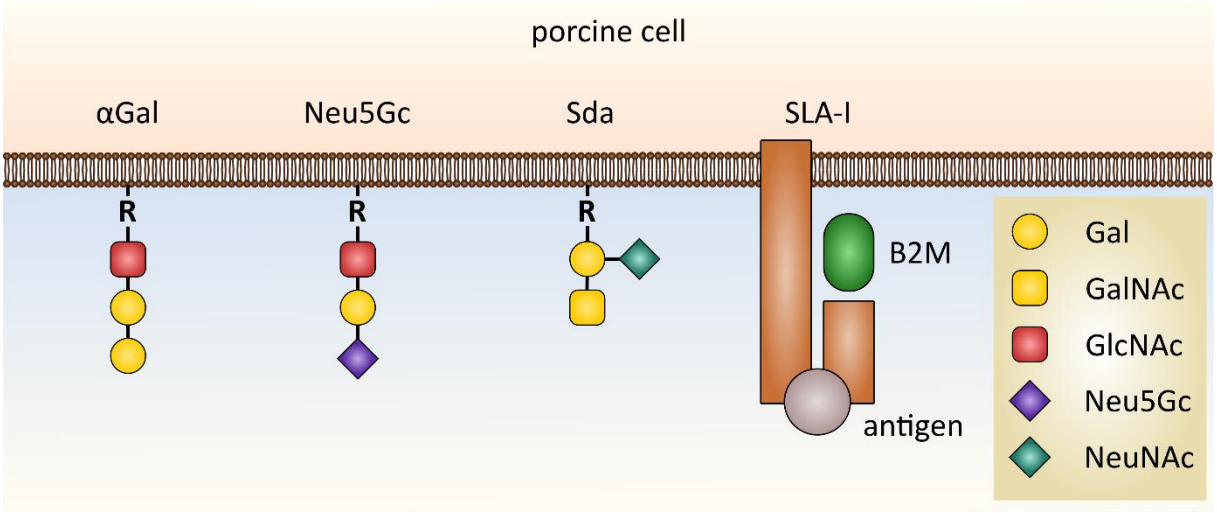

Figure 2 – Known xenorelevant antigens

The carbohydrate epitopes αGal, Neu5Gc and Sda, synthesized by GGTA1, CMAH and B4GALNT2, and SLA class I molecules, composed of a heavy α-chain and a light β-chain (B2M), contribute to the xenoantigenicity of porcine grafts.

αGal: Galα1-3Galβ1-(3)4GlcNAc-R; Neu5Gc: N-glycolylneuraminic acid; Sda: 'Sda antigen'; SLA-I: swine leukocyte antigen class I; Gal: galactose; GlcNAc: N-acetyl-D-glucosamine; NeuNAc: N-acetylneuraminic acid.

Removing xenogeneic surface molecules alone will not completely prevent AVXR. Coagulation dysfunctions, mainly caused by activation of the donor vascular endothelium and molecular incompatibilities in porcine and human coagulation factors, are still a major obstacle in pig-to-NHP transplantation. Endothelial activation includes exposition of tissue factor (TF), a key initiator of the clotting cascade, and internalisation of thrombomodulin (TM), an anti-coagulative surface receptor that blocks the procoagulant activities of thrombin [111, 112]. Coagulation is further promoted by the inability of porcine TM to effectively bind human thrombin, thereby impeding protein-C dependent inhibition of blood clotting [113, 114]. It was shown that expression of human TM on porcine aortic endothelial cells (AECs) helps to delay the coagulation process *in vitro* [115]. Beneficial effects of human TM expression on xenograft survival have also been suggested by Iwase *et al.* who used GGTA1-deficient hCD46/hTM transgenic hearts in heterotopic pig-to-baboon cardiac transplantation [116]. Introducing the human gene for tissue factor pathway inhibitor (TFPI), the principal inhibitor of the extrinsic coagulation pathway, into the donor's genome is another strategy to combat clotting dysregulation as porcine TFPI was discussed to be unable to neutralize the human coagulation factor Xa [117-119]. Significant reduction of human platelet aggregation was achieved when human TFPI was expressed on porcine AECs [120]. CD39 is another critical thrombo-regulatory protein that rapidly loses its activity during EC activation [121, 122]. It inhibits platelet aggregation by converting prothrombic adenine nucleotides that are released at the site of cellular injury [123-125]. The potential value of human CD39 expression to regulate coagulation disorders was supported in transgenic mouse studies. Cardiac allografts expressing human CD39 were significantly protected from thrombosis and revealed prolonged survival in a murine model of vascular rejection [126]. Moreover, human CD39 expression on murine islets was shown to prevent clotting of human blood *in vitro* [127]. Another strategy to reduce the risk of thrombosis and also to regulate inflammatory processes after xenotransplantation is the introduction of the human endothelial protein C receptor (*EPCR*) gene into the donor's genome. EPCR promotes protein C activation, which is strongly anticoagulative, by the TM-thrombin complex (see Figure 3) and induces a response in ECs that decreases synthesis of pro-inflammatory cytokines [128, 129]. Reduced platelet activation by human *EPCR* expression was shown *in vitro* in porcine AECs as well as in a xenogenic perfusion model, where porcine lungs transgenic for human *EPCR* also exhibited extended survival [120, 130].

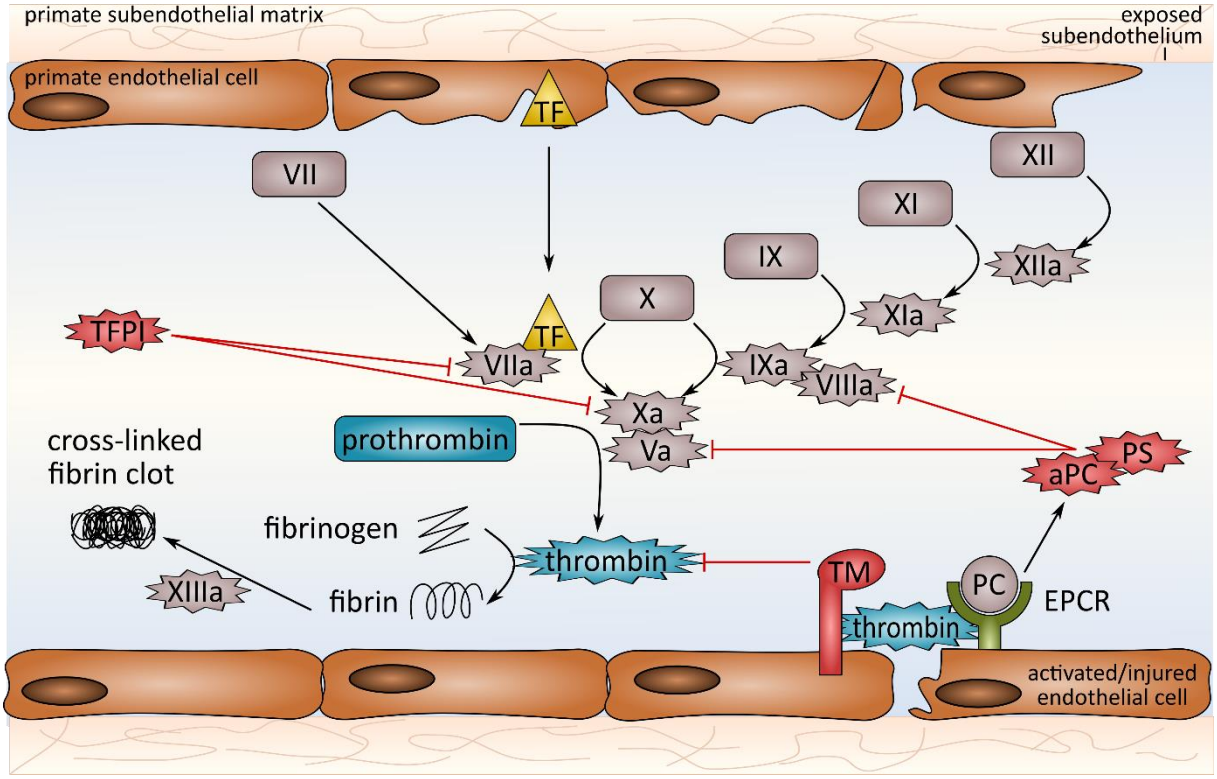

Figure 3 – The coagulation cascade in primates

Exposition of TF to the circulation initiates the coagulation cascade via the extrinsic pathway. Once activated, TF binds to factor VIIa (FVIIa). The TF/FVIIa complex induces activation of FX that binds to FVa, forming the FXa/FVa complex and converting prothrombin to thrombin. Fibrinogen is then cleaved by thrombin into fibrin monomers, which are cross-linked in presence of FXIIIa to form an insoluble clot. The intrinsic coagulation pathway is initiated by the exposed subendothelial matrix activating FXII. FXI and FIX are subsequently activated. The IXa/VIIIa complex then activates FX. Clot formation is regulated by several anticoagulant mechanisms. E.g. (A) TFPI inhibits Xa after binding and forms the TFPI/Xa complex, which neutralizes TF/VIIa. (B) TM binds thrombin and inhibits formation of fibrin. It also acts as a cofactor in the (C) thrombin-induced activation of PC, which is enhanced by EPCR. The aPC/PS complex inactivates FVIIIa and FVa by proteolysis.
TF: tissue factor; TFPI: tissue factor pathway inhibitor; TM: thrombomodulin; PC: protein C; EPCR: endothelial protein C receptor; PS: protein S (adapted from [131] and [132]).

A major challenge, especially in pig liver xenotransplantation, is the loss of platelets causing thrombocytopenia [133]. Inactivation of the asialoglycoprotein receptor (ASGR), a hetero-oligomeric transmembrane protein consisting of ASGR1 and ASGR2 subunits, might offer a solution to this problem [134]. Molecular differences in glycosylation of human and porcine platelets are assumed to cause ASGR-mediated phagocytosis of human thrombocytes by porcine Kupffer cells and liver sinusoidal endothelial cells (LSECs) [135-137]. Pig livers deficient in the ASGR1 protein exhibited decreased sequestration of human thrombocytes than wildtype organs in *ex vivo* perfusion experiments [138].

Transgenic expression of human proteins with anti-inflammatory and anti-apoptotic properties, like TNFα-induced protein 3 (also called A20) and heme oxigenase 1 (HO-1), can help to maintain integrity of the donor endothelium and prevent EC activation. A20 is an ubiquitin-editing enzyme that modulates pro-inflammatory cytokine responses, such as tumor necrosis factor (TNF) and interleukin (IL)-1β, through inhibition of nuclear factor-κB (NF-κB) activation (see section 4.3.4.2) [139]. The cytoprotective character of HO-1 arises from both the catabolization of free heme, an inflammatory molecule capable of inducing apoptosis at patho-physiological concentrations, and the downstream functions of its degradation products biliverdin, Fe^{2+} and carbon monoxide (CO) [140-143]. The latter scavenges reactive oxygen species and prevents apoptosis resulting from cellular stress during inflammation processes [144]. Human A20 and HO-1 were each shown to protect porcine AECs from TNF-mediated cell death, whereas human HO-1 also reduced IFNγ-induced MHC class II expression and prolonged kidney survival in *ex vivo* perfusion experiments [145-147].

Numerous genetic modifications have the potential to control AVXR at many different levels. Combination of multiple gene knockouts and transgenes will help to surmount short- to midterm xenograft rejection. Recently, several breakthroughs have been made in pig-to-NHP transplantation. Längin *et al*. achieved function of life-supporting cardiac xenografts (*GGTA1*$^{-/-}$/hCD46/hTM) up to 195 days. Xenografted kidneys (*GGTA1*$^{-/-}$/hCD55) have even been working for up to 499 days as reported by Kim *et al*. [148, 149]. Xenograft survival resulted not only from the genetic modifications and technical refinements of the transplantation procedure but also from the extensive use of immunosuppressive drugs mainly blocking immune cell responses. The latter is necessary as cellular components of the immune system destroy the porcine graft during a process called cellular xenograft rejection (CXR).

4.3.3.2.3 Cellular xenograft rejection (CXR)

Although cellular responses are one of the most common types of rejection in allotransplantation, CXR has not been characterized in xenografts in detail. In contrast to HAR and AVXR that are mainly relevant to whole organ xenotransplantation, CXR is relevant for both, solid organs and cellular grafts. However, it often accompanies AVXR in solid organ transplantation and involves both, cells of the innate and the adaptive immune system [150, 151]. Among other cells, NK cells, macrophages and T lymphocytes were associated with tissue

destruction [150]. Even though cellular rejection can be prevented by potent pharmacological immunosuppressants, it is desirable to minimize the causes of CXR, which will be discussed below [148, 149, 152, 153].

NK cells activity is triggered by an imbalance of activating and inhibitory signalling, mediated by various NK cell receptors and their ligands on potential target cells (see Figure 4), and finally results in degranulation of lytic molecules and secretion of cytokines (e.g. TNF and IFNγ). [154, 155]. The interaction between xenoreactive IgG-antibodies bound to porcine cells and the NK cell's FcγRIIIA (CD16a) receptor induces antibody-dependent cell-mediated cytotoxicity (ADCC) [156, 157]. Xenografts from multiple-knockout animals lacking the major xenoantigens (see section 4.3.3.2.2) may significantly curtail ADCC by human NK cells but will not prevent direct NK cell-mediated cellular lysis. SLA class I molecules cannot efficiently deliver inhibitory stimuli to human NK cells, making porcine xenografts highly prone for NK cell-mediated cytotoxicity [158]. Equipping porcine cells with human MHC class I molecules is a promising strategy to mimic human self-signals. Transgenic expression of HLA-E, a non-classical HLA class I molecule with only two functional variants, provided partial protection of porcine ECs from xenoreactive human NK cells *in vitro* [159, 160]). In *ex vivo* xenoperfusion experiments, HLA-E expression was also associated with a reduction of NK cell responses [161-163]. An important activating receptor of human NK cells is NK cell receptor D (NKG2D) that can be triggered by porcine UL16-binding protein 1 (ULBP1) present on the surface of ECs. Lilienfeld *et al.* have demonstrated that xenogeneic cytotoxicity can be inhibited by anti-porcine ULBP1 antibodies [164]. *In vitro* data suggest that the knockout of porcine *ULBP1* might reduce human NK cell-dependent lysis [165, 166].

Macrophages play a major role in the rejection of cellular xenografts mainly by amplifying T cell responses through cytokine release (e.g. IL-12). They are also involved in vascularized graft rejection, where they participate in CXR as well as in HAR and AVXR and can act in total absence of T cell activity [131, 167-170]. Interaction between porcine endothelial antigens and receptors on the surface of macrophages causes direct toxicity, which is mediated by the release of pro-inflammatory cytokines like TNF, IL-1 and IL-6 [171-175]. Macrophages can also eliminate antibody-coated target cells through phagocytosis (see Figure 4) [176]. Besides the variety of activating pathways, cross-species incompatibility between porcine CD47, a 'marker of self', and the inhibitory receptor SIRPα may contribute to macrophage responses in pig-to-

NHP xenotransplantation [177, 178]. *In vitro* studies demonstrated that expression of human CD47 in porcine cells dramatically reduces susceptibility to phagocytosis by human macrophages [177]. The protective effect of hCD47 expression *in vivo* was further reported by Tena *et al.* in a small animal model [179].

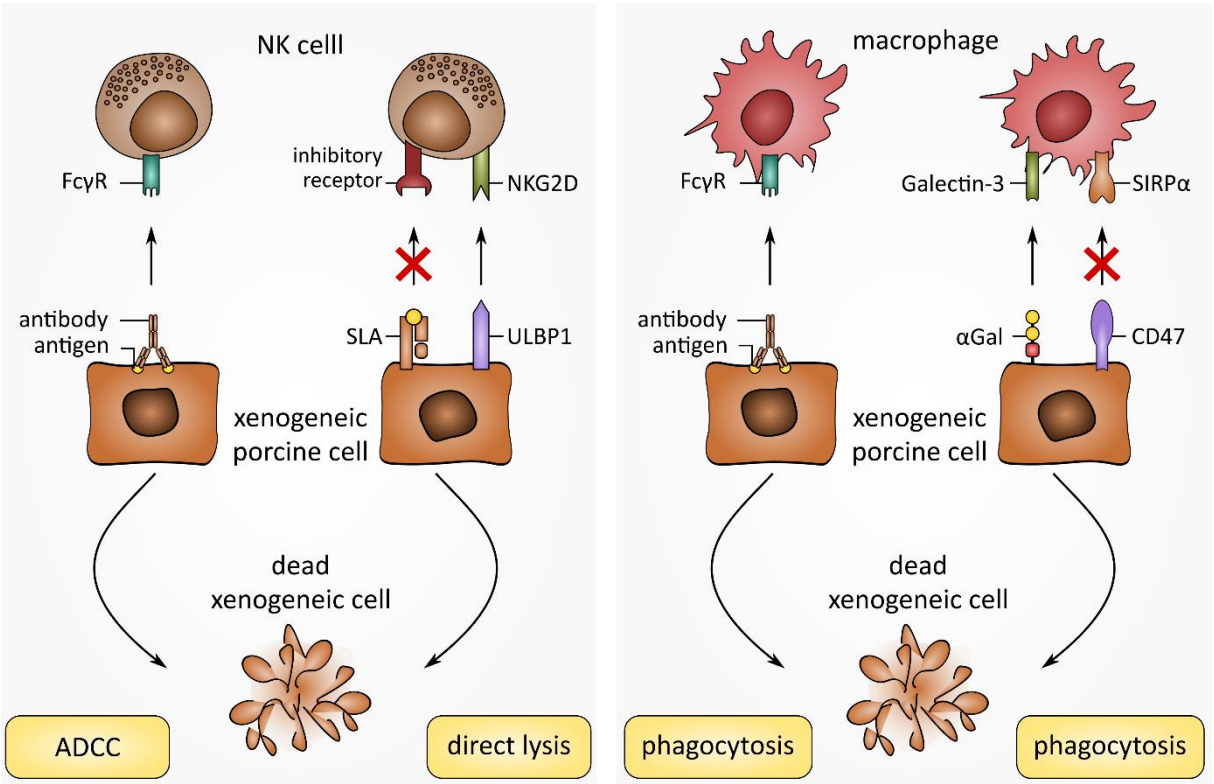

Figure 4 – Cellular rejection mediated by NK cells and macrophages

Left: Xenoreactive antibodies bound to porcine surface epitopes are recognized by the NK cell's FcγRIIIA receptor which induces antibody-dependent cell-mediated cytotoxicity (ADCC). Direct lysis of xenogeneic porcine cells by NK cells is initiated by an imbalance of activating and inhibitory signals. SLA class I molecules are unable to transmit inhibitory signals to human NK cells, while interaction between porcine ULBP1 and human NKG2D stimulates human NK cell activation. **Right:** Macrophages can be activated by antibodies bound to porcine antigens via FcγR receptors. They are also activated by interaction of porcine αGal epitopes with Galectin 3. Cross-species incompatibility between porcine CD47 and the human inhibitory receptor SIRPα makes porcine cells prone to phagocytosis by human macrophages.

FcγRIIIA: low affinity immunoglobulin γ Fc region receptor III-A; ULBP1: UL16-binding protein 1; NKG2D: natural killer group 2D; SIRPα: tyrosine-protein phosphatase non-receptor type substrate 1 (adapted from [131]).

The importance of T cells in xenotransplantation of solid organs has not been finally clarified. However, T cell-mediated rejection is the major cause of porcine islet loss [180, 181]. T lymphocytes damage the xenograft by direct killing activity of the CD8+ subpopulation, the production of cytokines that prime the innate immune system and their ability to provide help

for B cells to produce xenoreactive antibodies [65]. T cell response to porcine antigens can be initiated by direct and indirect xenoantigen recognition [182, 183]. The indirect pathway, where donor-derived peptides are presented by recipient MHC class II molecules, is stronger than its allogeneic counterpart, while the direct response seems to be weaker in xeno- than in allotransplantation [182-184]. The latter involves the direct recognition of SLA class I and class II molecules of porcine antigen presenting cells (APCs) by recipient (NHP or human) T cell receptors (TCRs) [185]. While conventional donor APCs, e.g. dentritic cells (DCs), are transient components of the graft, porcine ECs are permanently present in (vascularized) graft and pose a risk of enduring T cell stimulation (see Figure 5). The removal of SLA class I molecules (see section 4.3.3.2.2) and the reduction of SLA class II proteins in the donor animal by expressing a dominant-negative class II transactivator (mutCIITA) gene are promising approaches to attenuate direct human T cell activation [186]. Besides the interaction of MHC-peptide-complex and TCR, an appropriate cytokine environment as well as the binding between co-stimulatory molecules at the T lymphocyte (e.g. CD154, CD28) and the corresponding surface proteins at APCs (e.g. CD40, CD80/86) are required to induce antigen-specific T cell proliferation [187, 188]. Costimulation via the CD28-CD80/86 pathway can be inhibited by CTLA4-Ig, a potent immunosuppressive fusion protein consisting of the extracellular domain of cytotoxic T-lymphocyte antigen 4 (CTLA4) and the Fc region of IgG [189]. The same co-stimulatory pathway is inhibited by LEA29Y, a CTLA4-Ig variant exhibiting 10-fold enhanced affinity *in vitro* [190, 191]. Both molecules compete with CD28 for binding to CD80/86 (B7) molecules on APCs and are already used in clinical post-allotransplant therapy [189, 190, 192, 193]. Transgenic expression of CTLA4-Ig or LEA29Y is suggested to attenuate xenograft rejection, but pigs that ubiquitously overexpress these proteins are highly susceptible to infection [194, 195]. Tissue-specific transgene expression is one strategy to protect the graft from xenogeneic T cell responses while avoiding undesirable immunodeficiency in the donor pig [196-199].

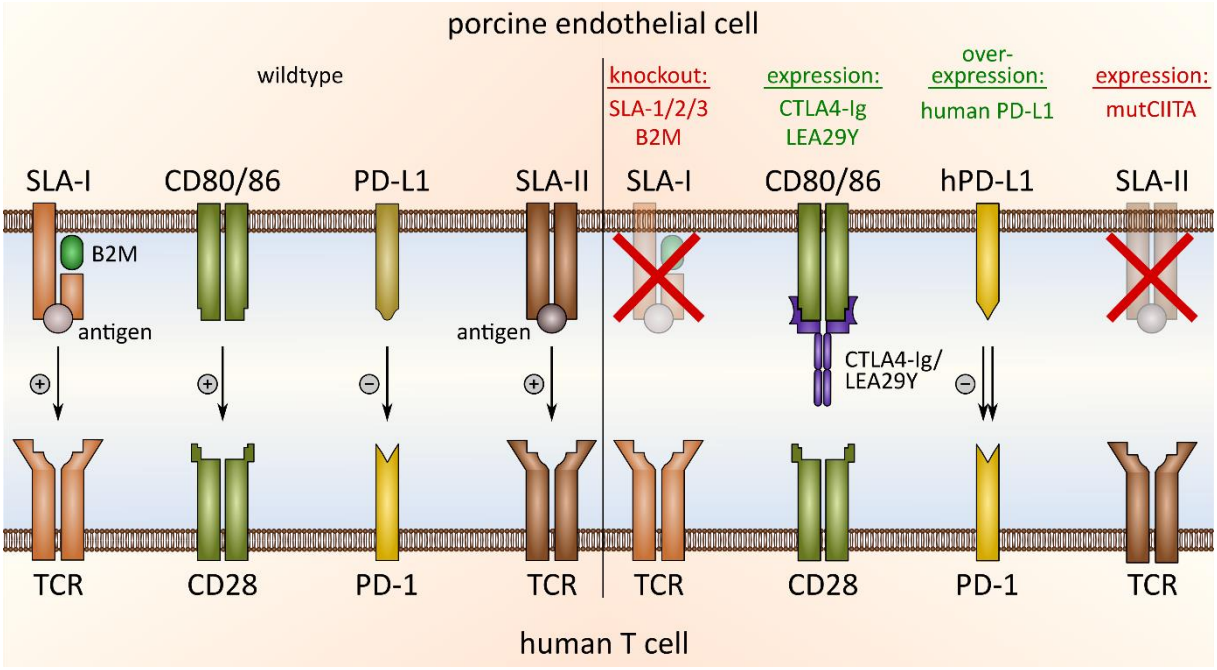

Figure 5 – Attenuating stimulatory signals for T cell activation

Porcine ECs of a wildtype xenograft can act as permanent stimulators of the human T cell response. They express type I and type II SLA molecules for antigen presentation via TCR. CD80/86 molecules constitutively expressed on porcine ECs interact with CD28 to provide a second signal for T cell activation. Binding of PD-L1 to PD-1, however, produces a suppressive stimulus to the T cell. Knocking out *SLA-1, SLA-2* and *SLA-3* or *B2M* eliminates functional SLA type I molecules from the donor cell. The expression of mutCIITA downregulates the production of SLA type II proteins. Costimulation by CD80/86 can be blocked by expressing CTLA4-Ig or LEA29Y. The inhibitory effect of endogenous PD-L1 can be amplified by overexpressing the human pendant.

In addition to costimulation blockade, the enhancement of inhibitory receptor-ligand interactions may help to overcome T cell-mediated rejection. Binding of programmed death 1 ligand 1 (PD-L1) to its receptor programmed cell death protein 1 (PD-1) on activated T cells initiates a negative signalling that modulates the balance between T cell activation and (self-) tolerance induction [200, 201]. Several studies indicate a protective effect of transgenic human PD-L1 expression. APCs derived from human PD-L1 transgenic pigs exhibited a reduced capacity to simulate activation and proliferation of human T cells *in vitro.* [202, 203]. Furthermore, fibroblasts expressing human PD-L1 were partially protected from lysis by human cytotoxic effector cells [203]. Overexpression of human PD-L1 on pig cells was also shown to stimulate the expansion of regulatory T cells (Treg), which play a role in the induction and maintenance of allograft tolerance [202, 204].

4.3.4 Immune modulation by cytokines

Cytokines are small proteins with essential immune-modulatory functions that can mediate anti- and pro-inflammatory responses. Important members of both categories are presented in the following sections. Table 1 summarizes the function of all cytokines mentioned below.

Table 1 – Function of selected cytokines

Name	Main functions	Ref.
IFNγ	Pro-inflammatory, activates macrophages, enhances expression of MHC molecules, inhibits viral replication	[205-209]
IL-1β	Pro-inflammatory, initiates APR, activates lymphocytes	[210-213]
IL-2	Proliferation and differentiation of naïve T cells	[214]
IL-5	Stimulates eosiophils, increases antibody secretion	[215, 216]
IL-6	Pro-inflammatory, initiates APR	[217]
IL-10	Anti-inflammatory (predominantly), inhibits macrophage functions, reduces antigen presentation	[218-220]
TGF-β	Anti-inflammatory, initiates immune privilege	[221]
TNF	Pro-inflammatory, activates ECs and macrophages	[222-224]

4.3.4.1 Anti-inflammatory cytokines

IL-10 and transforming growth factor (TGF) β are cytokines with potent anti-inflammatory properties and important for establishing immune tolerance [218, 225-227]. IL-10 is primarily produced by monocytes, T helper (Th) type 2 cells and CD4+ Tregs and is an effective inhibitor of macrophage functions and T cell responses [219, 228-231]. It inhibits the production of IL-2, IL-5 and TNF by T cells which reduces the expression of MHC- and costimulation molecules at APCs and consequently blocks antigen presentation [220, 232-235].

TGF-β is released by many different cell types including lymphocytes and monocytes/macrophages and is, like IL-10, involved in the formation of immunologically privileged environments [221, 236, 237]. At high concentrations and the simultaneous absence of pro-inflammatory signals (e.g. IL-6), TGF-β promotes the differentiation to CD4+ Tregs [238, 239]. TGF-β also suppresses the development of cytotoxic T cells and differentiation of Th cells and can inhibit or modulate activation, maturation and differentiation of dendritic cells (DCs), neutrophils and macrophages [240-242].

4.3.4.2 Pro-inflammatory cytokines

TNF, IL-1β and interferon (IFN) γ are important cytokines being involved in the upregulation of inflammatory reactions, also during xenograft rejection as mentioned in the previous sections.

TNF has a wide range of biological functions and plays a major role in inducing local and systemic inflammation [222, 243]. It is mainly produced and released by macrophages in response to bacterial products (e.g. lipopolysaccharides (LPS)), but also by NK cells, DCs, ECs and Th cells [244-249]. TNF belongs, alongside IL-1β and IL-6, to the important cytokines that initiate the acute phase response (APR) in the liver following infection, tissue injury, tumor growth or immunological disorders [217, 250]. As part of APR, C-reactive protein (CRP) and mannose-binding lectin (MBL) are synthesized and the complement system is activated [251, 252]. TNF is also a strong activator of ECs and macrophages and orchestrates the production of other pro-inflammatory cytokines [223, 224]. It stimulates migration of DCs to the lymph nodes thereby promoting the initiation of the adaptive immune response [253, 254].

IL-1β is, like TNF, a key mediator of the inflammatory response and essential for immune responses to infection and injury [210]. It is primarily expressed by macrophages and blood monocytes, contributes to the release of acute phase proteins and the differentiation of macrophages [217, 255, 256]. IL-1β also triggers activation of T and B lymphocytes and promotes cytokine synthesis and antibody production [212, 213, 257-260].

IFNγ is a crucial player in controlling intracellular pathogens and is released by cells of the innate immune system (e.g. NK cells, DCs and macrophages) during the early immune response and later by Th1 and CD8+ cytotoxic T lymphocyte (CTL) effector cells [261-266]. The main function of IFNγ is the activation of macrophages and to enhance the expression of MHC class I and class II molecules on these and other APCs [205-208]. IFNγ also has a direct inhibitory effect on viral replication [209].

The pro-inflammatory effects of TNF and IL-1β are largely due to the activation of transcription factor NF-κB [267]. After binding of TNF and IL-1β to their respective receptors (TNFR1 and IL1R1), downstream signalling results in phosphorylation-dependent ubiquitination and degradation of IκB, the inhibitor protein of cytoplasmic NF-κB (see Figure 6) [268, 269]. The active, dimeric NF-κB then enters the nucleus to mediate the expression of e.g. cytokines,

chemokines, adhesion molecules and further proteins of the inflammatory response, cell cycle regulators and anti-apoptotic factors [270].

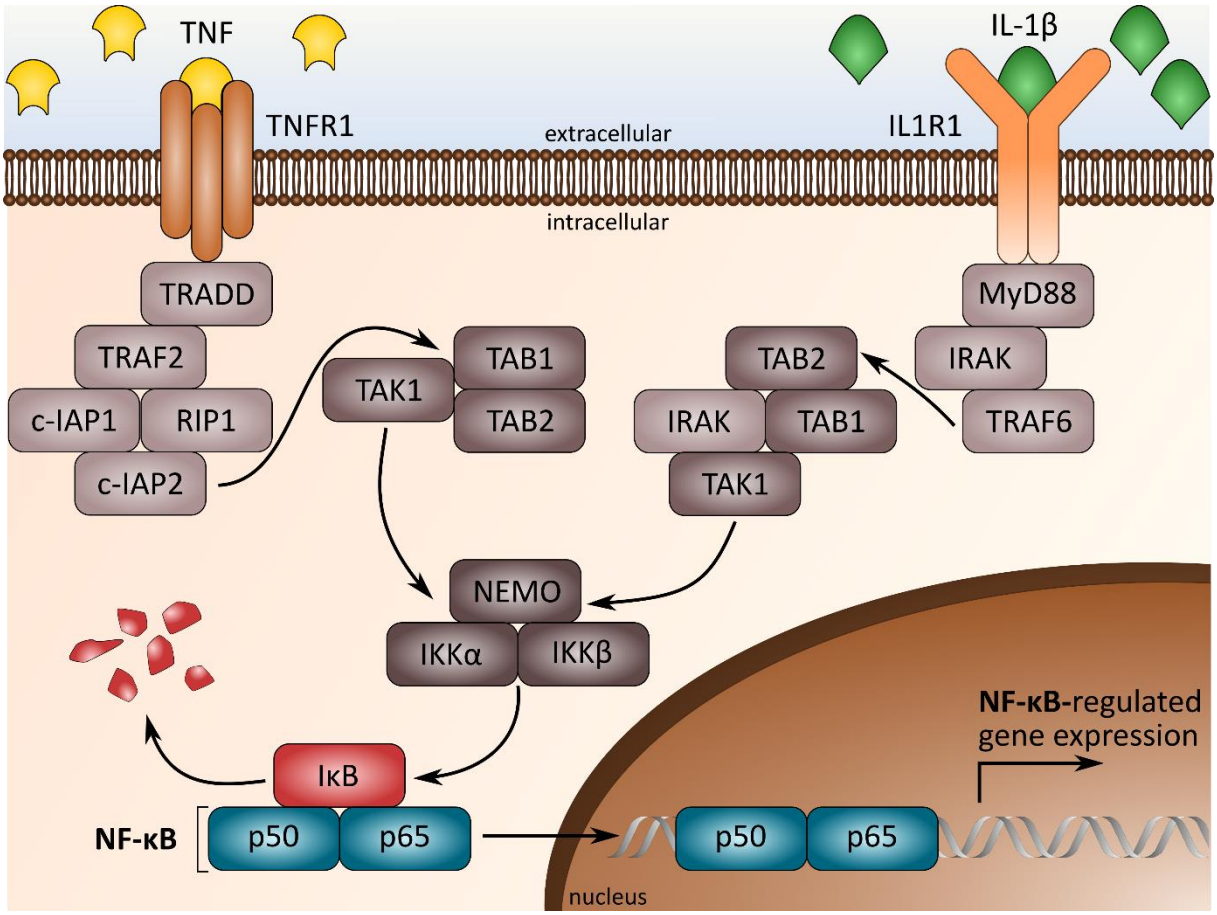

Figure 6 – TNF and IL-1β-associated intracellular signalling pathways inducing activation of NF-κB

Left: Interaction of TNF with TNFR1 induces association with the adapter protein TRADD and gradual binding by further adaptor proteins (e.g. TRAF2, cIAP1, cIAP-2, RIP1). The ubiquitinated RIP1 binds TAK1, TAB1 and TAB2 leading to phosphorylation of the IKK complex (IKKα/β, NEMO). **Right:** After binding of IL-1β to ILR1, the adaptor protein MyD88 attaches to the receptor and enables binding of IRAK family protein kinases. Recruitment of TRAF6 and subsequent binding of TAK1, TAB1 and TAB2 results in phosphorylation of the IKK complex. **Bottom:** The IKK complex induces phosphorylation of IκB, the inhibitor protein of NF-κB, which is subsequently ubiquitinylated and degraded. The cytosolic NF-κB protein consisting of e.g. p50 and p65 is then translocated to the nucleus where it modifies the expression of NF-κB-regulated genes.

TNF: tumor necrosis factor; TNFR1: TNF receptor 1; TRADD: TNFR1-associated death domain protein; TRAF2: TNF receptor-associated factor 2; c-IAP1/2: cellular inhibitor of apoptosis 1/2; RIP1: receptor-interacting protein 1; TAK1: orphan nuclear receptor; TAB1/2: TGF-β-activated kinase 1/2; IL-1β: interleukin 1 β; IL1R1: interleukin-1 receptor type 1; IRAK: interleukin-1 receptor-associated kinase; TRAF6: TNF receptor-associated factor 6; NEMO: NF-κB essential modulator; IKKα/β: IκB kinase α/β; IκB: inhibitor of NF-κB; p50/p65: subunits of proteins forming NF-κB; NF-κB: nuclear factor-κB (adapted from [269]).

Biological responses induced by IFNγ, however, are mediated through the transcription factor STAT1. Binding of IFNγ to its receptor (IFNGR) causes a series of phosphorylation reactions that leads to dimerization of two STAT1 proteins [271, 272]. The STAT1 homodimer then migrates into the nucleus where it induces or suppresses the transcription of IFNγ-regulated genes [272]. Many of those genes activated by STAT1 are transcription factors that initiate a second wave of transcription [273].

4.4 Generation of genetically modified pigs

The previous chapter demonstrated how genetic modifications of the donor animal can weaken and even prevent rejection of a xenograft. The following sections therefore focus on the techniques to specifically introduce new genetic constructs into porcine cells and to precisely inactivate genes (see section 4.4.1) and finally, on the reproductive methods commonly used to create genetically modified pigs (see section 4.4.2).

4.4.1 Genetic engineering approaches

The availability of embryonic stem cells (ESCs) dramatically accelerated site-directed mutagenesis experiments in mice as these cells can be cultured and modified for unlimited time spans [274, 275]. Although first approaches for ESC isolation and cultivation in pigs have already been published, these protocols are still missing independent reproducibility [276]. Therefore, genetic engineering approaches in pigs have been based on the use of somatic cells. Gene targeting based on homologous recombination was one of the first methods of choice for pigs [277]. This method enables the site-specific integration of exogenous DNA sequences, as well as the specific alteration or complete substitution of endogenous sequences. Locus-determining homology arms flanking the donor DNA comprise between 500 bp and several thousand bp for gene targeting in pigs [147, 278, 279].

To further increase efficiencies of homologous recombination and facilitate endogenous gene knockouts, synthetic and highly specific endonucleases were developed. Selectively introduced double-strand breaks (DSBs) can not only be repaired by homology directed repair (HDR), a high-fidelity mechanism depending on a homologous DNA template, but also by non-

homologous end joining (NHEJ), causing inactivation of endogenous genes by introducing small insertions or deletions (InDel), resulting in frameshift or missense mutation of critical codons [280-286]. Examples of such molecular scissors are zinc-finger nucleases (ZFNs) and transcription activator-like effector nucleases (TALENs) that emerged between the late 1990s and early 2010s [287-289]. Both technologies are based on DNA-binding protein domains fused to FokI-nuclease domains [287, 289, 290]. The field of genetic engineering was revolutionized in 2012, when the clustered regulatory interspaced short palindromic repeats (CRISPR)/CRISPR-associated (Cas) system was published as a novel tool for genome editing [291]. It originates from bacteria and archaea as an RNA-based, adaptive immune defence that sequence-specifically detects and silences foreign nucleic acids [292]. A complex of CRISPR RNA (crRNA), that determines the sequence specificity, and trans-activating crRNA (tracrRNA) guides the Cas9 DNA endonuclease to the target DNA sequence to introduce DSBs. This target recognition site usually comprises 18-20 nt followed by a protospacer adjacent motif (PAM). For efficient genetic modification of eukaryotic cells, crRNA and tracrRNA were fused to form a single chimeric molecule called single guide RNA (sgRNA) [291].

There are many advantages making CRISPR/Cas-based methods so successful: The ease of customization and the ability to target several loci simultaneously while being highly affordable and providing similar or greater efficiencies than ZNFs and TALENs [293-295]. The discovery and development of further Cas variants opened new applications for the CRISPR-technology. The Cas9 enzyme typically used for the introduction of DSBs in mammalian cells was derived from *Streptococcus pyogenes* (SpCas9) and creates a blunt cut 3 bp upstream of its PAM (5'-NGG-3') [291]. However, the Cas12a enzyme (formerly Cpf1) cleaves the target DNA 18-23 nt downstream of the PAM (5'-TTTV-3'; (V = A/G/C). This allows re-engineering of the locus of interest as the target recognition site remains intact. The staggered-ended DSBs produced by Cas12a may also improve the frequency of HDR over NHEJ [296]. Besides genetic modification via the DSB repair pathway, catalytically inactive Cas9 (dCas9) and Cas9 nickase variants (nCas9) can be fused to deaminase to allow precise conversion of a single base without double-stranded DNA cleavage [297, 298]. Another application of dCas9 is site-specific gene regulation when linked to transcriptional or epigenetic regulator proteins [299-301]. The development of these new classes of molecular scissors has decisively improved genome editing efficiencies. The following chapter will give insights into the subsequent generation of genetically modified animals.

4.4.2 Reproductive technologies

Due to the lack of ESCs in pigs, methods such as blastocyst complementation for the generation of chimeric animals as performed in mice, are not available. Therefore, gene-modified pigs have been mainly created by using somatic cell nuclear transfer (SCNT) or microinjection methods in fertilized oocytes.

SCNT involves the transfer of a somatic donor cell into an enucleated oocyte and was first developed in sheep and later optimized for additional species [302]. Genome-engineered somatic cells were then used to create genetically modified animals, including pigs, in subsequent years [76, 303]. SCNT provides many advantages for the challenging generation of livestock species. Somatic cells can be modified in cell culture, subsequently screened and pre-selected *in vitro*, thereby reducing the risk of generating animals with non-intended mutations or without the desired modifications. As the genetic background and gender is fixed by the somatic cells used, this further reduces the number of animals required. Compared to other methods, SCNT also ensures germ-line transmission of the genetic modifications. However, several disadvantages can be linked to SCNT including low efficiencies, epigenetic and imprinting defects as well as health disorders of the animals such as over-sized tongue, orofacial cleft and abnormalities of the legs [304-308].

Especially for the fast-track generation of genetically modified animals, other techniques have been preferred, such as cytoplasmic microinjection of nucleic acids into the fertilized oocyte. Although microinjection-based methods are not suitable for precise HDR-mediated transgene placements due to low efficiencies and consequently high numbers of experimental animals required, microinjection is nowadays frequently used for transposon-mediated or NHEJ-based approaches, particularly in combination with molecular scissors, to generate transgenic or knockout animals [309-312].

4.5 Objectives

The overall aim of this work was to establish new approaches for genetical optimization of porcine organ donors to improve graft acceptance in xenotransplantation.

Transgenic expression of powerful T cell regulatory proteins such as CTLA4-Ig/LEA29Y provide significant protection against T-cell-mediated rejection in pre-clinical xenotransplantation studies. Enduring ubiquitous expression at high levels, however, can greatly impair the immune competence of the donor animal and may induce adverse health effects on the xenograft recipient. The first project goal was therefore to develop a novel approach (the Smart Graft strategy) to enable dynamic expression of xenoprotective genes in response to pro-inflammatory cytokines secreted during incipient xenograft rejection. The idea was to use NF-κB-regulated promoters to achieve the inflammation-dependent transgene expression, since downstream-signalling of TNF and IL-1β, the key mediators of the inflammatory response, both result in activation of this transcription factor. A swift response to the cytokines released is desirable to enable immediate expression of protective proteins, thereby counteracting incipient xenograft rejection. Quick reversion to low basal promoter levels, once inflammation subsides, should prevent undesired permanent modulation of the recipient's immune system.

The number of known gene inactivations with beneficial effects on xenograft acceptance is steadily growing. The combination of all desired gene knockouts in a single animal through breeding, however, is a labour and time-consuming challenge. The second objective was therefore to provide CRISPR/Cas9-based means for an efficient fast-track knockout of up to seven genes or gene clusters in order to reduce immunogenicity and improve molecular as well as anatomical compatibility between xenograft and recipient.

5. MATERIALS

5.1 Equipment

Table 2 – Equipment

Name	Manufacturer
Block heater, ThermoQ	Bioer Technology, Tokyo, JPN
Blue light table	Serva, Heidelberg, GER
Centrifuges, Sigma 3-16, Sigma 1-14, Sigma 1-15, Sigma 1-15K, Sigma 4K15	Sigma, Osterode, GER
Digital graphic printer UP-D895MD	Syngene, Cambridge, UK
Droplet generator, QX200	Bio-Rad, Munich, GER
Droplet reader, QX200	Bio-Rad, Munich, GER
Electrophoresis system (buffer chamber, gel trays, combs)	Peqlab Biotechnologie, Erlangen, GER
Electroporator, Multiporator	Eppendorf, Hamburg, GER
ELISA reader, Multiskan Ex	Thermo Fisher Scientific, Waltham, USA
Freezer, - 20 °C	Liebherr, Bulle, CHE
Freezer, - 80 °C	Thermo Fisher Scientific, Waltham, USA
Freezing container, Mr. Frosty	Thermo Fisher Scientific, Waltham, USA
Gel documentation imaging system, Quantum ST5	Vilber Lourmat, Eberhardzell, GER
Gel electrophoresis mains adapter	Amersham Bioscience, Little Chalfont, UK
Glassware	Marienfeld GmbH, Landa, GER
Hybridisation oven, Shake 'n' stack	Thermo Fisher Scientific, Waltham, USA
Ice maker	Manitowoc Ice, Manitowoc, USA
Incubator shaker, Orbital- Shaker	Thermo Fisher Scientific, Waltham, USA
Incubator, BD 115	Binder, Tuttlingen, GER
Incubator, CO_2	Thermo Fisher Scientific, Waltham, USA
IVIS Lumina LT series III	Caliper Life Sciences, Waltham, USA
Laminar airflow cabinet, HERAsafe	Kendro, Langenselbold, GER
Luminometer, Glomax 20/20	Promega, Fitchburg, USA
Magnetic stirrer	Velp Scientifica, Usmate, ITA
Microscope, Axiovert 40 CFL	Carl Zeiss, Oberkochen, GER
Magnetic tube rack, DynaMag-15 Magnet	Life technologies, Carlsbad, USA
Microscope, DMIL LED	Leica, Wetzlar, GER
Microwave oven	MHA, Barsbüttel, GER
Microtome, Microme Cool Cut	Histoserve, Celle, GER
Microscope and Scanner, M8	PreciPoint, Freising, GER
PCR cycler, Peqstar 2x	Peqlab Biotechnologie, Erlangen, GER
PCR plate sealer, PX1	Bio-Rad, Munich, GER

pH meter, CyberScan 510	Thermo Fisher Scientific, Waltham, USA
Pipette controller, Accu-Jet Pro	Brand, Wertheim am Main, GER
Pipette, Gilson Pipetman (2, 20, 200, 1000 µL)	Gilson, Middleton, USA
Refrigerator	Siemens, München, GER
Spectrophotometer, NanoDrop Lite	Peqlab Biotechnologie, Erlangen, GER
Vortex Genie 2	Scientific Industries, Bohemia, USA
Water bath, WB14	Memmert, Schwabach, GER
StainTray	Simport, Saint-Mathieu-de-Beloeil, CAN

5.2 Consumables

Table 3 – Consumables

Name	Manufacturer
Cartridges for QX100/QX200 droplet generator, DG8	Bio-Rad, Munich, GER
Cell culture dishes, 10 cm, 15 cm	Corning, New York, USA
Cell culture flasks, T25, T75, T150	Corning, New York, USA
Cell culture plates, 6 well, 12 well. 24 well, 48 well, 96 well	Corning, New York, USA
Cell scraper	Faust Lab Science, Klettgau, GER
Centrifuge tubes, 15 mL, 50 mL	Sarstedt, Nümbrecht, GER
Counting chamber, C-Chip	NanoEntek, Waltham, USA
Cryogenic vials, 2.0 mL	Corning, New York, USA
Droplet generator DG8 gasket	Bio-Rad, Munich, GER
Electroporation cuvettes, 2 mm	Peqlab Biotechnologie, Erlangen, GER
Microscope slides, Polysine	VWR, Radnor, USA
Microtome blades, R35 Type	Feather, Osaka, JPN
Pasteur pipettes	Brand, Wertheim am Main, GER
PCR plate 96, twi.tec, semi skirted, colorless	Eppendorf, Hamburg, GER
Petri dishes, 10 cm	Grainer Bio-One, Frickenhausen, GER
Pierceable foil heat seal	Bio-Rad, Munich, GER
Pipette tips, 0.1–10 µL, 2–200 µL, 100–1000 µL	Brand, Wertheim am Main, GER
Pipette tips, filtered, 2–20 µL, 20–200 µL, 100–1000 µL	Fisher Scientific, Hampton, USA
Pipettes, serological, 1 mL, 2 mL, 5 mL, 10 mL, 25 mL	Corning, New York, USA
qPCR Plates, 96 well	4titude, Wotton, UK
Reaction tubes, 0.2 mL	Starlab, Hamburg, GER
Reaction tubes, 1.5 mL, 2.0 mL	Eppendorf, Hamburg, GER

Round-bottom tubes, 15 mL	Becton, Dickinson and Company, Franklin Lakes, USA
Scalpel	Braun, Melsungen, GER
Sterile filter, 0.22 µm	Sartorius, Göttingen, GER
Syringes	Becton, Dickinson and Company, Franklin Lakes, USA

5.3 Chemicals and buffers

Table 4 – Chemicals

Name	Manufacturer
3,3'-Diaminobenzidine (DAB) Enhanced Liquid Substrate System tetrahydrochloride	Sigma-Aldrich, Darmstadt, GER
Acidic acid	AppliChem, Darmstadt, GER
Agarose	Sigma-Aldrich, Darmstadt, GER
Boric acid	AppliChem, Darmstadt, GER
Bovine serum albumin, BSA (Fraction V)	Biomol, Hamburg, GER
ddPCR droplet reader oil	Bio-Rad, Munich, GER
Disodium hydrogen phosphate	Merck KGaA, Darmstadt, GER
Dithiothreitol, DTT, 0.1 M	Invitrogen, Carlsbad, USA
Dithiothreitol, DTT, 0.1 M	Nippon Genetics Europe, Düren, GER
dNTPs, 10 mM	New England Biolabs, Frankfurt, GER
dNTPs, 2 mM	Nippon Genetics Europe, Düren, GER
Droplet generation oil for probes	Bio-Rad, Munich, GER
Dynabeads Biotin Binder, streptavidin coupled	Invitrogen, Carlsbad, USA
Ethanol, EtOH, absolute	VWR, Radnor, USA
Ethylenediaminetetraacetic acid, EDTA	AppliChem, Darmstadt, GER
Eukitt quick-hardening mounting media	Sigma-Aldrich, Darmstadt, GER
Formaldehyde	Sigma, Osterode, GER
Gel Loading Dye, Purple, 6x	New England Biolabs, Frankfurt, GER
Glycerol, 100%	AppliChem, Darmstadt, GER
Haematoxylin, Gill's formula	Vector laboratories, Burlingame, USA
Hydrogen peroxide	Honeywell Riedel-de Haën, Morristown, USA
Paraformaldehyde	Sigma, Osterode, GER
Passive Lysis Buffer 2.0, 1x	Biotium, Fremont, USA
peqGREEN staining solution	Peqlab Biotechnologie, Erlangen, GER
Phenol chlorophorm isoamyl alcohol	AppliChem, Darmstadt, GER
Potassium chloride, KCl	Sigma-Aldrich, Darmstadt, GER
Potassium dihydrogen phosphate	Merck KGaA, Darmstadt, GER

Random Hexamers, 50 µM	Invitrogen, Carlsbad, USA
Roticlear	Carl Roth, Karlsruhe, GER
Sodium acetate	AppliChem, Darmstadt, GER
Sodium chloride, NaCl	AppliChem, Darmstadt, GER
Sodium citrate tribasic dihydrate	Sigma, Osterode, GER
Tris Base	AppliChem, Darmstadt, GER
Tris-HCl	Sigma-Aldrich, Darmstadt, GER
Triton X-100	Omnilab Life Science, Bremen, GER
ViviRen In Vivo Renilla Luciferase Substrate	Promega, Fitchburg, USA
XenoLight D-Luciferin, K^+ Salt Bioluminescent Substrate	PerkinElmer, Waltham, USA

Table 5 – Composition of buffer solutions

Name	Components	Mass/Volume/ Concentration
Antibody dilution buffer	BSA	0.4 g
	PBS, 10x	4 mL
	Triton-X100	120 µL
	H_2O	36 mL
Cytokine dilution buffer	PBS	50 mL
	BSA	50 mg
Lysis buffer	Tris base	0.1 M
	EDTA	5 mM
	SDS	28 mM
	NaCl	0.2 M
PBS buffer, 10x	NaCl	1.4 M
	KCl	27 mM
	Na_2HPO_4	0.1 M
	KH_2PO_4	18 mM
		Adjust to pH 7.4
Sodium citrate buffer, 10 mM (pH 6.0)	Trisodium citrate dihydrate	10 mM Adjust to pH = 6.0
TAE buffer, 50x (pH 8.0)	Acetic acid, 100%	2 M
	Tris base	2 M
	EDTA	50 mM
TBE buffer, 10 x (pH 8.0)	Boric acid	0.9 M
	Tris base	0.9 M
	EDTA	20 mM
		Adjust to pH = 8.0
TE buffer	Tris HCl	10 mM
	EDTA	1 mM

TL HEPES Ca^{2+} 296+ buffer	NaCl	114.0 mM
	KCl	3.2 mM
	$CaCl_2$ x 2 H_2O	2.0 mM
	NaH_2PO_4	0.4 mM
	$MgCl_2$ x 6 H_2O	0.5 mM
	$NaHCO_3$	2.0 mM
	HEPES	10.0 mM
	Sodium lactate	10.0 mM
	Sodium pyruvate	0.25 mM
	Succrose	32.0 ´mM
	BSA	0.4%

5.4 Kits

Name	Manufacturer
CloneJET PCR Cloning Kit	Fisher Scientific, Hampton, USA
Firefly & Renilla Single Tube Luciferase Assay Kit	Biotium, Fremont, USA
NucleoBond Xtra Midi	Macherey-Nagel, Düren, GER
SEAP Reporter Assay Kit	InvivoGen, San Diego, USA
SurePrep RNA/DNA/Protein Purification Kit	Fisher Scientific, Hampton, USA
VECTASTAIN Elite ABC Kit (Standard)	Vector laboratories, Burlingame, USA
Wizard SV Gel and PCR Clean-Up System	Promega, Fitchburg, USA

5.5 Animals, mammalian cells and bacteria

Table 6 – Animals

Mouse strain	Source
NOD.*Cg-Prkdc^{scid} Il2rg^{tm1Wjl}*/SzJ	Jochen Seißler, LMU, München

Table 7 – Mammalian cells

Name	Isolation no.	Genotype	Sex	Source
Primary cells				
Porcine kidney fibroblasts (pKDNF)	2505	Wt, GLR	f	Chair of Livestock Biotechnology, TUM, GER

Porcine kidney fibroblasts (pKDNF)	8616-3	Wt, PERV-C free, m BGr 0, GLR	Chair of Livestock Biotechnology, TUM, GER
Porcine kidney fibroblasts (pKDNF)	120419-1/7	Wt, GLR	Chair of Livestock Biotechnology, TUM, GER
Cell lines			
Porcine kidney 15 (PK-15)			Joachim Denner, Robert Koch Institut, Berlin, GER
Swine Tesis (ST)		*GGTA1*$^{-/-}$, CMAH$^{-/-}$, m B2M$^{-/-}$	Chair of Livestock Biotechnology, TUM, GER

Table 8 – Bacteria

Name	Manufacturer
Echerichia Coli, ElectroMAX DH10B	Invitrogen, Carlsbad, USA
Echerichia Coli, NEB 5-alpha Competent (High Efficiency)	New England Biolabs, Frankfurt, GER

5.6 Media, supplements and reagents

Table 9 - Cell culture media, supplements and reagents

Name	Manufacturer
Accutase solution	Sigma-Aldrich, Darmstadt, GER
Ala-Gln	Sigma-Aldrich, Darmstadt, GER
Amphotericin B	Sigma-Aldrich, Darmstadt, GER
Blasticidin S	InvivoGen, San Diego, USA
Dimethylsulfoxid, DMSO	Sigma-Aldrich, Darmstadt, GER
Dulbecco's Modified Eagle's Medium, DMEM high glucose	Sigma-Aldrich, Darmstadt, GER
FCS Superior	Biochrom, Berlin, GER
Hygromycin B Solution	PanReac AppliChem, Darmstadt, GER
IL-1β, recombinant human (rhIL1b)	PeproTech, Rocky Hill, USA
IL-1β, recombinant murine (rmIL1b)	PeproTech, Rocky Hill, USA
Lipofectamine 2000 Transfection Reagent	Life technologies, Carlsbad, USA
Lipofectamine 3000 Transfection Reagent	Life technologies, Carlsbad, USA
MEM Non Essential Aminoacid Solution, x100	Sigma-Aldrich, Darmstadt, GER
Opti-MEM Reduced Serum Medium	Life technologies, Carlsbad, USA
PBS, Dulbecco's	Sigma-Aldrich, Darmstadt, GER
Penicillin/Streptomycin	Sigma-Aldrich, Darmstadt, GER

Puromycin	InvivoGen, San Diego, USA
QuickExtract DNA Extraction Solution	Epicentre, Madison, USA
Sodium pyruvate, 100 mM	Sigma-Aldrich, Darmstadt, GER
TNF, recombinant human (rHuTNF)	Biomol, Hamburg, GER
TNF, recombinant murine (rmTNFa)	PeproTech, Rocky Hill, USA
IFNγ, recombinant human (rHuIFNgamma)	Biomol, Hamburg, GER
Trypan blue stain, 0.4%	InvivoGen, San Diego, USA
Water, cell culture grade	Sigma-Aldrich, Darmstadt, GER

Table 10 – Bacterial growth media, supplements and reagents

Name	Manufacturer
Ampicillin	Carl Roth, Karlsruhe, GER
Difco LB Agar, Miller	Becton, Dickinson and Company, Franklin Lakes, USA
Difco Luria Broth Base, Miller	Becton, Dickinson and Company, Franklin Lakes, USA

5.7 Antibodies

Table 11 – Antibodies and second step reagents

Name	Manufacturer
Anti-CD45 antibody, biotin anti-mouse	Biolegend, San Diego, USA
Anti-MHC I monoclonal antibody, biotin anti-bovine, clone PT85A	Kingfisher Biotech, Saint Paul, USA

5.8 Vectors

Table 12 – Vectors

Name	Plasmid no.	Source
Subcloned promoters		
pJET-hTNFAIP1	A033 #2	This thesis
pJET-hCCL2-2.9kb	A061 #13	This thesis
pJET-hCCL2-prox (A)	A032 #73	This thesis
pJET-hCCL2-prox (B)	A057 #6	This thesis
pJET-hCCL2-dis	A056 #2	This thesis
pJET-hCCL2-dis/prox	A058 #11	This thesis
SEAP reporter constructs		
pcDNA-pA20-SEAP	A006 #45	Nina Simm

		(Master's student)
pcDNA-hVCAM1-SEAP	A020 #24	Nina Simm (Master's student)
pcDNA-CAG-SEAP	A021 #18	Mona Baumgart (Master's student)
pcDNA-ELAM-SEAP	A022 #9	Mona Baumgart (Master's student)
pcDNA-hTNFAIP1-SEAP	A036 #1	This thesis
pcDNA-hCCL2-prox-SEAP	A039 #7	This thesis
pcDNA-pA20+3NFkB-SEAP	A043 #3	This thesis
pcDNA-pA20+5NFkB-SEAP	A044 #(30)9	This thesis
pcDNA-pA20+2SP1-SEAP	A049 #29	This thesis
pcDNA-pA20+7NFkB-SEAP	A050 #(3)11	This thesis
pcDNA-pA20+9NFkB-SEAP	A051 #(3)12	This thesis
pcDNA-pA20+8SP1-SEAP	A052 #91	This thesis
pcDNA-pA20+6SP1-SEAP	A053 #75	This thesis
pcDNA-pA20+4SP1-SEAP	A054 #19	This thesis
pcDNA-pA20+4SP1+3NFkB-SEAP	A055 #4	This thesis
pcDNA-hCCL2-dis/prox-SEAP	A059 #8	This thesis
pcDNA-hCCL2-2.9kb-SEAP	A062 #15	This thesis
pcDNA-pA20+5NFkB-4SP1-3NFkB-SEAP	A063 #xy	This thesis
pcDNA-pA20+4SP1+9NFkB-SEAP	A066 #166	This thesis
pcDNA-pA20+5NFkB+4SP1+9NFkB-SEAP	A067 #17	This thesis
pcDNA-pA20+10NFkB+4SP1+3NFkB-SEAP	A068 #312	This thesis
Dual luciferase constructs		
pSL1180+psiCHECK	A069 #5	Chair of Livestock Biotechnology, TUM, GER
pSL1180+psiCHECK-CAG	A072 #60	This thesis
pSL1180+psiCHECK-ELAM	A073 #8	This thesis
pSL1180+psiCHECK-hCCL2-dis/prox	A074 #18	This thesis
pSL1180+psiCHECK-pA20+3NFkB	A076 #3	This thesis
pSL1180+psiCHECK-pA20+10NFkB+4SP1 +3NFKB	A077 #5	This thesis
pSL1180+psiCHECK-CAG-Hygro	A080 #28	This thesis
pSL1180+psiCHECK-ELAM-Hygro	A081 #6	This thesis
pSL1180+psiCHECK-hCCL2-dis/prox-Hygro	A082 #3	This thesis
pSL1180+psiCHECK-pA20-Hygro	A083 #30g	This thesis
pSL1180+psiCHECK-pA20+3NFkB-Hygro	A084 #18	This thesis
pSL1180+psiCHECK-pA20+10NFkB+4SP1 +3NFKB-Hygro	A085 #9	This thesis

Gene targeting constructs		
ROSA26-SA-BS-LA	A118	Chair of Livestock Biotechnology, TUM, GER
ROSA26-BS-pA20multi-LEA29Y	A133 #43	This thesis
ROSA26-BS-pA20multi-LEA29Y-ELAM--PDL1-MIN	A166 #4	This thesis
CRISPR/Cas9 constructs and subclones		
px330-MCS-T2A-Puro-847	A141	Chair of Livestock Biotechnology, TUM, GER
pSL1180-U6-MCS-tracRNA-756	A142	Chair of Livestock Biotechnology, TUM, GER
px330-CMAH-E9-T1-Puro	A143 #1	This thesis
px330-CMAH-E7-T1-Puro	A144 #3	This thesis
px330-GGTA1-E8-T3-Puro	A145 #1	This thesis
px330-GGTA1-E8-T4-Puro	A146 #2	This thesis
px330-ASGR1-E1-T1-Puro	A147 #1	This thesis
px330-ASGR1-E4-T1-Puro	A148 #2	This thesis
px330-GHR-E10-T1-Puro	A149 #2	This thesis
px330-GHR-E14-T1-Puro	A150 #1	This thesis
pSL1180-U6-CMAH-E9-T1-Puro	A153 #1	This thesis
pSL1180-U6-GGTA1-E8-T3-Puro	A155 #1	This thesis
pSL1180-U6-ASGR1-E1-T1-Puro	A157 #1	This thesis
pSL1180-U6-ASGR1-E4-T1-Puro	A158	This thesis
px330-ULBP1-E1-T1-Puro	A167	Katharina Rinke (Bachelor's student)
px330-ULBP1-E1-T2-Puro	A168	Katharina Rinke (Bachelor's student)
px330-ULBP1-E2-T3-Puro	A169	Katharina Rinke (Bachelor's student)
px330-ULBP1-E2-T4-Puro	A170	Katharina Rinke (Bachelor's student)
pSL1180-ULBP1-E1-T2-Puro	A171 #2	Katharina Rinke (Bachelor's student)
pSL1180-ULBP1-E2-T4-Puro	A172 #5	Katharina Rinke (Bachelor's student)
pSL1180-B4GAL2NT2-E2-T3-Puro	A173 #1	Katharina Rinke (Bachelor's student)
px330-U6-MCS-tracRNA-705	A174	Chair of Livestock Biotechnology, TUM, GER
px330-GGTA1E8T3	A175 #1	Katharina Rinke (Bachelor's student)
px330-B2ME1F1	A176#3	Katharina Rinke

		(Bachelor's student)
px330-GGTA1E8T3-CMAHE9T1	A177#8	Katharina Rinke (Bachelor's student)
px330-B2ME1F1-ULBP1E1T2	A178 #7	Katharina Rinke (Bachelor's student)
px330-GGTA1E8T3-CMAHE9T1-ASGR1E1T1	A179 #10	Katharina Rinke (Bachelor's student)
px330-B2ME1F1-ULBP1E1T2-ULBP1E2T4	A180 #3	Katharina Rinke (Bachelor's student)
px330-B4GALNT2E3T3-CMAHE10T2-GGTA1E7T6-MHCIE4T1-MHCIE4T2-Puro	A190	Chair of Livestock Biotechnology, TUM, GER
px330-GGTA1E8T3-CMAHE9T1-ASGR1E1T1-ASGR1E4T1	A191 #3/#6	Katharina Rinke (Bachelor's student)
px330-B2ME1T1-ULBP1E1T2-ULBP1E2T4-B4GALNT2E2T3	A192 #2/#10	Katharina Rinke (Bachelor's student)
Miscellaneous		
pL452	A015	Chair of Livestock Biotechnology, TUM, GER
pJET1.2/blunt	A026	Thermo Fisher Scientific, Waltham, USA
px330-Cas9-MSC-Puro-Hygro-PERV1/2_BEA	A078	Chair of Livestock Biotechnology, TUM, GER
Vector-CAG-LEA29Y	A117	Nikolai Klymiuk, Chair for Molecular Animal Breeding and Biotechnology, LMU, GER
pJET1.2-LEA29Y	A120 #1	This thesis
pJET1.2-LEA29Y-bGHpA	A131 #23	This thesis
pJET1.2-pA20multi-LEA29Y-bGHpA	A132 #20	This thesis
pcDNA-ELAM-PDL1-BGHpA-MIN	A164	Gene synthesis by General Biosystems, Durham, USA

5.9 Oligonucleotides

Table 13 – Primers for PCR, RT-PCR and ddPCR

Primers were designed using Primer3web and synthesized by Eurofins Genomics (Ebersberg, GER).

Name	Sequence, 5‘→ 3‘
Screening, dual-luciferase clones	
ddpoGAPDH F1	CTCAACGACCACTTCGTCAA
ddpoGAPDH R1	CCCTGTTGCTGTAGCCAAAT

F.GAPDH S.scrofa	TTCCACGGCACAGTCAAGGC
hluc+ F1	CCGAGGCCATGAAGAGGTAC
hluc+fire F5	GGCATTCCGGTACTGTTGGTA
hluc+fire R5	CCGCCCCGACTCTAGAATTA
Hygro F3	CAGCTTCGATGTAGGAGGGC
Hygro R3	TCTTGCAACGTGACACCCTG
R.GAPDH S.scrofa	GCAGGTCAGGTCCACAAC
Promoter generation & optimisation	
hCCL2 NEB F2	GGCGTTTTGCGCTGCTTCG ATTTTCCCCATAG CCCCTCTG
hCCL2 NEB R2	AGTATAGAAGCTAAACGCTAGATCTAGC GCG AGAGTGCGAGCTTCA
hCCL2 prom F5	CCTGGAAATCCACAGGATG
hCCL2 prom F8	ATTTTCCCCATAGCCCCTCTG
hCCL2 prom R4	GCGGCAGAGACTTTCATG
hCCL2 prom R6	CTGTCTGCCTCCCACTTCTG
hCCL2 prom R7	GCGAGAGTGCGAGCTTCA
hCCL2 prom XbaI	TCTAGACCTGGAAATCCACAGGATG
hCCL2F5s NEB F1	GGCGTTTTGCGCTGCTTCGCCCTGGAAATCCA CAGGATG
hCCL2F5s NEB R1	TGCAGGGCCCCAGAACCATGGCTGGAGGCGAGA GTGCGAGCT
hTNFAIP1 NEB F1	GGCGTTTTGCGCTGCTTCGGGACAGCCGGTA CCCAGCCAG
hTNFAIP1 NEB R1	AGTATAGAAGCTAAACGCTACCCCTCAGCAGT CCCAAG
hTNFAIP1 prom F1	GACAGCCGGTACCCAGCCAG
hTNFAIP1 prom R1	CCCCTCAGCAGTCCCAAG
hVCAM1 F1	GGGCTATGTGTGTGCAAGGC
hVCAM1 R1	AGTTGCTGTCGTGATGAGAA
pA20 prom 1F	ACAGTGAGGCCAGCGTGGTA
pA20 prom 1R	TCCTAGTTTGCAGCGCTTGG
pA20 prom F4	CTGTCCGCGGGCGGTAAAAC
pA20 prom F4	CTGTCCGCGGGCGGTAAAAC
pA20 prom F5	CCCCTACAAGCACATCACGT
pA20 prom F7	ACTGGAAAGTCCCTGGGTGGAAATCCCCTGG
pA20 prom R2	TGAGTCACCTGGGCATTTCG
SEAP R3	TCCTCAACTGGGATGATGCC
SEAP R3	TCCTCAACTGGGATGATGCC
Generation of dual-luciferase constructs	
ELAM NEB F1	ATTAATATTCCGGAGTATACCGATCGCTGAAT TCTGGGGACTT

ELAM NEB R1	GGAAGCCATGGTGGCTAGCTGGCTCTGTCTC AGGTCAGTA
hCCL2 NEB F3	ATTAATATTCCGGAGTATACATTTTCCCCATAG CCCCTCTG
hCCL2 NEB R3	GGAAGCCATGGTGGCTAGCTGCGAGAGTGC GAGCTTCA
Hygro psi NEB R1	AGGCCTAGGATGCATATGGCGACCGAAATCG GCAAAATCC
Hygro psi NEB XhoI F1	ACGGCCAGTGCCAAGCTTAA*CTCGAGAA*CGG GCTATTCTTTTGATGTGTCA
pA20 NEB F1	ATTAATATTCCGGAGTATACACAGTGAGGCCA GCGTGGTA
pA20 NEB R1	GGAAGCCATGGTGGCTAGCTTTCCTAGTTTGC AGCGCTTGG
pX-Hygro-NEB-R1	AGGCCTAGGATGCATATGGCGACCGAAATCG GCAAAA
pX-Hygro-NEB-XhoI F1	ACGGCCAGTGCCAAGCTTAACTCGAGAACGG GCTATTCTTTTGATTGTGTGTCA
Generation of targeting vectors	
bGHpA NEB F2	TCTCCGGGTAAATGACCAATTCAGCCTCGACT GTGCCTTC
bGHpA NEB R4	ATTGCCAAGAAAACCCACGCCCTAGGAGCTG GTTCTTTCCGCCTCA
pA20 NEB F4	AATTGTCCCAATTAGTAGCATCACGACCGGTA CAGTGAGGCCAGCGTGGTA
pA20 NEB R4	CGAGCCATCCGGAAGATCTGTCCTAGTTTGCA GCGCTTGG
NEB_LEA_F1	GGCGGCCAAGCGCTGCAAACTAGGATCAGCA AGATAGCTTCACCCC
Lea hEx2 R1	ATCATGTAGGTTGCCGCACA
Screening & sequencing, gene targeting	
BS R neu	CGGCTGTCCATCACTGTCCT
hPDL1 E2-E3 F1	GGCATTTGCTGAACGCATTT
hPDL1 F1	GACCACCACCACCAATTCCA
hPDL1 R1	GGTCTTCCTCTCCATGCACA
LEA expr 1F	GGATGAGCTGACCAAGAACC
LEA Expr 1F	GGATGAGCTGACCAAGAACC
LEA expr 3R	CGGCTTTGTCTTGGCATTA
pA20 prom F8	GACCCAACAATGCTGCCATC
pA20 prom R8	TTACTGTCCTTGCCACGTCC
pSL1180 R1	CGGGCCTCTTCGCTATTACG
ROSA26 I1 F2	TATGGGCGGGATTCTTTTGC

ROSA26 I3 R2	CAGGTGGAAAGCTACCCTAGCC
ROSA26 LA F3	TTGGCTGTGCTGCTAATGTG
ROSA26 LA r43 red	GTCCTGGCAGTTTTACCCACG
ROSA26 SA F7	GGTGTTTGTGAAACTACCCCTGAA
SV40 polyA F	TTGGGCTTCGGAATCGTTTT
Screening & sequencing, knockout generation	
ASGR1 E2 F1	GCACCCTAATTCTCCAGCCTT
ASGR1 E3 F1	CCTGCCTCCTCCTGATTTCC
ASGR1 E6 R1	CGGACACAAACTGCTTCACG
ASGR1 Ex4 R1	TCCTGCAGCTTGGAGTCTGG
ASGR1 I2 F2	ACAAGAGGAGGCCCAGGATG
ASGR1 I2 R1	TTCTTCCGCTTACTCCCACG
B4G I1 F1	ACCAGACATCGTTCCCAGTG
B4G I2 R1	AACTGGCTGTAAAGTGGGCA
B4Gal Scr I2 F1	CCCTCACCTACCAGCCCACT
B4Gal Scr I3 R1	AGCTTCCGCTCCATCTCAGG
CMAH E8 R1	TGAACGCCATCCATCAAGATCA
CMAH I6 F1	GACGGAATTTGCACACCTGG
CMAH I8 F1	AGTGTCCTCATTCAGAACCCAC
CMAH I9 R	CTCAGGCTGCCCACACTCTG
CMAH Scr E10 F2	TGCCGTAAACAAAGAGGGGATT
CMAH Scr E10 R2	TTGTCTGCTGGGTGGGATTC
Gal I7 F1	TCTGGATGTGGGAGCAGGGC
Gal Scr E7 T56 F	GCCAGTCACCACAAGCCATG
Gal Scr E7 T56 R	TGGCCCTGTGACACCATTCT
Gal Scr E8 T3 R	GGCTTTCATCATGCCACTCG
GGTA1 E11 F1	AGAGGTGGCAAGACATCAGC
GHR I10 R1	CACTCCCGGAAACATCCTCC
GHR I13 F1	CCCCATTTCAGGAGCACTCA
GHR I14 R1	GTCCCTTGTAGCAGCACACA
GHR I8 F1	TTCCTGAGACAAGCACCCAC
MHCI Antigen F1	CCAGTGGTCACATGAGGCTGC
MHCI Antigen R1	GCGCCCTCCTTACCCCATCT
pB2M Scr 5'UTR F1	CCACCCAGTCCAACCTTTGCC
pB2M Scr I1 R1	CCAGAGTTAGCGCCCGGAGT
ULBP1 Ex1 F1	GCGCTGGGGAATCTGCAT
ULBP1 Ex2 F1	TTGCTATAACTTCATCATCATTCCAAA
ULBP1 I1 R1	GCCCCACCCAAGGAGAAGTT
ULBP1 I2 R1	CGAGGACCAGCACCCAATCT

Table 14 – ddPCR probes

Probes for ddPCR were designed using Primer3web and synthesized by Eurofins Genomics (Ebersberg, GER). They were equipped with a 5' fluorescence dye (HEX/FAM) and a 3' quencher (BHQ1).

Name	Sequence, 5'→ 3'
ddpoGAPDH	HEX-TGTGATCAAGTCTGGTGCCC-BHQ1
ddprobe Hygro 1	FAM-GCGCCGATGGTTTCTACAAA-BHQ1

Table 15 – Miscellaneous oligonucleotides

Name	Sequence, 5'→ 3'
sgRNA target site oligonucleotides	
PX-ASGR1-E1-T1 F	CACCGAGCCAGCCTTAGCATGACAA
PX-ASGR1-E1-T1 R	AAACTTGTCATGCTAAGGCTGGCTC
PX-ASGR1-E4-CRISP-T1 F	CACCGCCGCGAGCACAGACGCCA
PX-ASGR1-E4-CRISP-T1 R	AAACTGGCGTCTGTGCTCGCGGC
PX-pB2M-E1-F1	CACCGTAGCGATGGCTCCCCTCG
PX-pB2M-E1-R1	AAACCGAGGGGAGCCATCGCTAC
PX-B4GALNT2-E2-T3 F	CACCGTGTATCGAGGAACACGCTT
PX-B4GALNT2-E2-T3 R	AAACAAGCGTGTTCCTCGATACAC
PX-B4GALNT2-E3-T3 F	CACCGAGGAAAGCTATAACTTGG
PX-B4GALNT2-E3-T3 R	AAACCCAAGTTATAGCTTTCCTC
CMAH-E7-T1 F	CACCGACATTGATATTAGTCAAC
CMAH-E7-T1 R	AAACGTTGACTAATATCAATGC
CMAH-E9-T1 F	CACCGGATTGCACCAGACCCAA
CMAH-E9-T1 R	AAACTTGGGTCTGGTGCAATCC
PX-CMAH-E10-T2 F	CACCGAGAAACTCCTGAACTACA
PX-CMAH-E10-T2 R	AAACTGTAGTTCAGGAGTTTCTC
PX-GGTA1-E8-T3 F18	CACCGACGAGTTCACCTACGAG
PX-GGTA1-E8-T3 R18	AAACCTCGTAGGTGAACTCGTC
PX-GGTA1-E7-T6 F18	CACCGTCGTGACCATAACCAGA
PX-GGTA1-E7-T6 R18	AAACTCTGGTTATGGTCACGAC
PX -GGTA1-E8-T4 F	CACCGATGGTGGATGATATCTCC
PX -GGTA1-E8-T4 R	AAACGGAGATATCATCCACCATC
PX-GHR-E10-T1 F	CACCGTCCTACAGGTATGGATCTC
PX-GHR-E10-T1 R	AAACGAGATCCATACCTGTAGGAC
PX-GHR-E14-T1 F	CACCGTCAAAAGTGTTTCTCCGTTG
PX-GHR-E14-T1 R	AAACCAACGGAGAAACACTTTTGAC
PX330-ULBP1-E1-T1 F	CACCGTGGCTCCACGGCGGGTCT
PX330-ULBP1-E1-T1 R	AAACAGACCCGCCGTGGAGCCAC
PX330-ULBP1-E1-T2 F	CACCGCTCTCCGGTTATGCCCGG
PX330-ULBP1-E1-T2 R	AAACCCGGGCATAACCGGAGAGC
PX330-ULBP1-E2-T3 F	CACCGAAACACTCAAAGACGTT

PX330-ULBP1-E2-T3 R	AAACAACGTCTTTGAGTGTTTC
PX330-ULBP1-E2-T4 F	CACCGCTGAGAACTACACGGCCA
PX330-ULBP1-E2-T4 R	AAACTGGCCGTGTAGTTCTCAGC
PX-MHCI-E4-T1 F	CACCGCCAGGACCAGAGCCAGGACA
PX-MHCI-E4-T1 R	AAACTGTCCTGGCTCTGGTCCTGGC
PX-MHCI-E4 T2 F2	CACCGCCAGAAGTGGGCGGCCCTGG
PX-MHCI-E4 T2 R2	AAACCCAGGGCCGCCCACTTCTGGC
Promoter modification oligonucleotides	
2xNFkB XhoI F	TCGAGGGGGACTTTCCACTGGGGACTTTCCAC TC
2xNFkB XhoI R	TCGAGAGTGGAAAGTCCCCAGTGGAAAGTCC CCC
A20 3xNFkB F1	ACTGGAAAGTCCCTGGGTGGAAATCCCCTGC TCGAGGGGGACTTTCCACTGGGGACTTTCCAC TGGGGACTTTCCACTGGTACCCTGTCCGCGGG CGGTAAAAC
A20 3xNFkB F1	ACTGGAAAGTCCCTGGGTGGAAATCCCCTGC TCGAGGGGGACTTTCCACTGGGGACTTTCCAC TGGGGACTTTCCACTGGTACCCTGTCCGCGGG CGGTAAAAC
A20 3xNFkB R1	GTTTTACCGCCCGCGGACAGGGTACCAGTGG AAAGTCCCCAGTGGAAAGTCCCCAGTGGAAA GTCCCCCTCGAGCAGGGGATTTCCACCCAGG GACTTTCCAGT
A20 3xNFkB R1	GTTTTACCGCCCGCGGACAGGGTACCAGTGG AAAGTCCCCAGTGGAAAGTCCCCAGTGGAAA GTCCCCCTCGAGCAGGGGATTTCCACCCAGG GACTTTCCAGT
pA20 2xSP1 F	CGAAATGCCCAGGTGACTCACGCGGGGACAC CCCGGGGCGGGGCATATAGCTAGCCGGGGC GGGGCATATACGGGGCGGGGCGGCACGCGG CTCGCCTCCTGCGCCTCCTG
pA20 2xSP1 R	CAGGAGGCGCAGGAGGCGAGCCGCGTGCCG CCCCGCCCCGTATATGCCCCGCCCCGGCTAGC TATATGCCCCGCCCCGGGGTGTCCCCGCGTGA GTCACCTGGGCATTTCG
pA20 5xNFkB F1	AGCTTGGAAAGTCCCTGGGTGGAAATCCCCT GGCGGCCGCGGGGACTTTCCACTGGGGACTT TCCACTGGGGACTTTCCACTGGTACCA
pA20 5xNFkB R1	AGCTTGGTACCAGTGGAAAGTCCCCAGTGGA AAGTCCCCAGTGGAAAGTCCCCGCGGCCGCC AGGGGATTTCCACCCAGGGACTTTCCA

pA20 NheI Sp1 F	CTAGCCGGGGCGGGGCATATACGGGGCGGGGCG
pA20 NheI Sp1 R	CTAGCGCCCCGCCCCGTATATGCCCCGCCCCGG

5.10 Enzymes

Table 16 – Enzymes and buffers

Name	Manufacturer
ALLin 5x Buffer	highQu, Kraichtal, GER
ALLin HiFi DNA Polymerase	highQu, Kraichtal, GER
Calf Intestinal Alkaline Phosphatase	New England Biolabs, Frankfurt, GER
Cutsmart 10x Buffer	New England Biolabs, Frankfurt, GER
ddPCR Supermix for Probes (No dUTP)	Bio-Rad, Munich, GER
GoTaq 5x Green Reaction Buffer	Promega, Fitchburg, USA
GoTaq G2 DNA Polymerase	Promega, Fitchburg, USA
NEBuffer (2.1, 3.1), 10x	New England Biolabs, Frankfurt, GER
Q5 5x Reaction Buffer	New England Biolabs, Frankfurt, GER
Q5 High GC Enhancer	New England Biolabs, Frankfurt, GER
Q5 High-Fidelity Polymerase	New England Biolabs, Frankfurt, GER
Restriction enzymes	New England Biolabs, Frankfurt, GER
FastGene Scriptase II (200 U/µL)	Nippon Genetics Europe, Düren, GER
FastGene 5x RT buffer	Nippon Genetics Europe, Düren, GER
T4 DNA Ligase	New England Biolabs, Frankfurt, GER
T4 DNA Ligase 10x Reaction Buffer	New England Biolabs, Frankfurt, GER
T4 Polynucleotide Kinase	New England Biolabs, Frankfurt, GER
Proteinase K, 20 mg/mL	Bioline, London, GBR
RNAse A	Sigma, Osterode, GER

5.11 DNA size markers

Table 17 – DNA size markers

Name	Manufacturer
DNA ladder, 1 kb	New England Biolabs, Frankfurt, GER
DNA ladder, 100 bp	New England Biolabs, Frankfurt, GER
DNA ladder, 2-Log	New England Biolabs, Frankfurt, GER
DNA ladder, GeneRuler 1 kb Plus	Thermo Fisher Scientific, Waltham, USA

5.12 Computer software and webtools

Table 18 – Software and webtools

Name	Weblink/Manufacturer
Ascent Software, Version 2.6	Thermo Fisher Scientific, Waltham, USA
Basic Local Search Tool (BLAST)	https://blast.ncbi.nlm.nih.gov
Benchling	https://www.benchling.com
CRISPOR	http://crispor.tefor.net
EMBOSS Needle	https://www.ebi.ac.uk/Tools/psa/emboss_needle
Ensembl genome browser	https://www.ensembl.org
Glomax Sis, v1.10.0	Promega, Fitchburg, USA
Leica Application Suite X	Leica, Wetzlar, GER
Living Image 4.4	Caliper Life Sciences, Waltham, USA
MicroPoint, V. 2016-02-05	PreciPoint, Freising, GER
NCBI, Gene	https://www.ncbi.nlm.nih.gov/gene
Primer3	http://pimer3.ut.ee
QuantaSoft 1.7.4.0917	Bio-Rad, Munich, GER
QuantaSoft Analysis Pro 1.0.596	Bio-Rad, Munich, GER
Quantum ST5	Vilber Lourmat, Eberhardzell, GER
TIDE	https://tide.deskgen.com
Universal Protein Resource (UniProt)	https://www.uniprot.org
ViewPoint Online	PreciPoint, Freising, GER

6. METHODS

6.1 Cell culture methods

6.1.1 Cultivation and subcultivation of porcine cells

Mammalian cells were cultivated in antibiotic-free medium (DMEM, 10-20% FCS, 1 mM sodium pyruvate, 1x NEAA, 2 mM Ala/Glu) at 37°C in a CO_2 enriched (5%), humidified atmosphere and medium was exchanged every 2-3 days. All work with open cell culture vessels was performed within a laminar airflow cabinet using autoclaved material. Non-sterile solvents and solutions were filter sterilized (0.22 µm pore size).

Subcultivation was performed at a confluence level of about 80%. For this purpose, medium was aspirated, cells were washed with PBS and incubated with Accutase solution for 5-15 min at 37°C. Dissociation reaction was terminated by dilution with culture medium and cells were transferred to new culture vessels.

6.1.2 Cryoconservation and thawing of porcine cells

For long-term cryostorage, cells were dissociated using Accutase solution, centrifuged at 300x g for 5 min and resuspended in 1 mL cryopreservation medium (70% FCS, 20% DMEM, 10% DMSO). Cells were transferred to a cryo vial and cooled down to -80°C at 1°C/min using a Mr. Frosty freezing container placed inside a -80°C freezer. After two hours, the vials were removed from the container and either stored in liquid nitrogen or at -80°C.

For re-cultivation, cryopreserved cells were thawed at 37°C, mixed with 5 mL medium and centrifuged at 300x g for 5 min. Cells were resuspended in culture medium and transferred to a new culture vessel.

6.1.3 Determination of cell number

Single cell suspension was mixed with Trypan blue solution in a ratio of 1:2 and 10 µL of stained cells was applied to a disposable Neubauer counting chamber. The cell numbers of four squares were counted and cell concentration was calculated as follows:

$$cell\ concentration = 2 * (average\ cell\ number\ per\ square) *\ 10^4/mL$$

6.1.4 Transfection of genetic constructs

Cells were transfected using Lipofectamine 3000 (for pX330-based vectors) and Lipofectamine 2000 (for all other constructs) at 25-60% confluence according to the manufacturer's instructions. Transfection of pX330 vectors was carried out in 6-wells using 1 µg DNA per well. For transfecting reporter and targeting constructs, 4 and 10 µg linearized DNA were used per 10 cm dish, respectively.

6.1.5 Magnetic cell separation

Cells with functional *GGTA1* knockout and SLA class I inactivation were selected by magnetic cell separation for further use in SCNT. $3x10^6$ cells were resuspended in 600 µL TL HEPES Ca^{2+} 296+ buffer, labelled with 50 µg biotin-conjugated isolectin B4 by incubating for 15 min on ice, and washed twice with PBS. Streptavidin-conjugated magnetic beads (600 µL) were purified according to the manufacturer's instructions, mixed with the cells and incubated for 30 min on ice. After adding 5 mL PBS, the magnet was applied for 2 min to separate bead-bound cells. Cells with functional *GGTA1* knockout remained in suspension and were re-cultivated. A second round of magnetic cell separation was performed using 5 µg biotin-conjugated anti-MHC I monoclonal antibody to additionally select for SLA class I negative cells.

6.1.6 Antibiotic selection of transfected cells

Cells were treated with culture medium supplemented with selection antibiotic 24 to 48 hours after transfection. The type and duration of antibiotic selection was based on the transfected construct and the cell type used (see Table 19).

Table 19 – Type and duration of antibiotic selection of mammalian cells

Mammalian cells	Antibiotic	Concentration, µg/mL	Selection time, d
PK-15	Hygromycin B	1200-1600	6-9
pKDNF	Hygromycin B	600	6-9
	Blasticidin S	12	7-11
	Puromycin	1.5	2
ST	Hygromycin B	600	7

6.1.7 Cell clone generation

After antibiotic selection, single cell colonies with a size of 1-4 mm were either isolated directly from the 10 cm dish or after seeding onto 15 cm dishes (PK-15: 50 cells/dish; pKDNF: 1000 cells/dish; ST: 200-400 cells/dish). Clones were picked after washing with PBS: cloning cylinders (diameter: ~ 6.5 mm) were dipped into sterile silicone grease and placed around the single cell colony. The cells were detached filling the cylinder with 200 µL Accutase solution and incubating 5-15 min. The reaction was stopped by adding culture medium and cell clones were transferred into a 12/24-well plate.

6.1.8 *In vitro* promoter induction by human and murine cytokines

Different culture formats, cell numbers and cytokine concentrations were used for *in vitro* promoter induction depending on the type of experiment (see Table 20). Cells were seeded in triplicates in a defined volume of medium followed by cytokine addition after 0.5-3 h. Untreated cells served as control (ctrl). Collection of cell culture supernatants for SEAP reporter assays or cell lysis for Dual Luciferase assays was conducted 3-72 h after cytokine treatment. Supernatants and lysates were stored up to 14 days at -20°C.

Table 20 – Cell numbers, medium volumes, cytokine concentrations and time of supernatant collection selected for individual promoter induction experiments

Experiment, chapter	Cell number	Medium volume	Cytokine concentration, ng/mL	Time of supernatant collection
Basic evaluation of cytokine-inducibility, 7.1.1.3	$4.0x10^5$ per 6 well	2 mL	hTNF: 30, 10, 1, 0.1 hIL-1β: 50, 5 2.5, 0.5, 0.05 hIFNγ: 10, 1, 0.1, 0.01	72 h
Determining initiation of promoter induction, 7.1.1.4	$1.0x10^5$ per 12 well	0.8 mL	hTNF: 10	3, 4, 5, 6, 8, 24, 48, 72 h
Analysis of PK-15 responsiveness to murine and human cytokines, 7.1.2.1.1	$0.33x10^5$ per 24 well	0.4 mL	hTNF: 30 mTNF: 90 hIL-1β: 62.5 mIL-1β: 150	72 h
Induction of PK-15 clones used for *in vivo* studies, 7.1.2.1.2	$2.1x10^6$ per T25	4 mL	hTNF: 30	24 h

6.2 Microbiological methods

6.2.1 Cultivation of *E. coli*

Bacterial cells were cultivated over night at 37°C, either on LB (lysogeny broth) agar plates or in liquid LB medium while shaking at 250 rpm. Medium was supplemented with 100 µg Ampicillin (Amp) per mL for selection of Amp^R positive bacteria.

6.2.2 Transformation of electro- and chemical competent *E. coli*

Competent *E. coli* were either transformed by electroporation or heat shock. After transformation, 50-100 µL bacteria suspension was plated on LB agar plates (Amp^{100}) incubated at 37°C over night.

6.2.2.1 Transformation by electroporation

To transform electrocompetent *E. coli* (strain DH10b), 50 µL bacteria suspension was incubated with 50-300 ng DNA for 2 min on ice and transferred to pre-cooled electroporation cuvettes (electrode distance: 2 mm). Electroporation was carried out by applying an electric impulse of 2500 V for 5 ms. Cell suspension was added to 500 µL LB media, incubated for 30 min at 37°C and 250 rpm and plated as described above.

6.2.2.2 Transformation by heat shock

Heat shock transformation of chemically-competent *E. coli* (NEB 5-alpha competent *E. coli*, High Efficiency) was carried out according to the manufacturer's instructions.

6.2.3 Cryoconservation of *E. coli*

Glycerol stocks of bacterial clones were generated by mixing 1000 µL of an overnight culture with 500 µL sterile glycerol and stored at -80°C. For re-cultivation, the glycerol stock was thawn on ice and 100 µL was used to inoculate liquid LB medium.

6.3 Molecular biological methods

6.3.1 Isolation of nucleic acids from mammalian cells

6.3.1.1 Genomic DNA isolation using QuickExtract DNA Extraction Solution

Cells of a confluent 12 well were harvested and resuspended in 30 µL QuickExtract DNA Extraction Solution to screen for positive targeting events. Cells were lysed by incubating for 15 min at 65°C and 8 min at 95°C. DNA was stored at -20°C.

6.3.1.2 Genomic DNA isolation by phenol chloroform isoamyl alcohol extraction

Phenol chloroform isoamyl alcohol extraction was conducted when large quantities of high purity DNA were required. Cells of a confluent T150 flask were resuspended in 1000 µL Lysis

Buffer and 60 µL proteinase K (20 µg/µL) added. After incubating for 2 h at 37°C, RNA was degraded by adding 2 µL RNAse A solution (20 µg/µL) and incubating for 5 min at RT. The lysate was mixed with an equal volume of phenol chloroform isoamyl alcohol (25:24:1), vortexed and incubated for 10 min at RT. After centrifugation for 15 min at 12,000xg, the aqueous phase was mixed a second time with an equal volume of phenol chloroform isoamyl alcohol. Centrifugation for 10 min at 12,000xg was followed by adding 0.1 volume of sodium acetate (5 M) and 1 volume isopropanol to the aqueous phase and mixing by inverting. After centrifugation for 5 min at 12,000xg, the DNA pellet was washed wit 500 µL EtOH (70%) and centrifuged a second time. This step was repeated once, the EtOH removed and the pellet dried at room temperature. The DNA was resuspended in 50 µL TE buffer and stored at -20°C.

6.3.1.3 Isolation of genomic DNA and total RNA using SurePrep RNA/DNA/Protein Purification Kit

To isolate small amounts of high purity gDNA and total RNA from mammalian cells, the SurePrep RNA/DNA/Protein Purification Kit was used according to the manufacturer's instructions.

6.3.2 Reverse transcription of RNA

For gene expression analysis at transcript level, RNA isolated from mammalian cells was transcribed using FastGene Scriptase II. Synthesis of cDNA was conducted following the manufacturer's instructions using 20-500 ng total RNA and random hexamer primers.

6.3.3 Polymerase chain reaction (PCR)

The Polymerase chain reaction (PCR) was used to screen bacterial and eukaryotic cell clones, amplify DNA sections for further cloning and to detect cDNA for gene expression analysis. Different DNA polymerases were used depending on the purpose following the manufacturer's instructions. ALLin HiFi DNA Polymerase was used to detect positive *ROSA26* targeting events in transfected cell clones. Q5 High-Fidelity DNA Polymerase was used to amplify GC-rich regions and DNA sequences with repetitive elements. GoTaq G2 DNA

Polymerase was used for all other PCR reaction. Table 21 summarizes the standard PCR reaction mixtures and thermal cycling conditions for each polymerase.

Table 21 – Reaction mixtures and thermal cycling conditions for GoTaq G2 DNA Polymerase, Q5 High-Fidelity DNA Polymerase and ALLin HiFi DNA Polymerase

Reaction mixture		**Thermal cycling conditions**			
Component	**Final concentration**	**Step**	**Temper-ature**	**Time**	**Cycles**
GoTaq G2 DNA Polymerase					
Template:					
* plasmid DNA	200-500 ng	Initial Denaturation	95°C	2 min	1
* gDNA	200 ng				
* cDNA	2 µL	Denaturation	95°C	40 sec	
dNTPs	200 µM each	Annealing	58-62°C	40 sec	30-40
Forward primer	0.5 µM	Extension	72°C	1 min/kb	
Reverse primer	0.5 µM	Final Extension	72°C	5 min	1
5x Green GoTaq Reaction Buffer	1x	Storage	8°C	Infinite	1
Polymerase	1.25 U				
H_2O, cell culture grade	to 50 µL				
Q5 High-Fidelity DNA Polymerase					
Template	200-500 ng				
dNTPs	200 µM each	Initial Denaturation	98°C	30 sec	1
Forward primer	0.5 µM				
Reverse primer	0.5 µM	Denaturation	98°C	10 sec	
5x Q5 Reaction Buffer	1x	Annealing	58-62°C	30 sec	30
5x Q5 High GC Enhancer	1x	Extension	72°C	30 sec/kb	
Q5 High-Fidelity DNA Polymerase	1.0 U	Final Extension	72°C	2 min	1
H_2O, cell culture grade	to 50.0 µL	Storage	8°C	Infinite	1
ALLin HiFi DNA Polymerase					
Template	350 ng				
		Initial Denaturation	95°C	1 min	1
Forward primer	0.4 µM				
Reverse primer	0.4 µM	Denaturation	95°C	15 sec	
5x ALLin HiFi Buffer	1x	Annealing	60°C	15 sec	35
ALLinPolymerase	0.5 U	Extension	72°C	30 sec/kb	
H_2O, cell culture grade	to 50.0 µL	Storage	8°C	Infinite	1

6.3.4 Droplet digital PCR

Droplet digital PCR (ddPCR) was used to determine the absolute copy numbers of transgenes present in a certain cell clone. High purity gDNA was fragmented by restriction digest to enable optimal accuracy by separating tandem gene copies. Prior to droplet generation with the QX200 Droplet Generator, 20 µL reaction mixture (Table 22) and 70 µL droplet generation oil for probes were loaded into the corresponding wells of the DGX8 cartridge. The droplets were transferred into a 96-well plate and PCR reactions conducted as described in Table 22. Data were subsequently acquired and analysed using the QX200 droplet reader and the application QuantaSoft.

Table 22 – Reaction mixture and cycling conditions for ddPCR

Reaction mixture		**Cycling conditions**			
Component	**Final concentration**	**Step**	**Temper-ature[#]**	**Time**	**Cycles**
gDNA, fragmented	9-100 ng				
GOI specific:					
* forward primer	900 nM	Enzyme activation	95°C	10 min	1
* reverse primer	900 nM				
* probe (HEX)	250 nM	Denaturation	94°C	30 sec	
Reference gene-specific:		Annealing/ extension	58°C	1 min	40
* forward primer	900 nM				
* reverse primer	900 nM	Enzyme deactivation	98°C	10 min	1
* probe (FAM)	250 nM				
2x ddPCR Supermix for Probes (No dUTP)	1x	Store	4°C	Infinite	1
H_2O, nuclease free	to 20.0 µL	*[#]Ramp rate: 2°C/sec*			

6.3.5 Restriction digestion

Preparative restriction digestions were performed to enable cloning of DNA fragments into vectors, to linearize targeting and reporter constructs for stable transfection and to fragment genomic DNA for ddPCR. Analytical digestions were conducted to verify correct vector sizes. The reaction mixture (Table 23) was incubated for 2 h at 37°C and either frozen at -20°C or used immediately for agarose gel electrophoresis.

Table 23 – Reaction mixture for preparative and analytical restriction digestions

Component	Final concentration
DNA:	
* preparative digestion (vector)	5-10 µg
* preparative digestion (gDNA)	0.2-2 µg
* analytical digestion	2 µg
10x NEB Buffer	1x
Restriction enzyme	3 U per µg DNA
H_2O, cell culture grade	to 50.0 µL

6.3.6 Removing single-stranded overhangs

Single-stranded overhangs of restriction fragments were removed using DNA polymerase I (Klenow Fragment) to enable ligation into blunt-end vector backbones. 1.5 µL dNTPs (2 mM each) and DNA polymerase I (1 U / µg DNA) were added to 50 µL restriction mixture and incubated at 25°C for 15 min. The enzyme was heat inactivated by incubation at 75°C for 20 min.

6.3.7 Dephosphorylation of 5'-ends of DNA

Enzymatical dephosphorylation of 5'-ends was performed prior to DNA ligation to prevent religation of linearized vector backbones. 2 µL calf intestine phosphatase (CIP) was added to 50 µL restriction mixture and incubated at 37 °C for 30 min. DNA was stored at -20 °C until purification.

6.3.8 Assembly of complementary single-stranded oligonucleotides

Complementary oligonucleotides were annealed for subsequent cloning by dissolving 1 µg of each oligonucleotide in 100 µL TE buffer, heating to 100°C and slowly cooling to room temperature (10°C per 30 sec).

6.3.9 Phosphorylation of double-stranded oligonucleotides

Phosphorylation of double-stranded oligonucleotides was performed to increase ligation efficiency and to enable multiple-integration for promoter optimization. The reaction mixture (Table 24) was incubated for 30 min at 37°C followed by enzyme inactivation for 20 min at 65°C.

Table 24 – Reaction mixture for phosphorylating double-stranded oligonucleotides

Component	Final concentration
Double-stranded oligonucleotides	44.0 pmol
10x T4 Ligase Buffer	1x
T4 Polynucleotide Kinase	100 U
H_2O, cell culture grade	to 50.0 µL

6.3.10 Ligation of DNA fragments and alternative DNA assembly

6.3.10.1 Ligation using T4 DNA ligase

Conventional cloning of digested DNA fragments and double-stranded oligonucleotides into linearized vectors was performed using T4 DNA ligase. The amount of insert DNA was chosen according to the molar vector:insert ratios of 1:3 to 1:10. The ligation mixture (Table 25) was incubated at 25°C for 2 h and at 4°C overnight.

Table 25 – Reaction mixture for ligation using T4 DNA ligase

* The amount of insert DNA was chosen according to molar vector:insert ratios of 1:3 to 1:10.

Component	Final concentration
Vector DNA	50-100 ng
Insert DNA	variable*
10x T4 DNA Ligase Bufffer	1x
T4 DNA Ligase	400 U
H_2O, cell culture grade	to 10.0 µL

6.3.10.2 DNA assembly using NEBuilder HiFi DNA Assembly Cloning Kit

The NEBuilder HiFi DNA Assembly Cloning Kit was used as an alternative strategy for DNA assembly. The reaction was performed according to the manufacturer's instructions.

6.3.11 Purification of DNA fragments

DNA was purified from gel slices, PCR- and restriction mixtures using the Wizard SV Gel and PCR Clean-Up System following the manufacturer's recommendations.

6.3.12 Sanger sequencing

Sequencing of selected DNA fragments was conducted using the Mix2Seq service by Eurofins Genetics. The samples were prepared as recommended by the company.

6.3.13 Agarose gel electrophoresis

Agarose gel electrophoresis was conducted to separate DNA fragments by size. Gels were prepared by boiling the appropriate buffer with 0.8-2.0% (w/v) agarose, adding 4 µL pegGREEN staining solution per 100 mL liquid gel and pouring into the gel tray. For preparative purposes 1x TBE buffer was used, whereas analytical gels were prepared with 1x TAE buffer. PCR reactions performed in GoTaq 5x Green Reaction Buffer were loaded directly into the gel, all other samples were pre-mixed with 6x Gel Loading Dye. 4 µL of a DNA size marker was loaded in a separate well for fragment length determination. After running the gel for 1-3 h at 80-120 V, DNA fragments were visualized under UV light and documented using the Quantum ST5 gel documentation imaging chamber.

6.3.14 Preparation of plasmid DNA

Plasmid DNA was prepared from 100 mL overnight bacterial cultures using the NucleoBond Xtra Midi kit according to the manufacturer's instructions. DNA was resuspended in 100 µL TE buffer and stored at -20°C.

6.3.15 Determining the concentration of nucleic acids

The concentrations of nucleic acids were determined using NanoDrop lite spectrophotometer measuring the absorption at 230 nm for RNA and 260 nm for DNA, respectively.

6.3.16 SEAP reporter assay

The activity of secreted embryonic alkaline phosphatase (SEAP) in cell culture supernatants (see chapter 6.1.8) was determined using the SEAP Reporter Assay Kit according to the manufacturer's instructions. The optical density at λ=405 nm was measured for 120 min at 15 min intervals using a Multiskan Ex ELISA reader.

Relative activity of a promoter x was defined as

$$Relative\ promoter\ activity\ (x) = \frac{OD_{405nm}(x)}{OD_{405nm}(CAG, ctrl)} * 100\%$$

and mean values of triplicate measurements of the control and the studied group were compared using T test and R script (The R project for statistical computing, version 3.2.1). The degree of promoter upregulation ('induction factor') was calculated as follows:

$$Induction\ factor\ (x) = \frac{relative\ promoter\ activity\ (x, test)}{relative\ promoter\ activity\ (x, ctrl)}$$

6.3.17 Dual-luciferase reporter assay

The Firefly & Renilla Single Tube Luciferase Assay Kit was used for *in vitro* analysis of transfected cell clones to be used for *in vivo* promoter evaluation in mice. Cells were harvested by centrifugation (300x g, 5 min) and lysed by resuspension and incubation in Passive Lysis Buffer for 10 min at RT. The assay was conducted following the company's instructions, whereas the lysate of $1.5x10^5$ cells was utilized per sample. Standardized precise timing was important to enable comparison of data between experiments, so substrate addition and luminescence measurement (Glomax 20/20 luminometer) were performed according to the scheme shown in Figure 7.

The degree of promoter x upregulation ('induction factor') was calculated as followed:

$$Induction\ factor\ (x) = \frac{\frac{RLU_{Rluc}\ (x, test)}{RLU_{Fluc}\ (x, test)}}{\frac{RLU_{Rluc}\ (x, ctrl)}{RLU_{Fluc}\ (x, ctrl)}}$$

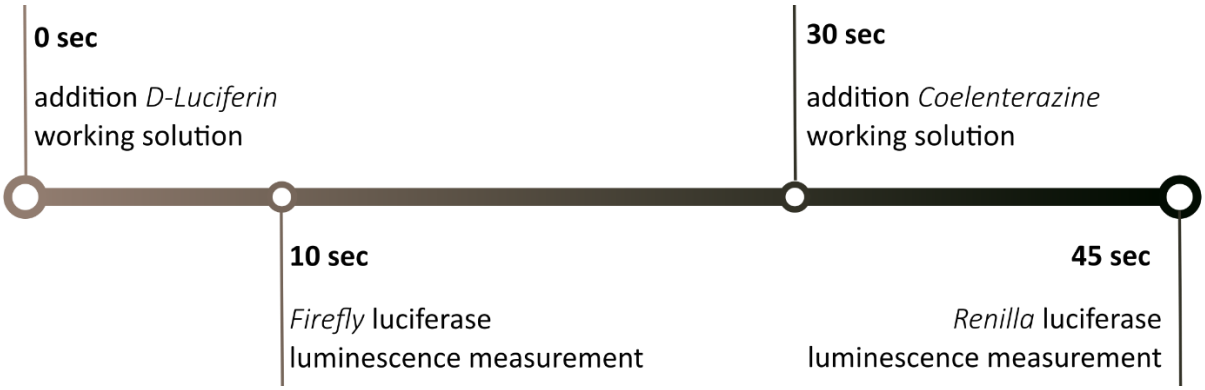

Figure 7 – Timeline for substrate addition and luminescence measurement
D-Luciferin was added to the sample at timepoint *0 sec* and *Firefly* luciferase (Fluc) induced luminescence measured 10 sec later. At timepoint *30 sec* Coelenterazine solution was added, thereby quenching Fluc activity. Luminescence produced by Rluc was measured at timepoint *45 sec*.

6.3.18 Design and evaluation of sgRNA target recognition sites

6.3.18.1 In silico design of sgRNA target recognition sites

For CRISPR/Cas9-induced gene editing, suitable sgRNA target recognition sites were determined *in silico* using the CRISPOR webtool (http://crispor.tefor.net). This application identifies 20-bp target recognition sites for Sp-Cas9 within a selected genomic sequence, evaluates off-target probability and guide specificity and scores the predicted cleavage efficiency at this position.

6.3.18.2 Quantitative assessment of CRISPR/Cas9-mediated genome editing

The frequency of CRISPR/Cas9-mediated insertions and deletions (InDels) in pools of transfected cells was evaluated using the TIDE web tool. Default parameters for analysis were applied as summarized in Table 26.

Table 26 – Parameter settings for CRISPR/Cas9-mediated InDel analysis using TIDE

Parameters	Setting
Alignment window:	
* left boundary	1-100 bp
* right boundary	Set at 'breaksite minus 10 bp'
Decomposition window	Maximum
Indel size range	2-10
P-value threshold	0.001

6.4 Animal experiments and histological methods

6.4.1 Transplantation of porcine cells into immune-deficient mice and splenocyte transfer

For *in vivo* promoter evaluation, transfected PK-15 cell clones were transplanted into NOD scid gamma (NSG) mice. A defined number of cells (see Table 27) was resuspended in 10 µL PBS and injected subcutaneously (*s.c.*) into the hind leg using a 31G needle. Splenocytes isolated from NOD mice (1x 10^7 in 100 µL PBS) were transferred via the tail vein of the NSG mice to reconstitute the immune system after an engraftment time of 1 to 4 weeks (see Table 27). Splenocyte transfer was not performed for the control group. Animal housing, PK-15 cell transplantation and splenocyte transfer were carried out by Prof. Jochen Seißler and colleagues at Klinikum der LMU München, GER.

Table 27 –Details for individual transplantation experiments

Experiment, chapter	Cell type implanted	Cell number	Time span, engraftment	Time span, splenocyte transfer to histology
Validation of cell engraftment, 7.1.2.1.1	PK-15 (wt), ST (3xKO)	2x10^6	7 days, 4 weeks	No splenocyte transfer
Validation of immune cell infiltration, 7.1.2.1.1	PK-15 (A080, pool)	1x10^5	10 days	10 days

In vivo induction experiments, 7.1.2.2	PK-15 (A080-A085, cell clones)	$1x10^5$	8 days	10 days

6.4.2 *In vivo* bioluminescence imaging

10 days after transplantation of NOD splenocytes, mice were transferred to Klinikum rechts der Isar (TUM, GER) where *in vivo* bioluminescence imaging and tissue collection were performed. The mice were anaesthetized with 3.0% isoflurane in a whole-body chamber and narcosis was maintained with 2.5% isoflurane within the imaging system (IVIS Lumina LT series III). To evaluate *Renilla* luciferase (Rluc) activity, 100 µL of ViviRen substrate (0.3 µg/µL in PBS) was injected into the tail vein and photon emission was detected after 1 min (exposure time: 60 sec). Not earlier than one hour after the first measurement, the remaining Rluc activity was determined and 200 µL of XenoLight D-Luciferin solution (14 µg/µL in PBS) was administered intraperitoneally (*i.p.*). *Firefly* luciferase (Fluc) activity was measured 7 min after substrate injection and mice were subsequently euthanized by cervical dislocation. The optimal times for detection of bioluminescence were determined in an initial experiment. All work on living animals was performed by Dr. Dirk Wohlleber and Katrin Manske (Institute of Molecular Immunology and Experimental Oncology, TUM, GER).

Relative activity of a promoter x was defined as

$$Relative\ promoter\ activity\ (x) = \frac{radiance_{Rluc}(x)}{radiance_{Fluc}(x)}$$

and the degree of promoter upregulation ('induction factor') was calculated as follows:

$$Induction\ factor\ (x) = \frac{mean\left(relative\ promoter\ activity\ (x, spleno)\right)}{mean\ (relative\ promoter\ activity\ (x, without\ speno)}$$

6.4.3 Immunohistochemistry

Murine hind legs were fixed without skin for 3-4 days in 4% paraformaldehyde and subsequently preserved in 70% EtOH. After removing the thighbone, samples were embedded in paraffin blocks by Nico Gebhardt (Chair of Nutrition and Immunology, TUM, GER). Histological sections, thickness 4-5 µm, were prepared using a Microm Cool-Cut microtome

prior to deparaffinisation. Microscope slides carrying the tissue sections were incubated three times in Roticlear for 5 min, then washed twice in 100% EtOH, 95% EtOH, 80% EtOH and H_2O for 5 min. For antigen unmasking, tissue slides were boiled for 10 min in 10 mM citrate buffer (pH 6.0) and cooled to room temperature. Slides were washed three times in H_2O for 5 min, then endogenous peroxidases were inhibited by incubating for 10 min in 3% H_2O_2 (dilution in PBS). After three 5 min washes in H_2O, slides were drained and 90 µL of the primary antibody dilution (Biotin anti-mouse CD45, 1:200 in Antibody Dilution Buffer) applied to the sections. The sections were covered using coverslips and incubated overnight at 4°C in a closed staining tray. The next day, the slides were washed in PBS for 5 min, covered with VECTASTAIN Elite ABC Reagent (prepared following the manufacturer's instructions) and incubated for 30 min. After washing for 5 min in PBS, sections were stained with peroxidase substrate (3,3'-Diaminobenzidine Enhanced Liquid Substrate System tetrahydrochloride) mixed according to the manufacturer's instructions. The staining process was monitored under the microscope and stopped after 40 min by removing the substrate and washing with PBS. Counterstaining was performed by incubating in haematoxylin for ten seconds. The slides were subsequently washed twice in H_2O for 5 min, twice in 95% EtOH for 10 sec and finally in 100% EtOH. For fixation, the stained tissue sections were mounted with Eukitt quick-hardening mounting media. To double-check staining quality, all tissue samples were additionally stained and histologically evaluated by Prof. J. Seißler.

6.4.4 Somatic cell nuclear transfer (SCNT) and embryo transfer

Cell cycles were synchronized by incubating primary cell clones for 2 days in starvation medium (DMEM, 1x NEAA, 1 mM sodium pyruvate, 2 mM Ala-Gln, 0.5 % FBS). Serum-starved cells (12-well, 100% confluency) were transferred to Prof. Eckhard Wolf's group (Chair for Molecular Animal Breeding and Biotechnology, LMU, GER), where SCNT was performed as described previously [313]. Reconstructed embryos were then transferred laparoscopically into the oviducts of hormone-primed German landrace (GLR) sows for gestation [313].

7. RESULTS

7.1 The Smart Graft strategy

Constitutive and systemic expression of T cell regulatory molecules in xeno-donor pigs is undesirable because it can lead to immunodeficient animals and possibly to uncontrollable immunosuppression in human recipients. It would be preferable if the expression of immune-modulatory transgenes such as CTLA4-Ig or LEA29Y becomes activated or upregulated in response to incipient rejection and tissue injury after transplantation. This strategy based on dynamic, cytokine-dependent expression of xenoprotective molecules in the donor tissue was termed the Smart Graft strategy. It envisaged the use of NF-κB-dependent promoters that are induced by human pro-inflammatory cytokines (e.g. TNF, IL-1β) to direct an appropriate transgene expression response (see Figure 8).

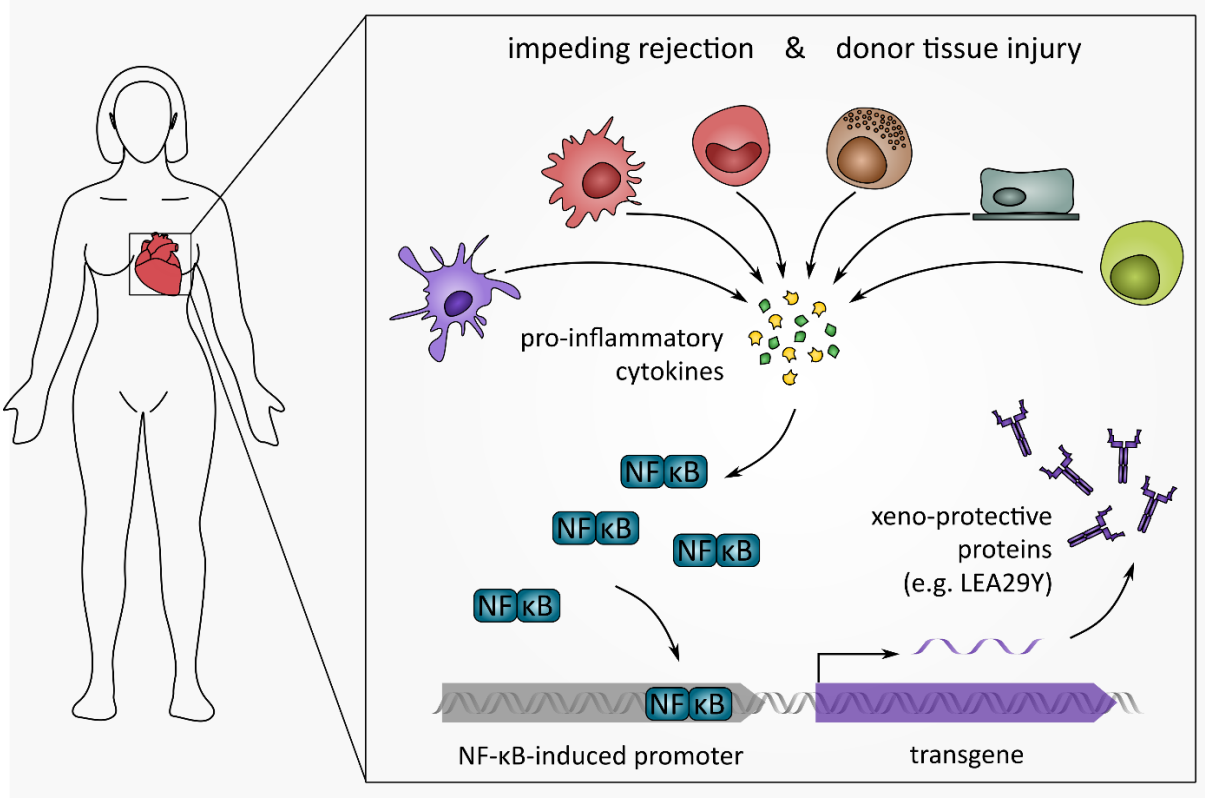

Figure 8 – Cytokine-dependent expression of protective proteins (the Smart Graft strategy)
Pro-inflammatory cytokines including TNF and IL-1β are released by diverse immune cells (e.g. DCs, macrophages, blood monocytes, NK cells, lymphocytes) and porcine ECs in response to incipient xenograft rejection and donor tissue injury. Downstream signalling of TNF and IL-1β results in activation of NF-κB that then attaches to specific binding-elements of NF-κB-regulated promoters. This induces cytokine-dependent expression of protective molecules (e.g. CTLA4-Ig, LEA29Y) to counteract the loss of the xenograft.

The first aim was thus to identify or engineer suitable promoters that provide strong and swift responsiveness to human TNF and IL-1β while having low activity in absence of these cytokines and to characterize them *in vitro* and *in vivo*. Gene constructs were then generated to introduce different cytokine-inducible transgenes into the porcine *ROSA26* locus by gene targeting. Much of the data described here have already been published [199].

7.1.1 *In vitro* promoter evaluation

This section focusses on the generation and *in vitro* evaluation of several candidate promoters. The first part (7.1.1.1) describes the selection of various promoter regions and the cloning of the corresponding reporter constructs. Different variants of the endogenous promoters pA20 and hCCL2 were generated to improve sensitivity to human cytokines and to create promoters with different activity levels, which is described in section 7.1.1.2. The *in vitro* investigation of promoter-inducibility with human cytokines is the subject of section 7.1.1.3, and section 7.1.1.4 describes timing of promoter induction.

7.1.1.1 Selection of promoter regions

Various human (hTNFAIP1: TNF alpha induced protein 1, hVCAM1: vascular cell adhesion protein 1, hCCL2: C-C motif chemokine 2), porcine (pA20: zinc finger protein A20) and semi-synthetic (ELAM: E-selectin) promoters, known to respond to inflammatory pathways, were considered as candidates for implementing the Smart Graft strategy. The CAG promoter (CMV enhancer/chicken β-actin promoter/rabbit globin intron), known to provide high and ubiquitous expression levels in pigs, was used as a reference. The sequences of the promoter regions described below originated from Ensembl Genome Browser (Ensembl Release 95; https://www.ensembl.org/) using the genome assemblies GRCh38.p12 (*Homo sapiens*) and SScrofa11.1 (*Sus scrofa*). The promoter structures are shown in Figure 9.

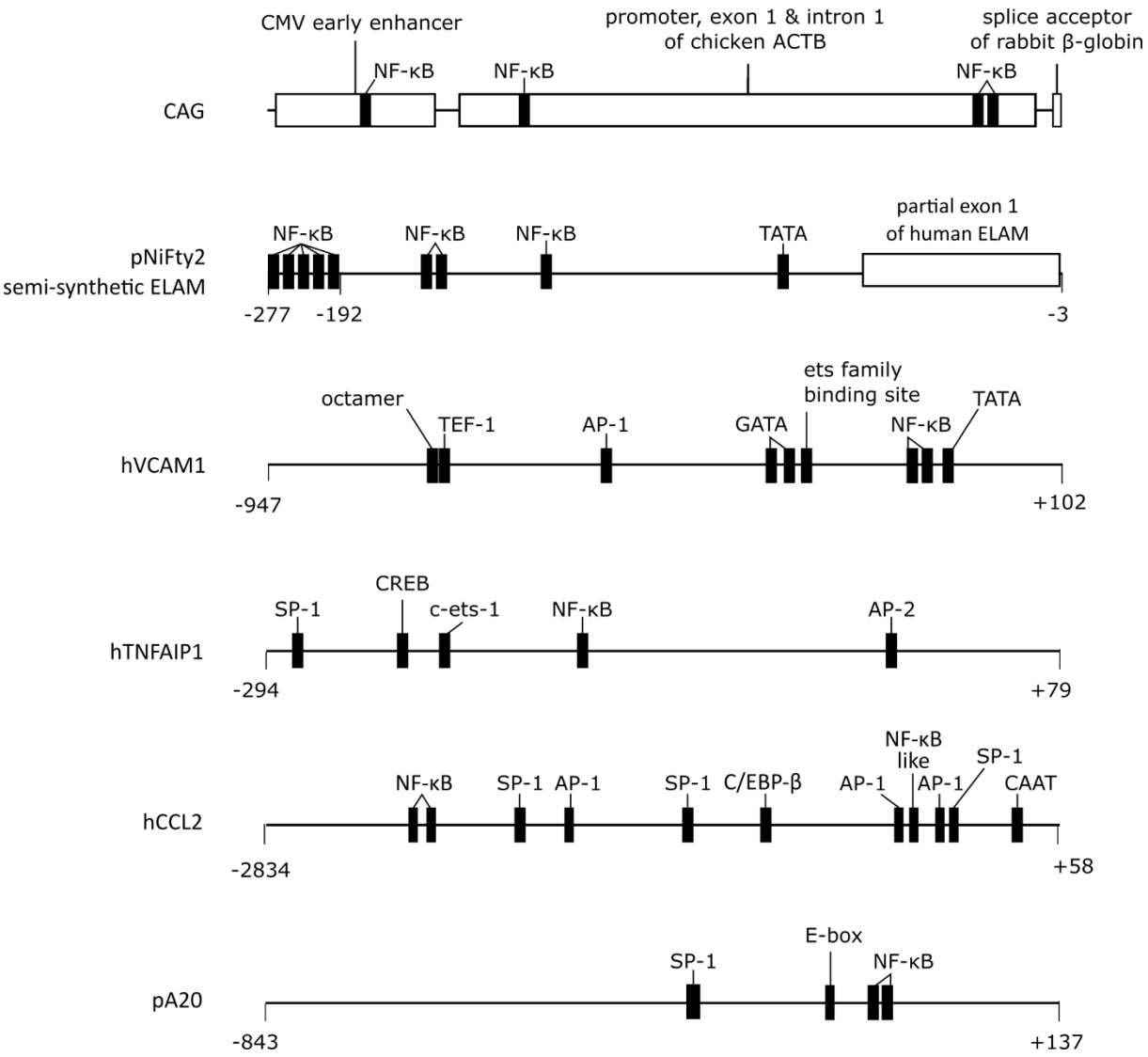

Figure 9 – Structures of the unmodified promoters tested for cytokine-responsiveness *in vitro*

Functional promoter elements were annotated according to the previous publications: ELAM [314, 315], hVCAM1 [316], hTNFAIP1 [317], hCCL2 [318-323]. Functional elements of the porcine A20 promoter were identified by sequence alignment with the human A20 promoter [324-326]. Putative NF-κB binding sites in the CAG promoter sequence were identified *in silico* and not functionally verified. Promoter elements are marked as boxes. NF-κB: NF-κB binding site; ACTB: actin, cytoplasmic 1; TATA: TATA box; octamer: octamer transcription factor binding site; TEF-1: transcriptional enhancer factor 1; AP-1/2: adaptor protein complex 1/2 binding site; GATA: GATA-binding factor binding site; ETS: epithelium-specific transcription factor binding site; SP-1: transcription factor specificity protein 1 binding site; CREB: cyclic AMP responsive element-binding protein binding site; C/EBP- β: CCAAT/enhancer-binding protein beta; CAAT: CAAT box; E-box: enhancer box (published in [199]).

The chosen promoter sequence of h*TNFAIP1* comprised bp -294 to +79 relative to the transcription start site (Transcript ID: ENST00000226225.6), the hVCAM1 promoter included bp -947 to +102 (Transcript ID: ENST00000294728.6) and the hCCL2 promoter region consisted of bp -2,834 to +58 (Transcript ID: ENST00000225831.4). The pA20 promoter was

composed of two parts: bp -843 to -180 and -101 to +137 (Transcript ID: ENSSSCT00000034426.2). The semi-synthetic ELAM promoter construct was commercially available (pNiFty-SEAP, InvivoGen) and consisted of the human ELAM proximal promoter (bp -149 to -1; Transcript ID: ENST00000333360.11) and five repeated NF-κB transcription factor binding sites.

For *in vitro* analyses of cytokine-inducibility and activity levels, the endogenous promoters described above were PCR amplified using genomic DNA (gDNA) of human SCP1 and porcine kidney fibroblast (pKDNF) isolate 2505 as a template and inserted into a SEAP reporter plasmid (see Figure 10). For detailed cloning information see Appendix 13.1.1.

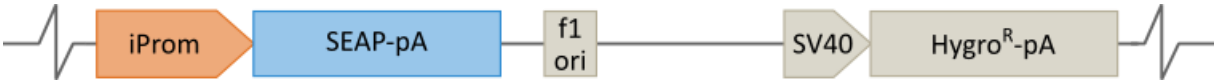

Figure 10 – Structure of the SEAP reporter plasmids
iProm: (cytokine-inducible) candidate promoter; SEAP: coding sequence of secreted embryonic alkaline phosphatase; f1 ori: origin of DNA replication of bacteriophage f1; SV40: Simian virus 40 promoter; Hygro^{R}: hygromycin resistance gene; pA: polyadenylation signal.

7.1.1.2 Promoter modification

The endogenous promoters of hCCL2 and pA20, that already showed some significant induction by hTNF *in vitro* (see Figure 13), were modified to further enhance cytokine responsiveness and to cover a wider activity spectrum.

A hCCL2 variant (hCCL2 prox) was generated that comprised the proximal promoter portion only (bp -145 to +65; Transcript ID: ENST00000225831.4). It includes a CAAT motif, two AP-1 sites and binding sites for transcription factor specificity protein 1 (SP-1) and NF-κB as summarized by Deng *et al.* (see Figure 11) [323]. The third variant (hCCL2 dis/prox) additionally contained the distal promoter region [323] with two extra NF-κB sites and included bp -2,834 to 2,519 and -145 to +58. Cloning details are described in Appendix 13.1.1. Some of the annotated promoter elements of the human CCL2 promoter might have negative effects on inducibility. AP-1 sites were shown to bind AP-1 molecules and cyclic AMP responsive element-binding proteins (CREBs) as well. CREB transcription factors are essential for gene regulation and were also show to downregulate transcription in response to TNF and other inflammatory cytokines [327-330]. Both shortened hCCL2 promoters had a deletion of an

adaptor protein complex 1 (AP-1) and a CCAAT/enhancer-binding protein beta (C/EBP-β) element to improve TNF responsiveness of hCCL2 prox and hCCL2 dis/prox.

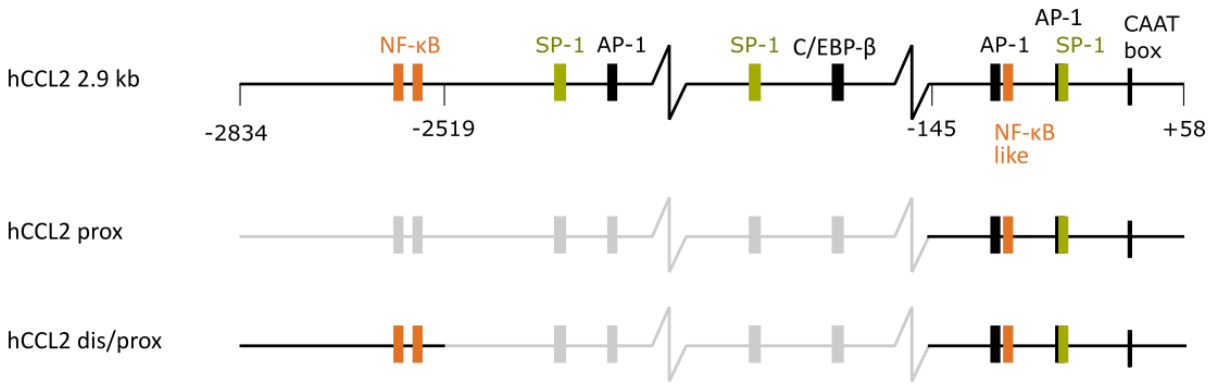

Figure 11 – Structure of the generated human CCL2 promoter variants

Top: endogenous hCCL2 promoter spanning 2.9 kb. Nucleotide positions refer to hCCL2 transcript ID ENST00000225831.4. Endogenous promoter elements are marked as boxes. **Below:** shortened hCCL2 promoter variants. Grey lines and boxes indicate removed promoter elements (published in [199]). Abbreviations as in Figure 9.

Sequence alignment between the porcine and human sequences was conducted to identify the functional elements of the pA20 promoter. High sequence homology allowed identification of an E-box element, two endogenous NF-κB and one SP-1 binding site [324-326]. SP-1 was reported to modulate basal activity of some NF-κB-regulated promoters and to enhance activity in response to TNF as well [317, 319]. Therefore, thirteen additional variants of the pA20 promoter were generated by sequential insertion of different clusters of SP-1 and/or NF-κB binding sites into plasmid pcDNA-pA20-SEAP (A006, see Figure 12) to optimize basal expression levels and inducibility. NF-κB sequences were inserted at position -404 and/or downstream of both endogenous NF-κB binding sites at position +52. The SP-1 cluster was introduced at position -101, upstream of the endogenous SP-1 site (Transcript ID: ENSSSCT00000034426.2). For cloning details see Appendix 13.1.1.

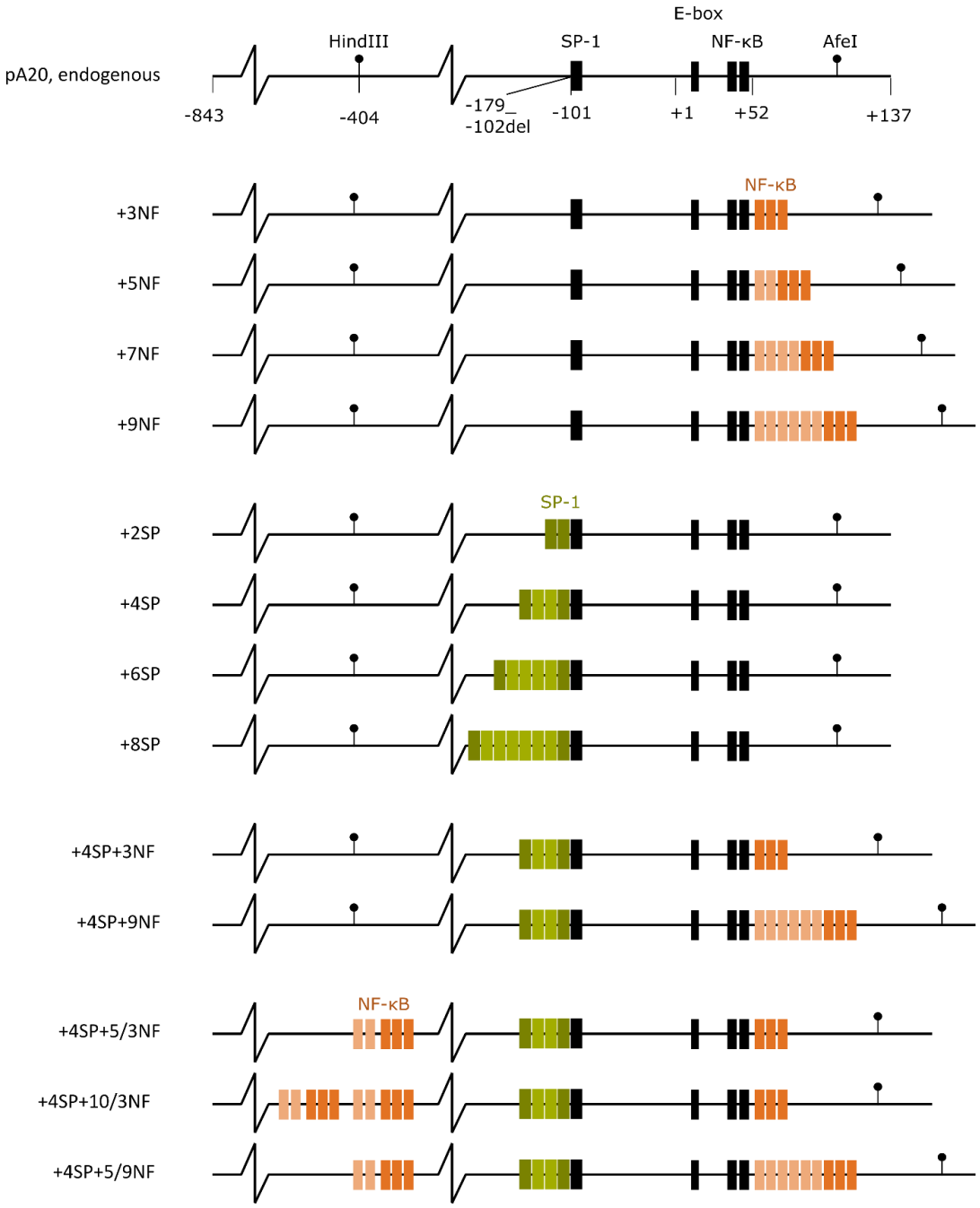

Figure 12 – Structure of the generated porcine A20 promoter variants

Top: endogenous pA20 promoter. Nucleotide positions refer to pA20 transcript ID ENSSSCT00000034426.2. Endogenous promoter elements are marked as black boxes. Restriction sites relevant for cloning are indicated as black circles. **Below:** pA20 promoter variants featuring different clusters of added transcription factor binding sites. Orange and green boxes indicate additional NF-κB and SP-1 binding sites, respectively (published in [199]). Abbreviations as in Figure 9.

7.1.1.3 Analysis of promoter inducibility by human cytokines

TNF and IL-1β are potent pro-inflammatory cytokines and produced by blood monocytes and tissue macrophages during early inflammatory reactions of the innate immune system [88, 331]. They also play an important role in xenograft rejection [174, 175]. TNF and IL-1β are thus suitable to mediate activation of xenoprotective transgenes within the graft.

The activity and cytokine response of candidate promoters (described in section 7.1.1.1 and 7.1.1.2) were quantified by a SEAP reporter assay in stably transfected wild-type pKDNF 2505 cells. Cell pools were treated with various concentrations of human TNF and IL-1β for 72 h, ranging from 0.1 to 50.0 ng/mL. Some promoters were also tested for inducibility by human IFNγ, another crucial pro-inflammatory cytokine released by innate immune cells and cytotoxic T lymphocytes (CTL). Figure 13 shows promoter activity levels with and without hTNF treatment (**A**) and the extent of induction (**B**) after exposure to hTNF (30 ng/mL), hIL-1β (50 ng/mL) and hIFNγ (10 ng/mL).

The 21 promoter variants tested provide a broad range of activity: CAG and hCCL2 dis/prox had strong activity, while the promoters pA20, pA20+2/4/6/8SP and pA20+5NF had lower activity. All constructs other than CAG, hVCAM1 and hTNFAIP1 showed a clear response to different concentrations of hTNF. The ELAM promoter exhibited the greatest inducibility with both cytokines, hTNF and hIL-1β. The combination of the distal and proximal promoter region and deletion of inhibitory elements in hCCL2 dis/prox resulted in a significantly increased sensitivity to hTNF and hIL-1β, when compared to hCCL2 2.9 kb and hCCL2 prox. Interestingly, also CAG showed a considerable response to hIL-1β. This finding would be explained by four potential NF-κB binding sites, that were previously identified at positions -245, -286, -904 and -1492 by *in silico* analyses (Nina Simm, Master's student) [332].

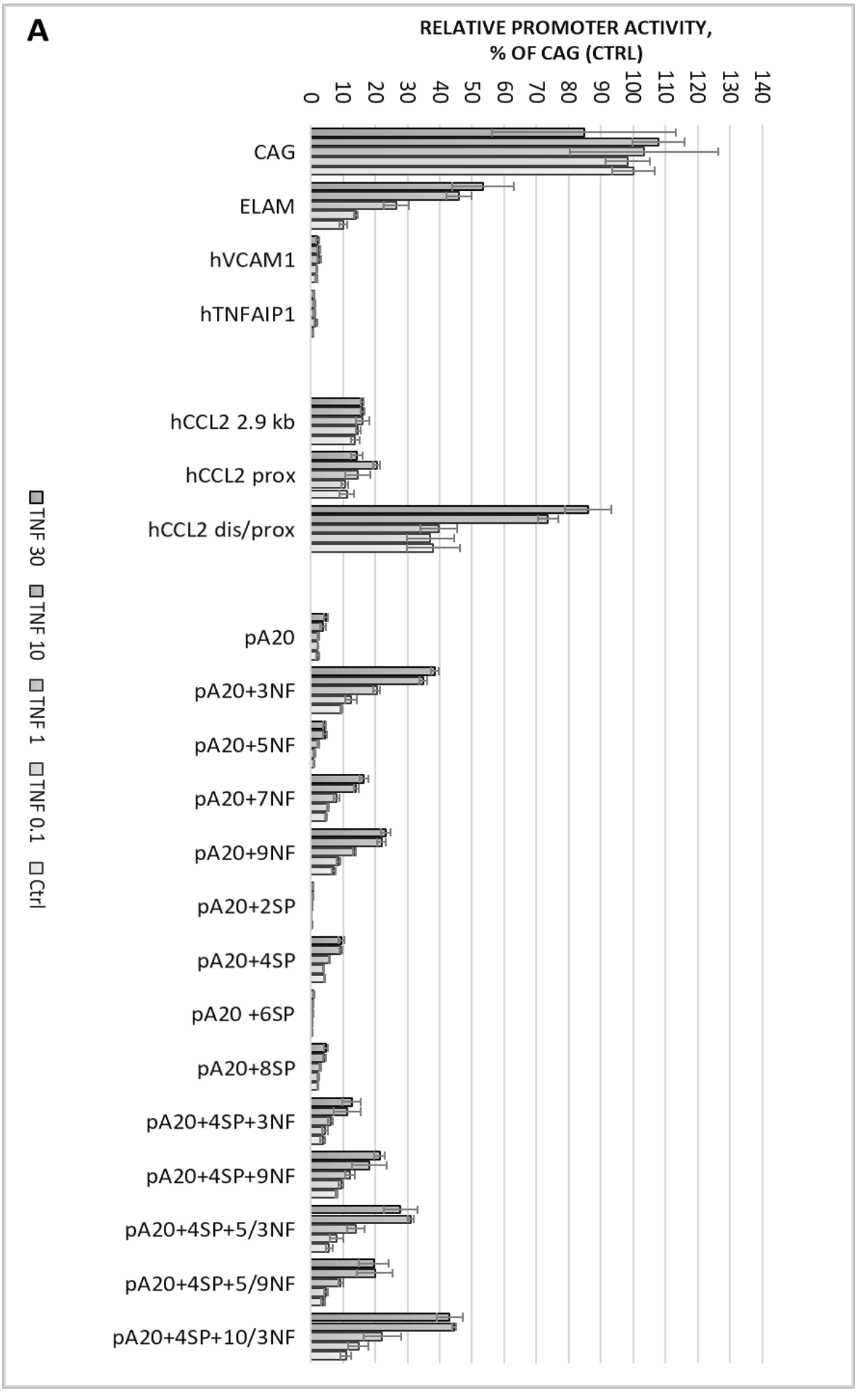
A
RELATIVE PROMOTER ACTIVITY,
% OF CAG (CTRL)
0
10
20
30
40
50
60
70
80
90
100
110
120
130
140
CAG
ELAM
hVCAM1
hTNFAIP1
hCCL2 2.9 kb
hCCL2 prox
hCCL2 dis/prox
pA20
pA20+3NF
pA20+5NF
pA20+7NF
pA20+9NF
pA20+2SP
pA20+4SP
pA20 +6SP
pA20+8SP
pA20+4SP+3NF
pA20+4SP+9NF
pA20+4SP+5/3NF
pA20+4SP+5/9NF
pA20+4SP+10/3NF
TNF 30
TNF 10
TNF 1
TNF 0.1
Ctrl

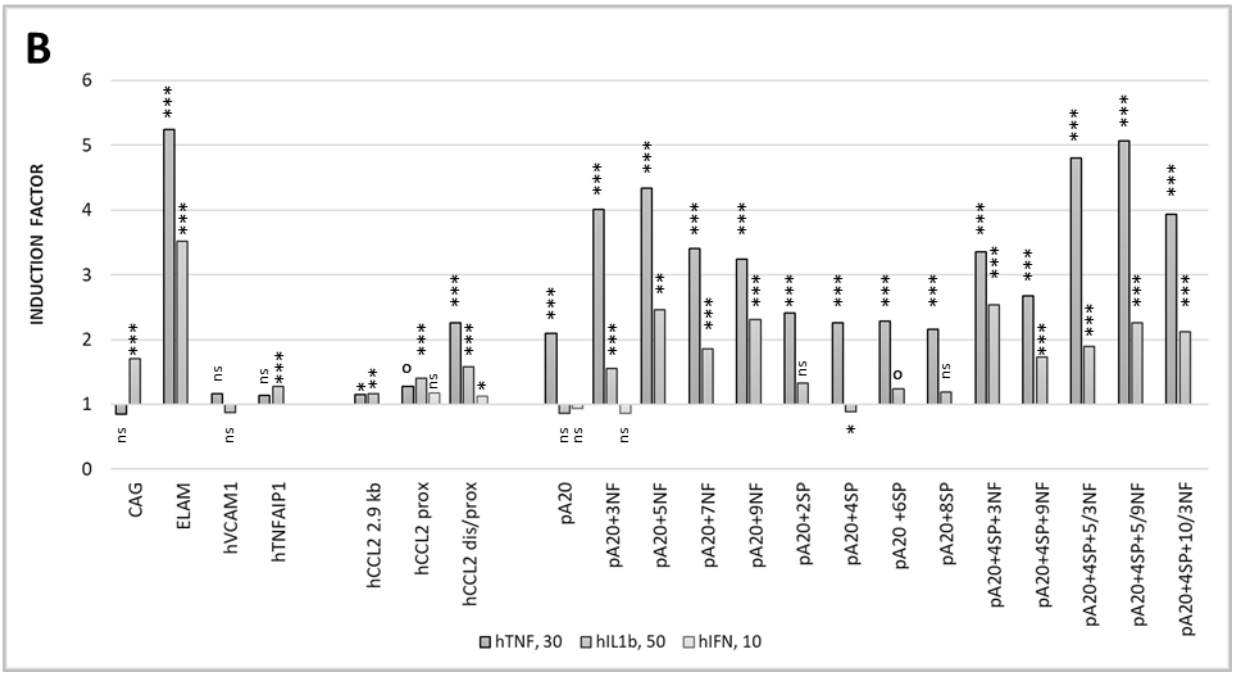

Figure 13 – *In vitro* promoter induction by human TNF, IL-1β and IFNγ

A: Relative promoter activity in pKDNF 2505 cells stably transfected with SEAP reporter plasmids ± SD. CAG promoter activity at control level = 100%. Cells were induced with human TNF in different concentrations (ng/mL) for 72 h. **B:** Factor of promoter induction in pKDNF 2505 cells 72 h after cytokine treatment compared to untreated control (published in [199]).

Significance codes: P-value <0.001 (***), 0.001 to 0.01 (**), 0.01 to 0.05 (*), 0.05 to 0.1 (°), > 0.1 (ns).

The additional NF-κB binding sites within the pA20 promoter variants clearly increased hTNF inducibility. Moreover, these also conferred sensitivity to hIL-1β that was not observed with the unmodified pA20 promoter. However, the effect of IFNγ on the promoters tested was negligible due to very low induction factors and significance levels. This is concordant with observations of other groups that suggested the incompatibility between human IFNγ and porcine IFNγ receptors [333, 334]. Six of the 21 promoters analysed were chosen for subsequent *in vivo* studies, based on promoter strength and responsiveness to hTNF and hIL-1β (summarized in Table 28).

Table 28 – Characteristics (activity level, inducibility) of promoters chosen for *in vivo* studies
Activity levels High/Medium/Low correspond to relative promoter levels (ctrl) of >35% / 35-5% / <5%. Inducibility levels High/Medium/Low correspond to induction factors of >3.5 / 3.5-2.0 / <2.0.

Promoter	Activity level, ctrl	Inducibility, hTNF	Inducibility, hIL-1β
CAG	High	x	Low
ELAM	Medium	High	High
hCCL2 dis/prox	High	Medium	Medium
pA20	Low	Medium	X
pA20+3NF	Medium	High	Low
pA20+4SP+10/3NF	Medium	High	Medium

7.1.1.4 Determining initiation and termination of promoter induction

In addition to promoter strength and inducibility, the timing of activation is also important. The time span between the release of pro-inflammatory cytokines and promoter induction should be as short as possible. After inflammation subsides, the expression of T-cell modulatory molecules should quickly reduce and then turn off or maintain at low level to avoid chronic systemic immunosuppression.

The kinetics of induction after hTNF challenge and promoter deactivation after removal of hTNF from the cell culture medium was determined for the promoters ELAM, hCCL2 dis/prox, pA20, pA20+3NF and pA20+4SP+10/3NF using the cell pools from section 7.1.1.3 (see Figure 14). Samples with readings too low for reliable evaluation (OD_{405nm} < 0.030) are indicated by square brackets. Armin Mauerer (Bachelor's student) partially executed the SEAP measurements [335].

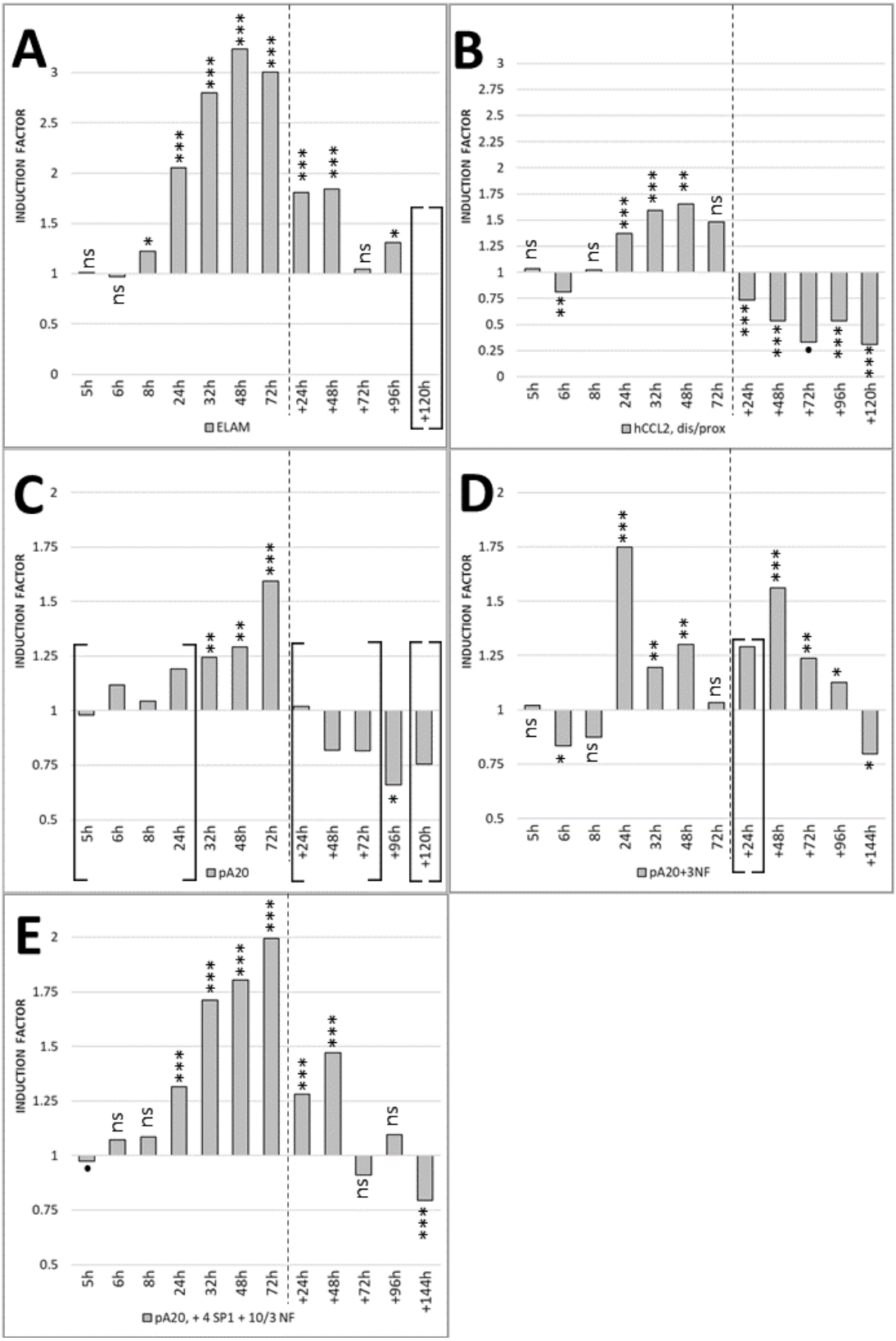

Figure 14 – *In vitro* analysis of initiation and termination of promoter induction

Factor of promoter induction in pKDNF 2505 cells relative to untreated control. Left to dashed line: promoter induction after hTNF treatment (10 ng/mL). Right to dashed line: promoter induction after hTNF removal. **A**: ELAM; **B**: hCCL2 dis/prox; **C**: pA20; **D**: pA20+3NF; **E**: pA20+4SP+10/3NF. Samples excluded from the analysis due to low SEAP measuring values (OD_{405nm} < 0.030) are indicated by square brackets.

Significance codes: P-value <0.001 (***), 0.001 to 0.01 (**), 0.01 to 0.05 (*), 0.05 to 0.1 (•), > 0.1 (ns).

All promoters tested showed a highly significant increase in promoter activity within 8 (ELAM) to 32 h (pA20+4SP+10/3NF) after hTNF-addition, compared to the untreated control. In almost all cases, promoter activity reduced on withdrawal of hTNF. This reduction was observed within 24 h for the ELAM and pA20+4SP+10/3NF promoters. Although pA20+3NF showed a greater induction factor 48 h after switching to TNF-free medium, promoter activity steadily decreased within the next few days compared to the control. Human CCL2 and pA20 also showed a significant reduction in activity, but promoter strength was below that of the control cells resulting in an induction factor <1.0. This can be explained by the substantially reduced cell viability of the sample cells due to exposure to hTNF.

7.1.2 *In vivo* mouse studies for promoter evaluation

In the previous section, a series of 21 promoters was designed that provide a broad range of activity and cytokine-responsiveness *in vitro*. Six of these were selected to investigate *in vivo* inducibility: CAG, ELAM, hCCL2 dis/prox, pA20, pA20+3NF and pA20+4SP+10/3NF (see Table 28).

For *in vivo* promoter evaluation, porcine cells expressing a luciferase reporter gene under the control of the inducible promoters were transplanted into NSG mice. These animals lack mature lymphocytes and NK cells and were used to facilitate engraftment [336]. The immune system was reconstituted after stable xenotransplant growth. This allowed infiltration of immune cells, such as macrophages, NK cells and T lymphocytes, into the graft with consequent production and release of pro-inflammatory cytokines to stimulate reporter gene expression. Reporter activity determined via bioluminescence imaging could thus be used as an indicator of *in vivo* induction of each promoter by the murine immune system.

The first section focusses on the preparation and analysis of genetic constructs and cells used for transplantation. The selection of a suitable cell type is covered in paragraph 7.1.2.1.1. The reporter constructs used for the mouse studies and the final selection of transfected cell clones is described in paragraph 7.1.2.1.2.

The second section (7.1.2.2) gives details of the bioimaging, including the experimental strategy, optimisation of bioluminescence detection and the findings regarding *in vivo* promoter inducibility derived from two runs of bioimaging.

7.1.2.1 Preparation of constructs and cells

7.1.2.1.1 Selection of a suitable cell line for in vivo application

Cells suitable for these *in vivo* experiments had to meet several criteria: They must be of porcine origin, since the inducible promoters are intended to drive transgenes in a porcine graft in the future, and able to grow stably within NSG mice. Moreover, the grafted cells must be recognized by murine immune cells after splenocyte transfer and respond to murine cytokines.

Two different porcine cell lines were used for the first transplantation experiments conducted by Prof. J. Seißler: Swine Testis (ST) and Porcine Kindey-15 (PK-15) that were derived both by spontaneous immortalisation. ST cells were originally isolated from testicular tissue from swine fetuses, possess fibroblast-like morphology with a diploid set of chromosomes and have a reported doubling time of 30 to 40 hours [337-339]. Whereas PK-15 cells are derived from an adult porcine kidney, show epithelial morphology with faster growth *in vitro* (generation time: 12 h) and an unstable karyotype [340-344].

Subcutaneous (*s.c.*) and intramuscular (*i.m.*) engraftment of ST and PK-15 cells within the tissue of NSG mice was analysed at different times. While 7 days after transplantation a small number of ST cells were present in the tissue, none were detected histologically after 4 weeks (see Figure 15, A+B). ST cells were therefore excluded from further studies. In contrast, PK-15 cells were stably engrafted 4 weeks after injection by both methods resulting in large tumors approx. 5 mm in diameter (see Figure 15, C+D). A follow-up experiment was then conducted to investigate whether reconstitution of the recipient's immune system results in invasion of murine leukocytes into the PK-15 cell aggregates. Ten days after PK-15 transplantation, NOD splenocytes were transferred into the recipient mice. After a further ten days, massive infiltration of CD45-positive immune cells was detected immunohistochemically, indicating the PK-15 cell line being suitable for *in vivo* promoter evaluation (see Figure 15, E).

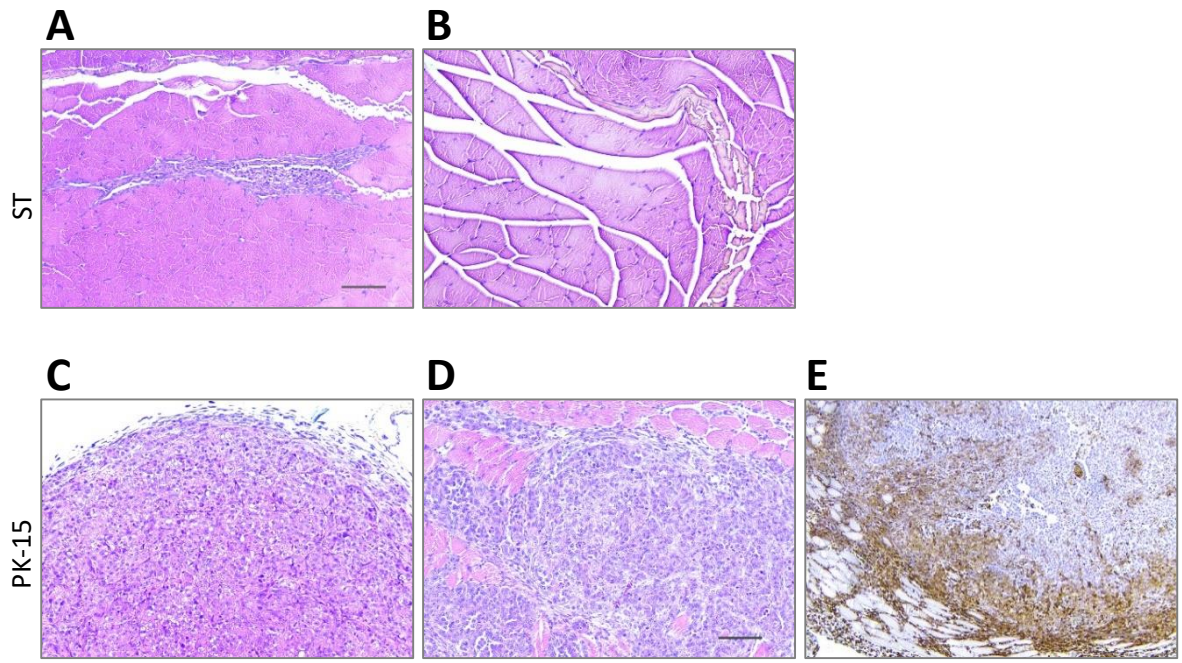

Figure 15 – Engraftment of porcine cells and infiltration of CD45-positive cells into PK-15 aggregations
Shown are HE-stained sections of graft sites in NSG mice after transplant of porcine ST (A, B) and PK-15 (C, D) cells and HE, mCD45-staining of PK-15 aggregates after immune reconstitution with NOD splenocytes (E). Scale bar: 500 µm.
A: A few ST cells are visible in muscle tissue 7 days after transplantation *i.m.* **B:** After 4 weeks, ST cells are not detectable. **C, D:** After 4 weeks, PK-15 cells are stably engrafted, *s.c.* (C) and *i.m.* (D). **E:** 10 days after transfer of NOD splenocytes, the PK-15 tumor shows massive infiltration of murine CD45-positive cells (partially published in [199]).

The *in vivo* bioluminescence assay requires that the inducible promoters in the porcine xenotransplanted cells respond to murine cytokines produced by cells of the mouse immune system. PK-15 cells were thus stably transfected with SEAP-reporter plasmid A068 (promoter: pA20+2SP+10/3NF) and treated for 72 h with murine cytokines then promoter activity evaluated (see Figure 16). Significant promoter induction was shown for both mTNF (P-value=$1.8*10^{-15}$) and mIL-1β (P-value=$9.9*10^{-2}$), verifying cross-species response to these cytokines.

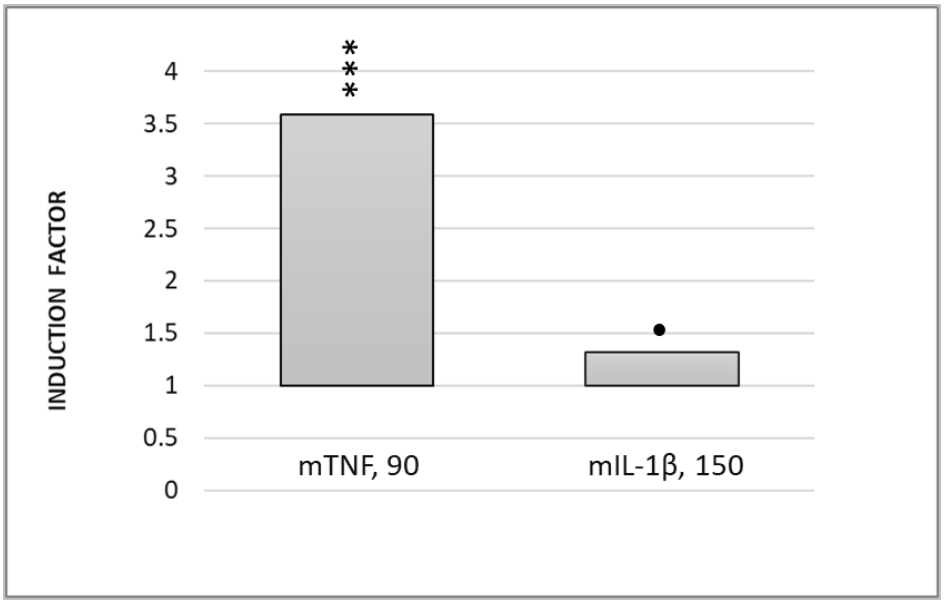

Figure 16 – *In vitro* verification of PK-15 sensitivity to murine TNF and IL-1β
Factor of promoter induction in PK-15 cells, transfected with SEAP-reporter plasmid A068 (pcDNA-pA20+10NFkB+4SP1+3NFkB-SEAP), 72 h after cytokine treatment (ng/mL) compared to untreated control (published in [199]).
Significance codes: P-value <0.001 (***), 0.001 to 0.01 (**), 0.01 to 0.05 (*), 0.05 to 0.1 (•), > 0.1 (ns).

7.1.2.1.2 Selection of clones for cell transplantation into mice

PK-15 cells were identified in the previous section as suitable for the *in vivo* assay. Thus, they were stably transfected with dual luciferase constructs. These vectors comprise cDNA sequences encoding Rluc, driven by one of the candidate promoters described and summarized in section 7.1.1 Table 28, and also Fluc directed by the herpes simplex virus thymidine kinase (HSV-TK) promoter as an internal control for normalisation (see Figure 17). Detailed cloning information is provided in Appendix 13.1.2.

Figure 17 – General structure of dual luciferase constructs for *in vivo* promoter evaluation
SV40: Simian virus 40 promoter; Hygro^{R}: hygromycin resistance gene; iProm: cytokine-inducible candidate promoter; Rluc: *Renilla* luciferase; HSV-TK: Herpes simplex virus thymidine kinase promoter; Fluc: *Firefly* luciferase; pA: polyadenylation signal.

The expression level of randomly integrated DNA constructs is strongly influenced by the integration locus and the number of copies integrated. This source of variability was reduced by preselecting stably transfected single cell clones by the criteria described below, and thus increase the validity of comparisons between different promoters.

The first strategy was to choose clones with only a single copy of the reporter construct. However, only 10% of single-copy-clones identified by droplet digital PCR (ddPCR) showed Fluc activity, which may have been due to the known chromosomal instability of the PK-15 cell line [341, 342]. So, for further clones, the integrity of the Fluc gene was first validated by PCR and Fluc transcription verified by RT-PCR before the activity of both luciferases was measured. The final selection was conducted according to the signal strength of the Fluc control, which ranged from $1.3x10^3$ to $1.4x10^8$ RLU: Cell clones with similar Fluc activities, around $1.0x10^5$ RLU, were chosen (see Figure 18, A) for *in vivo* assays: A080-45 (CAG), A081-49 (ELAM), A082-70 (hCCL2 dis/prox), A083-61 (pA20), A084-42 (pA20+3NF) and A085-17 (pA20+4SP+10/3NF). In this way, the influence of the integration site and copy number on the *in vivo* promoter evaluation was reduced. The number of integrated vector copies of these cell clones were determined by ddPCR (see Figure 18, B). Prior to transplantation the cells were checked for responsiveness of Rluc expression to murine TNF. For all the five clones analysed, increased Rluc activity was detected 24 h after addition of murine TNF (30 ng/mL) compared to the untreated control (see Figure 18, C).

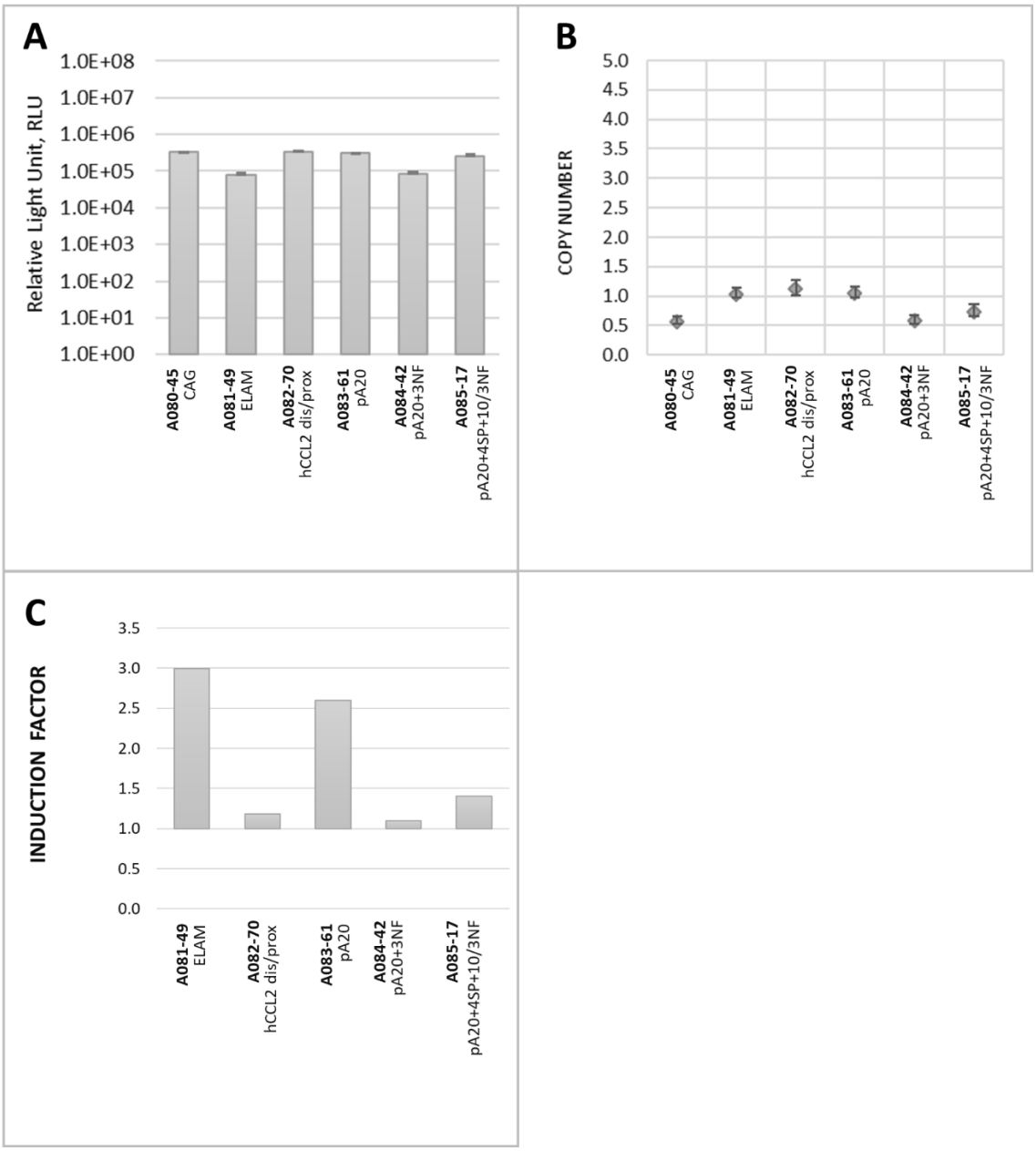

Figure 18 – Selection and further characterisation of transfected PK-15 cell clones used for *in vivo* promoter evaluation

A: Cell clones for *in vivo* promoter evaluation selected according to Fluc activity ± SD, with values around $1.0x10^5$ RLU. **B:** Copy numbers of integrated dual luciferase plasmids ± SD determined by ddPCR using HindIII-digested gDNA and glyceraldehyde 3-phosphate dehydrogenase (*GAPDH*) as a reference gene. **C:** Verification of Rluc inducibility in cell clones compared to untreated control: PK-15 cells were induced with murine TNF (30 ng/mL) and harvested after 24 h at full confluence (partially published in [199]).

7.1.2.2 In vivo promoter induction analyses

PK-15 cell clones containing the dual luciferase reporter construct under the control of the CAG promoter (A080-45), ELAM (A081-49), hCCL2 dis/prox (A082-70), pA20 (A083-61), pA20+3NF (A084-42) and pA20+4SP+10/3NF (A085-17) were used to analyze the extend of *in vivo* promoter inducibility. After subcutaneous cell transplantation to NSG mice (day 0) and reconstitution of the immune system by transferring splenocytes from non-obese diabetic (NOD) mice (day 8; not performed in the control group), bioimaging was conducted to determine Rluc and Fluc expression levels at day 18. In addition, the size and morphology of PK-15-induced tumors and progression of immune cell infiltration into the porcine tissue were investigated histologically. The workflow is shown in Figure 19.

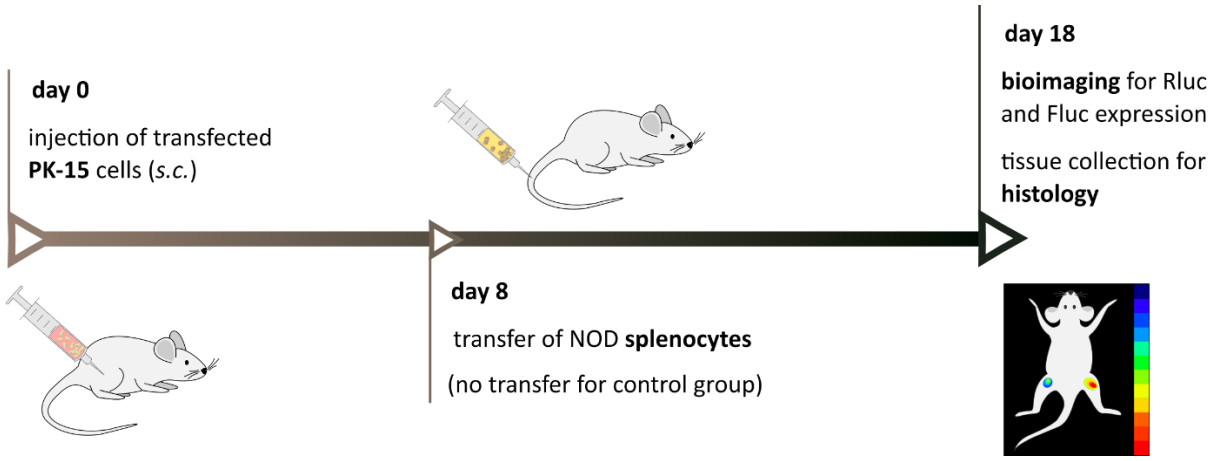

Figure 19 – Workflow for *in vivo* promoter induction analyses
Procedure for the bioluminescence assay of promoter activity in mice: transplantation of transfected PK-15 cell clones; reconstitution of the murine immune system; then *in vivo* bioimaging and tissue collection for histology (adapted from [199]).

The experiment was sub-divided into two runs. The first run served as a proof-of-principle experiment with only one PK-15 transplantation per promoter for induction analysis ($n_{test} = 1$) and for control ($n_{ctrl} = 1$) and is described in section 7.1.2.2.2. The second experiment was then scaled up to $n_{test} = 2\text{-}3$ and $n_{ctrl} = 2\text{-}3$ to test data reproducibility and is subject of section 7.1.2.2.3. The optimal times for detection of bioluminescence after substrate application were determined in an initial experiment, which is described in section 7.1.2.2.1.

7.1.2.2.1 Optimisation of bioluminescence detection

In three out of four tumors, Rluc-mediated bioluminescence dramatically decreased after the first measurement at 1 min. In contrast, Fluc-induced photon emission increased continuously until the end of the measurement at 7 min (see Figure 20). Bioluminescence detection was therefore conducted 1 min after *i.v.* application of the Rluc substrate and 7 min after intraperitoneal (*i.p.*) injection of the Fluc substrate for all subsequent experiments.

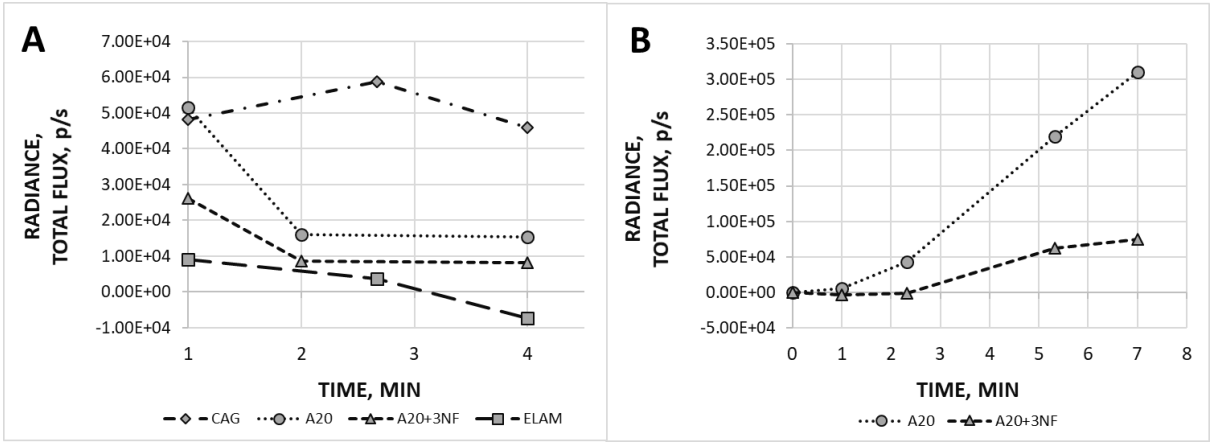

Figure 20 – Optimisation of bioluminescence detection after substrate application
Bioluminescence values at different times after substrate application for Rluc (**A**; *i.v.*) and Fluc (**B**; *s.c.*) (published in [199]).

7.1.2.2.2 In vivo bioimaging – first run

In the first run, a strong variation of Fluc signals used for normalisation was observed. Also activities of Rluc driven by the six promoters varied a lot (see Figure 21, A). The highest levels were detected in tumors containing the CAG promoter (Fluc: 5.2×10^6 p/s; Rluc: 4.29×10^5 p/s) whereas the lowest levels were found in a tumor with the hCCL2 dis/prox promoter construct (Fluc: -2.1×10^4 p/s; Rluc: -8.65×10^3 p/s). Negative values were a result of subtracting the background signal from very low measured values and these values were excluded from determining *in vivo* promoter induction (see below).

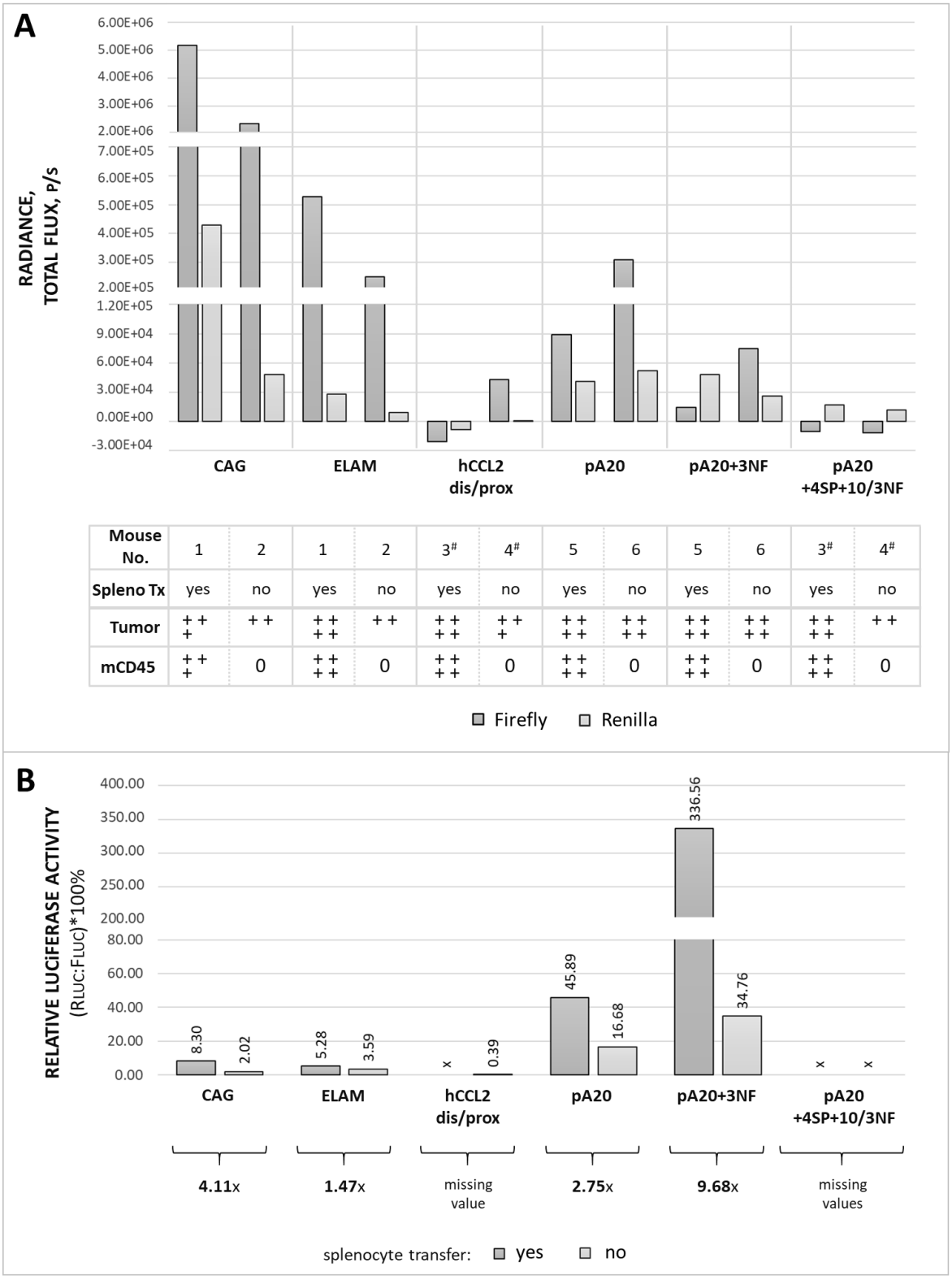

Figure 21 – Analysis of bioimaging results (first run) and evaluation of histological sections

A: Bioluminescence values induced by Fluc and Rluc after background subtraction and analysis of tumor size and immune cell infiltration from HE and mCD45 stained sections. Spleno Tx: splenocyte transfer; Tumor: tumor size; mCD45: level of immune cell infiltration. Values excluded from induction analysis due to low luminescence (radiance < 5.0×10^3 p/s) are indicated by superscript '*#*'. **B:** Rluc activities normalized to Fluc expression. *In vivo* promoter induction is given below, referring to the control group (no splenocyte transfer).

In vivo promoter inducibility in the xenograft mouse was indicated in four out of six promoters tested (see Figure 21). The CAG promoter showed a 4.1-fold increase in activity *in vivo*, markedly greater than observed *in vitro* in the SEAP reporter assays with human cytokines (hTNF: 0.9, hIL-1β: 1.7; see section 7.1.1.3, Figure 13). The relative activity of the ELAM promoter increased by a factor of 1.5 in the mouse with a reconstituted immune system compared to the animal without splenocyte transfer. In this case, promoter induction was not as strong as detected in the *in vitro* SEAP (hTNF: 5.2; hIL-1β: 3.5; see section 7.1.1.3, Figure 13) and luciferase (mTNF: 3.0, see section 7.1.2.1.2, Figure 18) reporter assays. In contrast, induction of the endogenous porcine A20 promoter by a factor of 2.8 almost perfectly correlated with the *in vitro* data (SEAP, hTNF: 2.1, see section 7.1.1.3, Figure 13; luciferase, mTNF: 2.6, see section 7.1.2.1.2, Figure 18). The A20 promoter equipped with three additional NF-κB binding sites showed a considerably higher induction than the unmodified variant (factor 9.7), promoter induction *in vivo* was more than double that *in vitro* with human TNF (SEAP, 4.0, see section 7.1.1.3, Figure 13).

7.1.2.2.3 In vivo bioimaging – second run

Data reproducibility was evaluated by performing a second run of PK-15 implantation, splenocyte transfer and *in vivo* bioimaging. Just as in the first run, Fluc signal intensities were widely scattered in the second experiment and CAG-containing tumors showed the highest Fluc luminescence values of up to 1.43×10^6 p/s. In contrast, Rluc signals of all PK-15-induced tumors were in a similar range between 4.27×10^4 p/s (ELAM) und -1.14×10^4 p/s (pA20+4SP+10/3NF). Luminescence values below 5.0×10^3 were excluded from subsequent analyses due to the proximity to the background signal.

The activity of the promoters tested was consistently higher in tumors of animals that underwent splenocyte transfer than in those of the respective control group. This confirms *in vivo* inducibility of the promoters CAG, ELAM and pA20 that was already postulated after the first bioimaging experiment. Furthermore, there is also evidence of promoter hCCL2 dis/prox being responsive to the murine cytokines. CAG promoter was induced by a factor of 5.1, even higher than in the first run (4.1, see Figure 22). The ELAM and pA20 promoters showed an increase in promoter activity by the factors 1.9 and 2.8. These correlated well with the findings of the first bioimaging experiments (ELAM: 1.5; pA20: 2.3, see Figure 22). While the CCL2

dis/prox promoter could not be evaluated in the first run, an induction by the factor 2.0 was determined in the second run. This corresponds to the findings of the SEAP assay (hTNF: 2.3; hIL-1β: 1.6, see section 7.1.1.3, Figure 13). Compared to the stimulation of the PK-15 cell clone with murine TNF *in vitro* (mTNF: 1.2; see section 7.1.2.1.2, Figure 18), hCCL2 dis/prox promoter induction within the grafted cells was even higher.

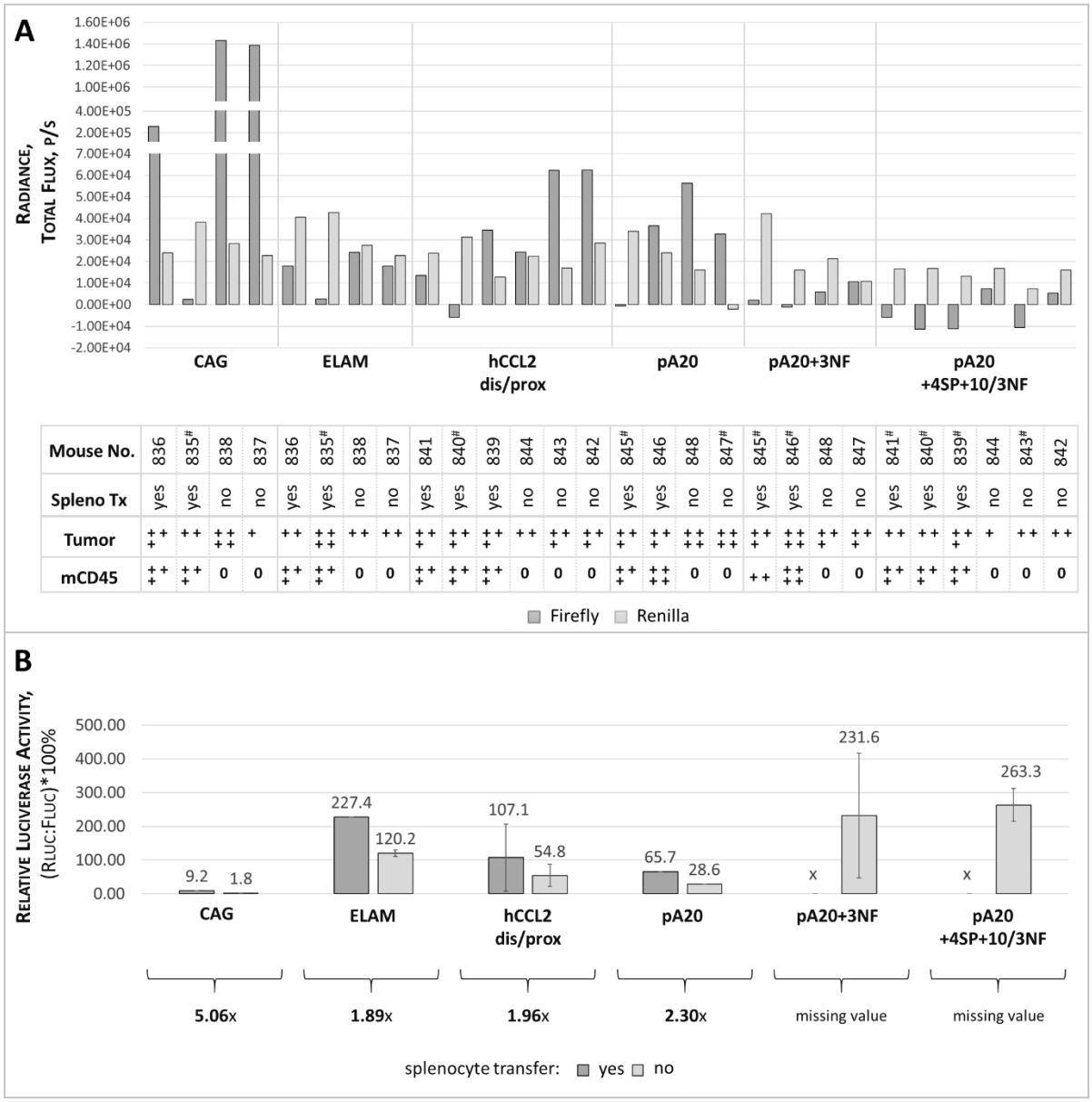

Figure 22 – Analysis of bioimaging results (second run) and evaluation of histological sections

A: Bioluminescence values induced by Fluc and Rluc after background subtraction and analysis of tumor size and immune cell infiltration from HE and mCD45 stained sections. Spleno Tx: splenocyte transfer; Tumor: tumor size; mCD45: level of immune cell infiltration. Values excluded from induction analysis due to low luminescence (radiance < $5.0x10^3$ p/s) are indicated by superscript '*#*'. **B:** Rluc activities normalized to Fluc expression ± SD. *In vivo* promoter induction is given below, referring to the control group (no splenocyte transfer).

The average *in vivo* inducibility of both bioimaging runs is visualized in Figure 23. To conclude this chapter, five out of six promoters tested were shown to be upregulated by the murine immune reaction to the xenograft. Furthermore, not only the proof-of-principle but also data reproducibility was demonstrated.

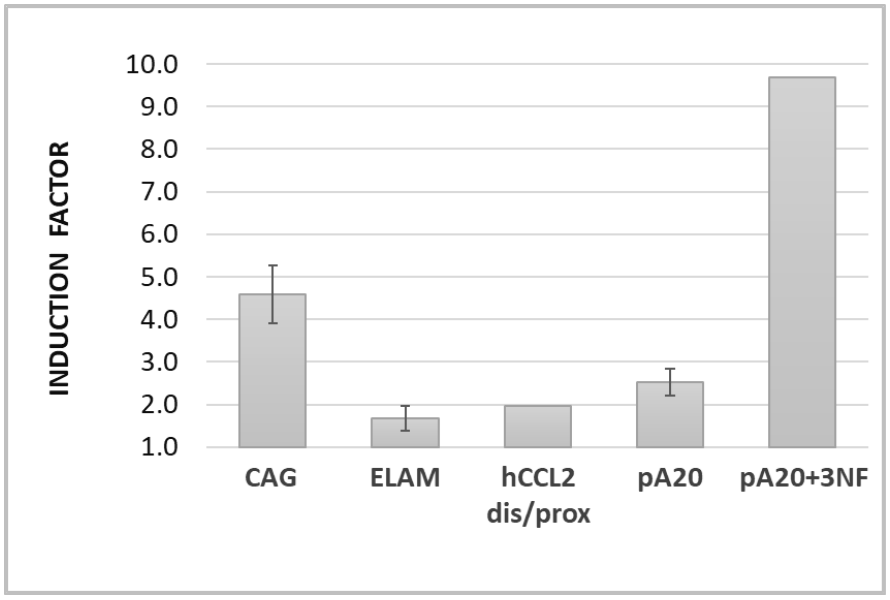

Figure 23 – Average *in vivo* promoter inducibility in the xenograft mouse model
Shown is the average x-fold upregulation of promoter activity ± SD, calculated from the first (Figure 21, B) and second (Figure 22, B) bioimaging run due to cytokine release by murine immune cells compared to the control groups (published in [199]).

7.1.3 Placement of dynamically expressed transgenes at the *ROSA26* locus

In the previous sections, different promoters have been analysed *in vitro* and *in vivo* for cytokine-dependent changes in activity. Future experiments should now clarify whether (A) dynamic transgene expression can also be achieved within organs and tissues of a transgenic pig model and (B) a biological functional concentration of xenoprotective molecules can be produced using these promoters. Two gene-targeting vectors were thus generated for placing cytokine-inducible transgene cassettes into intron 1 of the porcine *ROSA26* gene. This locus was reported to support efficient targeting in primary somatic cells and to provide ubiquitous expression of an inserted transgene [345]. The structure of the targeting vectors generated is subject of section 7.1.3.1. The results of first gene-targeting experiments are described in section 7.1.3.3.

7.1.3.1 Vectors targeting the porcine ROSA26 locus

Two promoter-trap vectors were generated to introduce cDNA sequences of *LEA29Y* and human *PD-L1* into intron 1 of the *ROSA26* gene, directed by the promoters pA20+4SP+10/3NF and ELAM. The vectors comprise a short (2.2 kb) and a long (4.7 kb) homology arm. After successful recombination, the endogenous *ROSA26* promoter drives a blasticidin resistance cassette which includes a splice acceptor sequence and a Kozak ribosome entry site. A triple polyadenylation signal prevents promoter leakage into the 3' flanking transgene cassettes. Generation of these vectors based on plasmid ROSA26-SA-BS-LA (A118, Chair of Livestock Biotechnology, TUM, GER) and is described in Appendix 13.1.3. The final constructs were called ROSA26-BS-pA20multi-LEA29Y (A133) and ROSA26-BS-pA20multi-LEA29Y-ELAM-PDL1-MIN (A166) and are depicted in Figure 24. Vector A166 was additionally equipped with a multifunctional integrase (MIN) site. Once integrated into the porcine genome, the MIN site will allow easy placement of additional transgenes using Bxb1 integrase [346]

Transgenic expression of *LEA29Y* in the donor tissue was shown to inhibit costimulation of xenoreactive T cells as described in section 4.3.3.2.3. The *LEA29Y* sequence being part of the targeting vectors A133 and A166 was kindly provided by Nikolai Klymiuk (Chair for Molecular Animal Breeding and Biotechnology, LMU, GER) and comprises the signal peptide sequence of the human *OSM* gene, portions of exons 2 and 3 of the human *CTLA4* gene (Transcript-ID:

ENST00000302823.8, Ensembl release 95) and of the human *IGHG1* gene (Transcript-ID: ENST00000390549.6, Ensembl release 95). The fully annotated *LEA29Y* sequence is given in Appendix 13.2.1.

Cells derived from h*PD-L1* (programmed cell death ligand1) transgenic pigs were shown to be less susceptible to human cytotoxic cells and have reduced potential to stimulate human $CD4^+$ T cells [203]. Human PD-L1 is thus the second xenoprotective protein encoded on targeting vector A166 and comprises exons 1 to 6 and a short part of exon 7 (Transcript-ID: ENST00000381577.3, Ensembl release 95). The complete h*PD-L1* sequence present on vector A166 is shown in Appendix 13.2.2..

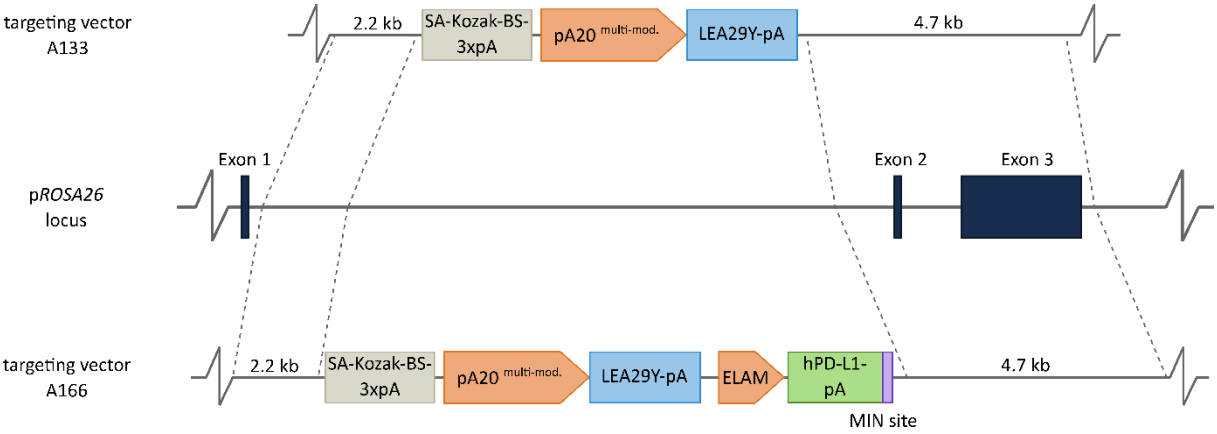

Figure 24 – Strategy to introduce dynamically expressed *LEA29Y* and h*PD-L1* genes into the porcine *ROSA26* locus

Middle: Organisation of the porcine *ROSA26* locus. Exons are indicated as dark boxes. **Top, bottom**: Promoter-trap targeting vectors A133 and A166. The transgene cassette is flanked by a short (2.2 kb) and long (4.7 kb) homology arm. A selection element – consisting of splice acceptor (SA), Kozak sequence, blasticidin S desaminase gene (BS) and a triple polyadenylation signal (pA) – facilitates selection of correctly targeted clones. The xenoprotective transgenes *LEA29Y* and h*PD-L1* are directed by pA20+4SP+10/3NF ($pA20^{multi\text{-}mod.}$) and ELAM promoter, respectively. Presence of a multifunctional integrase site (MIN) can be later used to easily place further transgenes using Bxb1 integrase.

7.1.3.2 Gene placement of LEA29Y

Primary porcine kidney fibroblasts (pKDNFs, isolates 2505 and 8616-3) were transfected in six runs with targeting vector ROSA26-BS-pA20multi-LEA29Y (A133) resulting in 519 cell clones isolated. 53 of them showed stable cell growth and were analysed for correct gene targeting using the primers depicted in Figure 25, A. Cell clones A133-138, -207, and -208 showed PCR fragments of the desired size, indicating correct homologous recombination at the short

homology arm (see Figure 25, B). As 3' targeting PCR of these clones did not provide reliable results, they were checked for integrity of the transgene cassette to be introduced (see Figure 25, C). Only the 5' portion of the transgene construct was present in clone A133-138, which was thus not used for further analyses. In contrast, DNA amplificates of the correct sizes indicated presence of the complete cassette in clone A133-207 and -208. However, both cell clones stopped growing and could therefore not be used for SCNT.

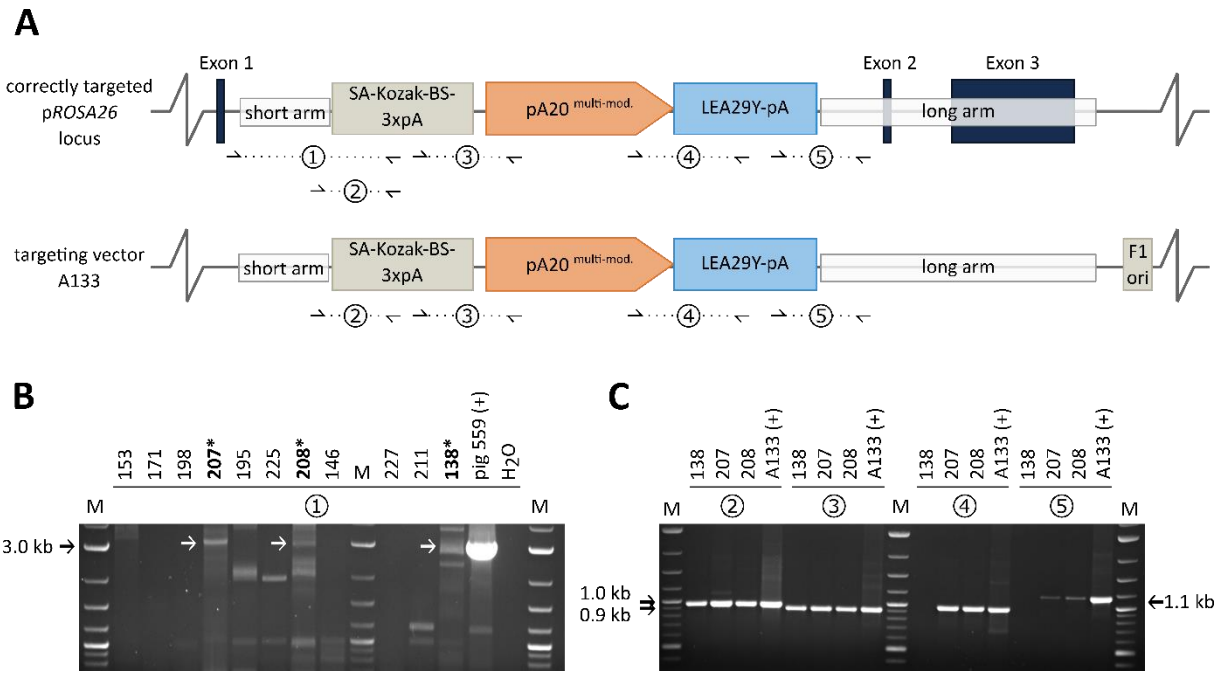

Figure 25 – Screening for positive targeting events (ROSA26-BS-pA20multi-LEA29Y, A133)
A: Correctly targeted porcine *ROSA26* locus and targeting vector A133. Exons are indicated as dark boxes. Primers used to screen A133-transfected single cell clones are displayed as black arrows connected by dotted lines. Primer combination ① is unique for correct 5' targeting and ②-⑤ bind in both, correctly targeted clones and the random integrated targeting vector A133. ①: ROSA26 I1 F2/ BS R neu, 2978 bp; ②: ROSA26 SA F7/ BS R neu, 978 bp; ③: SV40 polyA F/ pA20 prom R8, 923 bp; ④: pA20 prom F8/ LEA expr 3R, 950 bp; ⑤: LEA expr 1F/ ROSA26 LA r43 red, 1150 bp. **B:** Screening for positive 5' targeting events (①). Cell clones A133-138, -207 and -208 show DNA amplificates of the correct size. **C**: Checking the integrity of the integrated transgene cassette (②-⑤). Correct DNA fragment sizes were verified for cell clones A133-207 and -208.
SA: splice acceptor; BS: blasticidin S desaminase gene; pA: polyadenylation signal; pA20$^{multi-mod}$: promoter pA20 +4 SP-1 +10/3 NF-κB, F1 ori: origin of DNA replication of bacteriophage f1; A133: plasmid A133.

For all following transfection experiments, the vector ROSA26-BS-pA20multi-LEA29Y-ELAM-PDL1-MIN (A166) was used to enable simultaneous placement of two xenoprotective transgenes, directed by the cytokine-inducible promoters pA20+4SP+10/3NF and ELAM, and the MIN site.

7.1.3.3 Simultaneous gene placement of LEA29Y, hPD-L1 and the MIN site

PKDNF cells (isolate 8616-3) were transfected in two runs with targeting vector ROSA26-BS-pA20multi-LEA29Y-ELAM-PDL1-MIN (A166). 36 out of 155 cell clones isolated were analysed for positive targeting events using the primer combinations shown in Figure 26, A. Screening PCR of cell clone A166-54 indicated correct 5' targeting at the short homologous arm. The lack of a positive control and a sufficient quantity of high-purity DNA disabled optimisation of the long-range 3' screening PCRs (5.6 kb and 6.2 kb) which remained without specific amplificates after the first try. However, presence of the transgene cassette in the genome was verified by another PCR, spanning the 3' portion of the *LEA29Y* sequence to the middle of the h*PD-L1* construct (see Figure 26). The cell clone A166-54 was then used for SCNT that resulted in one successfully established pregnancy. However, embryos were resorbed and no piglets born. New targeting approaches will now be performed based on a highly-efficient CRISPR/Cas-based gene placement method ('CRISPlace').

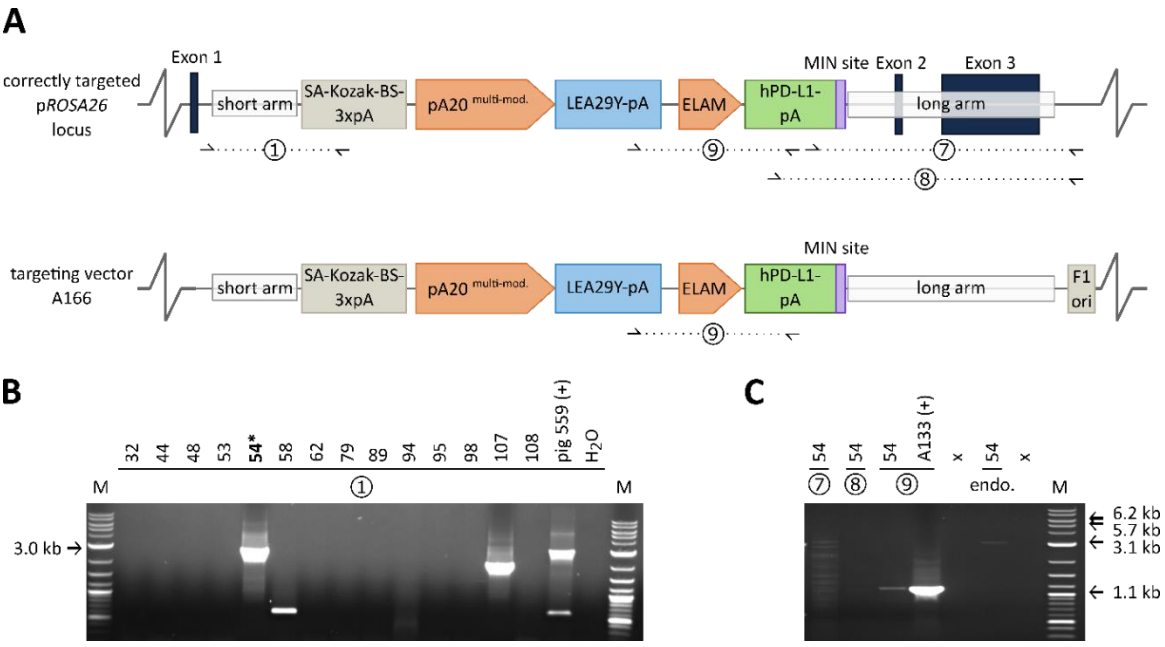

Figure 26 – Screening for positive targeting events (ROSA26-BS-pA20multi-LEA29Y-ELAM-PDL1-MIN, A166)
A: Correctly targeted porcine *ROSA26* locus and targeting vector A166. Exons are indicated as dark boxes. Primers used to screen A166-transfected single cell clones are displayed as black arrows connected by dotted lines. Primer combinations ①, ⑦ and ⑧ are unique for correct targeting and ⑨ binds in both, correctly targeted clones and the random integrated targeting vector A166. ①: ROSA26 I1 F2/ BS R neu, 2978 bp; ⑦: hPDL1 F1/ ROSA26 I3 R2, 5681 bp; ⑧: hPDL1 E2-E3 F1/ ROSA26 I3 R2, 6177 bp; ⑨: LEA Expr 1F/ hPDL1 R1, 1133 bp. **B:** Screening for positive 5' targeting events (①). Cell clone A166-54 shows a DNA fragment of the correct size. **C:** Screening for positive 3' targeting events (⑦, ⑧) and presence of one transgene cassette section ⑨. Homologous recombination into the long arm region could not be finally verified, but presence of the transgene

cassette was proven for clone A166-54. Endo.: endogenous pROSA26 locus, ROSA26 I1 F2/ ROSA26 I1 R3, 3105 bp.
SA: splice acceptor; BS: blasticidin S desaminase gene; pA: polyadenylation signal; $pA20^{multi\text{-}mod}$: promoter pA20+4SP+10/3NF, MIN site: multifunctional integrase site, F1 ori: origin of DNA replication of bacteriophage f1.

7.2 Multi-knockouts for xenograft improvement

The first project of this thesis was to identify suitable promoters for future transgene expression in genetically modified pigs. Experiments for gene addition have already been performed to create Smart Graft donors. This chapter focusses on inactivation of various genes to enhance immunological and anatomical compatibility between organ donor and recipient: *CMAH*, *GGTA1* and *B4GALNT2* to reduce antibody-mediated rejection processes, *ASGR1* to decrease xenogeneic hepatic degradation of human thrombocytes, *ULBP1* to provide protection against NK cells, *SLA-1*, *SLA-2*, *SLA-3* or *B2M* to inhibit activation of xenoreactive cytotoxic T cells and *GHR* to reduce the size of the donor organs.

The first aim was to identify and evaluate sgRNA target recognition sites for inactivation of xenorelevant genes (section 7.2.1). Some of these and other sgRNA sequences were then incorporated into two multi-knockout vectors (section 7.2.2) and used to induce multiple gene-inactivations in primary porcine cells for subsequent generation of multi-knockout pigs by SCNT (section 7.2.3).

7.2.1 Selection and evaluation of sgRNA target recognition sites

CRISPR/Cas9-mediated knockouts require a sgRNA target recognition site within a translated exon which is shared by all known protein-coding transcripts. All exons of the genes-of-interest were thus annotated using cDNA sequence information provided by Ensembl Genome Browser (Ensembl Release 95) and National Center for Biotechnology Information (NCBI, annotation release 106).

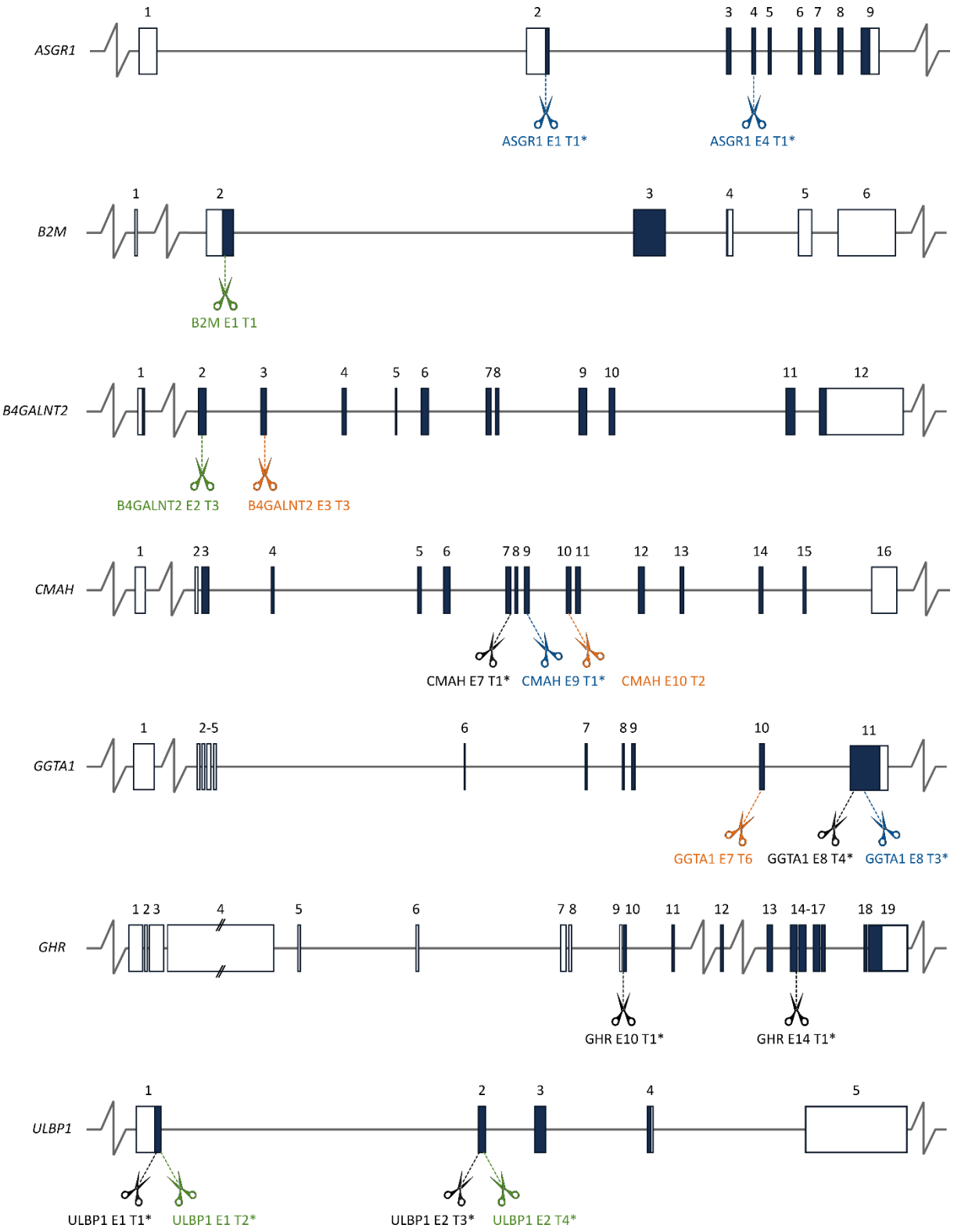

Figure 27 – sgRNA target recognition sites to inactivate *ASGR1*, *B2M*, *B4GALNT2*, *CMAH*, *GGTA1*, *GHR* and *ULBP1*

Exons translated in all known transcripts are marked as black boxes. Any other exons are represented by white boxes. Scissors symbols indicate the positions of sgRNA target recognition sites. Red, blue and green scissors: targeted by multi-knockout vector A190, A191 and A192, respectively (section 7.2.3). Target sites analysed individually in pKDNF cells (section 7.2.1) are marked with an asterisk.

Up to four sgRNA target recognition sites were designed per gene (*ASGR1*, *CMAH*, *GGTA1*, *GHR*, *ULBP1*; see Figure 27) and cloned each into the vector px330-MCS-T2A-Puro-847 (A141) carrying the sgRNA scaffold and *SpCas9* gene. The plasmids were transiently transfected into pKDNF cells (isolates: 2505, 8616-3, 120419-1/7) and functionality of all CRISPR guides was verified using the webtool TIDE. The primer combinations used for pool analyses and sanger (see Table 29) sequencing are listed in Appendix 13.3.1. Design, cloning and analysis of sgRNA sequences targeting *ULBP1* were conducted by Katharina Rinke (Bachelor's student) [347].

Table 29 – InDel frequencies in pKDNF cell pools after sgRNA-Cas9 transfection and puromycin selection
Analysis using TIDE webtool. SgRNA target recognition sites designed by: [a] Beate Rieblinger (Chair of Livestock Biotechnology, TUM, GER), [b] Bao *et al.* 2014 [348], [c] Katharina Rinke (Bachelor's student), [d] identified by agarose gel electrophoresis.

Target site	pKDNF isolate no.	InDel frequency	R^2 value
ASGR1 E1 T1	2505	17.6%	0.91
	8616-3	48.2%	0.78
ASGR1 E4 T1[a]	2505	90.0%	0.94
	8616-3	53.5%	0.84
CMAH E9 T1	2505	>100 bp insertion[d]	-
	8616-3	42.5%	0.71
CMAH E7 T1	2505	46.0%	0.88
	8616-3	13.2%	0.97
GGTA1 E8 T3[a]	2505	25.5%	0.92
	8616-3	66.0%	0.82
GGTA1 E8 T4[b]	8616-3	59.5%	0.91
GHR E10 T1	2505	98.7%	0.99
	8616-3	47.9%	0.95
GHR E14 T1	2505	79.7%	0.90
	8616-3	46.9%	0.95
ULBP1 E1 T1[c]	120419-1	24.2%	0.93
	120419-7	25.2%	0.92
ULBP1 E1 T2[c]	120419-1	48.4%	0.96
	120419-7	51.8%	0.88
ULBP1 E2 T3[c]	120419-1	9.3%	0.98
	120419-7	5.4%	0.99
ULBP1 E2 T4[c]	120419-1	49.4%	0.98
	120419-7	54.3%	0.98

7.2.2 Generation of multi-knockout vectors

Having verified guide functionality (see section 7.2.1), two multi-knockout vectors were generated with sgRNAs binding within *ASGR1* exon 2 and 4 (ASGR1 E1 T1, ASGR1 E4 T1), *CMAH* exon 7 (CMAH E7 T1), *GGTA1* exon 11 (GGTA1 E8 T3) and *ULBP1* exon 1 and 2 (ULBP1 E1 T2, ULBP1 E2 T4). Additionally, guides binding within *B2M* exon 2 (B2M E1 T1) and *B4GALNT2* exon 2 (B4GALNT2 E2 T3), published by Estrada *et al.*, were used [100]. The high-efficiency guides targeting *GHR* were not required at this point but are available for future experiments.

Specific sgRNA oligonucleotides with additional BbsI overhangs were subcloned into plasmid pSL1180-U6-MCS-tracRNA-756 (A142) that carries a 0.2 kb U6 promoter followed by a BbsI restriction site and the sgRNA scaffold sequence. Restriction fragments were sequentially cloned into plasmid px330-MCS-T2A-Puro-847 (A141) (K. Rinke). The two final vectors (px330-GGTA1E8T3-CMAHE9T1-ASGR1E1T1-ASGR1E4T1-Puro, A191; px330-B2ME1T1-ULBP1E1T2-ULBP1E2T4-B4GALNT2E2T3-Puro, A192) contained four sgRNA sequences with individual U6 promoters and a 4.2 kb h*SPCas9* gene driven by a 0.8 kb chicken β hybrid (CBH) promoter as depicted in Figure 28. Detailed cloning procedure is described in Appendix 13.3.2.

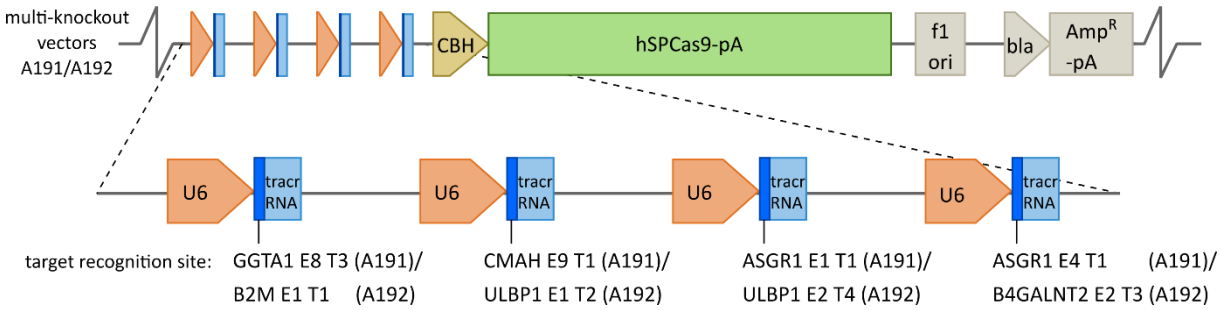

Figure 28 – Structure of the multi-knockout vectors A191 and A192
The vectors were designed to specifically recognize four different genomic loci each. CBH: chicken β hybrid promoter; hSPCas9: humanized *Streptococcus pyogenes* Cas9 gene; f1 ori: origin of DNA replication of bacteriophage f1; bla: beta lactamase promoter; Amp: Ampicillin resistance gene; pA: polyadenylation signal; U6: RNA polymerase III promoter U6; tracrRNA: trans-activating CRISPR (cr)RNA.

7.2.3 Generation of multi-knockout cells for SCNT

The vectors A191 and A192 described in chapter 7.2.2 (see Figure 28) were used to inactivate multiple genes in primary porcine cells to generate multi-knockout pigs by SCNT. They were transfected simultaneously with a third vector px330-B4GALNT2E3T3-CMAHE10T2-GGTA1E7T6-MHCIE4T1-MHCIE4T2-Puro (A190, Chair of Livestock Biotechnology) into pKDNF

cells (isolates 120419-1/7). In each case, two different sgRNA sequences were used for *ASGR1*, *B4GALNT2*, *CMAH*, *GGTA1* and *ULBP1* to increase the probability of a functional knockout. One guide recognising *B2M*, which encodes the β-light chain of SLA class I, and two guides binding in *SLA-1*, *SLA-2* and *SLA-3*, coding for the α-heavy chain, (see Figure 29) were used to inactivate the SLA class I complex.

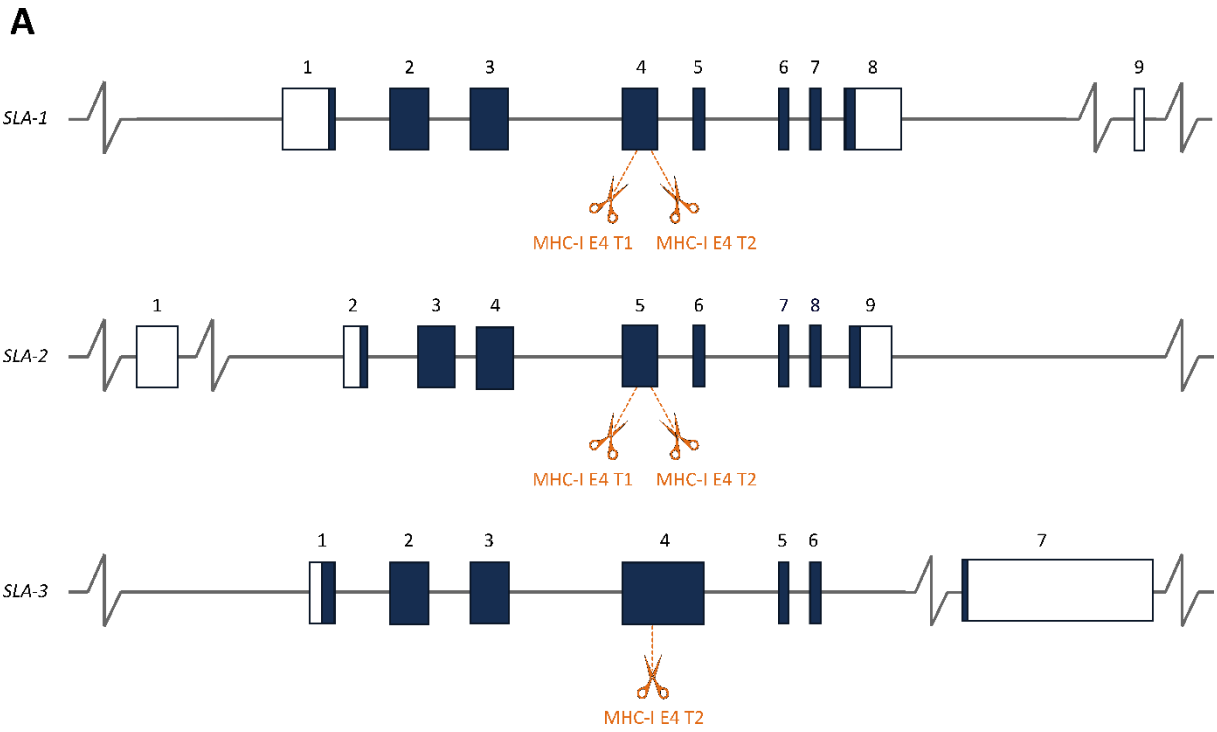

Figure 29 – sgRNA target recognition sites to inactivate the α-heavy chain of porcine MHC class I (SLA-I)
The sgRNA sequences MHC-I E4 T1 and MHC-I E4 T2 on vector A190 bind to conserved sequences within *SLA-1*, *SLA-2* and *SLA-3* that encode the α-heavy chain of the porcine MHC class I (SLA-I). Exons translated in all known transcripts are marked as black boxes. Any other exons are represented by white boxes. Scissors symbols indicate the positions of sgRNA target recognition sites.

After antibiotic selection, knockout cells were enriched for *GGTA1* and SLA-I inactivation. This enrichment strategy has already been used in the past to successfully generate viable pigs with four-fold knockouts [110]. Gene editing was then determined in two cell pools by sequencing across the sgRNA target recognition sites and subsequent TIDE analysis (see Table 30). Selection and enrichment resulted in a very high frequency of InDel mutations in *GGTA1* (up to 98.7%) and *B2M* (up to 98.0%). High gene editing rates were also detected for most of the other target genes: Up to 96.0% for CMAH, 95.5% for ASGR1, 84.1% for ULBP1 and 80.5% for B4GALNT2. The mutation frequency of *SLA-1* (MHC-I E4 T1) was up to 26.5%. However,

detailed SLA-I analysis would have required subcloning and sequencing of specific sgRNA target recognition sites due to the high sequence similarity of SLA-1, SLA-2 and SLA-3.

Table 30 – InDel frequencies in pKDNF cell pools after transfecting multi-knockout vectors A190, A191 and A192

InDel frequencies analysed using TIDE webtool after puromycin treatment and counter-selection for αGal- and SLA-I-deficiency. The primer used are given in Appendix 13.3.1. [a] no detection possible, [b] analysis of *SLA-1.*

Target site	pKDNF isolate no.	InDel frequency	R^2 value
ASGR1 E1 T1	120419-1	63.1%	0.65
	120419-7	95.8%	0.96
ASGR1 E4 T1[a]	120419-1	x	x
	120419-7	x	x
B2M E1 T1	120419-1	85.0%	0.97
	120419-7	98.0%	0.99
B4GALNT2 E2 T3	120419-1	80.3%	0.80
	120419-7	74.6%	0.79
B4GALNT2 E3 T3	120419-1	13.2%	0.97
	120419-7	10.3%	0.97
CMAH E9 T1	120419-1	96.0%	0.99
	120419-7	75.7%	0.97
CMAH E10 T2	120419-1	24.7%	0.99
	120419-7	32.6%	0.99
GGTA1 E7 T6	120419-1	98.7%	0.99
	120419-7	97.3%	0.98
GGTA1 E8 T3	120419-1	94.0%	0.99
	120419-7	98.0%	0.98
ULBP1 E1 T2	120419-1	28.9%	0.95
	120419-7	84.1%	0.84
ULBP1 E2 T4	120419-1	30.7%	0.94
	120419-7	42.0%	0.59
MHC-I E4 T1[b]	120419-1	24.7%	0.79
	120419-7	26.5%	0.28
MHC-I E4 T2[a, b]	120419-1	x	x
	120419-7	x	x

In summary, the probability of multiple, functional knockouts was optimized by different factors: (A) pre-selection of the most efficient sgRNAs, (B) usage of two guide sequences per target gene, (C) enrichment of cells with *GGTA1*/SLA-I double-knockout and (D) manipulating the SLA-I complex using guides against the α- and β-chain genes. The cell pools are now available for SCNT.

8. DISCUSSION

8.1 Cytokine-inducible promoters for dynamic transgene expression

T lymphocytes were described to damage a porcine xenograft by direct cytotoxic activity of the CD8+ subpopulation, the production of cytokines priming the innate immune system, and the ability of CD4+ T cells to provide help for B cells to produce xenoreactive antibodies [65]. Inactivation of SLA class I molecules by CRISPR/Cas9 and reduction of SLA class II proteins by expressing mutCIITA are promising approaches to attenuate the direct T cell response to the porcine graft [108, 110, 186]. However, additional strategies are required to inhibit xenoreactive T cell activity that is induced by donor-derived peptides presented by human APCs, such as transgenic expression of the inhibitory ligand hPD-L1 or costimulation blockade via the CD154-CD40 pathway using extensive anti-CD154 or anti-CD40 antibody therapy [349, 350]. Potent immunosuppressive effects can also be achieved by direct inhibition of the CD28-CD80/86 co-stimulatory pathway using an artificial, soluble form of the cytotoxic T lymphocyte-associated antigen 4 (CTLA4) molecule. CTLA4 is a high-affinity CD28 homolog and binds to the CD80/CD86 (B7) receptors on APCs, directly preventing T cell activation [351, 352]. Recombinant CTLA4 fusion proteins (Abatacept or the affinity-enhanced variant Belatacept) are used for several clinical immunosuppressive regimens and post-operative follow ups after allotransplantation [353]. Transgenic expression of soluble CTLA4 in pigs was performed by combining the extracellular domain of porcine or human CTLA4 with a human IgG1 Fc domain (CTLA4-Ig) [194, 197]. As porcine CTLA4-Ig compared to human CTLA4-Ig contains a leucine to methionine substitution at position 97 in the MYPPPY motif, it binds inefficiently to human CD80/CD86 and shows a weaker inhibition of the xenogeneic human T cell response [354, 355]. LEA29Y is a high-affinity hCTLA4-Ig variant that causes slower dissociation rates for CD80/CD86 and a 10-fold increase in potency *in vitro* compared to hCTLA4-Ig [190]. Pigs with ubiquitous expression of pCTLA4-Ig or hCTLA4-Ig (LEA29Y), however, showed a very similar phenotype, e.g. developmental abnormalities due to exposure to these molecules *in utero*, acute susceptibility to opportunistic pathogens and diminished humoral immunity, and were dependent on prophylactic antibiotic treatment [194, 195].

The work presented here comprises a unique method to drive dynamic transgene expression. As discussed in the following sections, former approaches focused on constitutive promoters that provided high and in some cases ubiquitous expression of foreign genes. However, especially immunomodulatory transgenes such as *LEA29Y* should not always be expressed at high levels. Alternative approaches were based on tissue-specific promoters to reduce detrimental effects on the immune system. Our new strategy can provide high and ubiquitous transgene expression without provoking negative effects on the host's immune response.

8.1.1 Constitutive and inducible transgene expression

8.1.1.1 Viral, hybrid (CAG) and mammalian promoters

Viral, hybrid and mammalian promoters of different species have been commonly used to express human proteins in transgenic pigs. Widely used viral promoters include the cytomegalovirus (CMV) and the simian virus 40 (SV40) promoters. Both were reported to provide high expression levels and to be suitable for transient or stable expression of exogenous genes *in vitro* [356, 357]. However, the use of viral promoters *in vivo* faces the risk of a strong variation in tissue-specific expression levels up to complete promoter silencing due to extensive promoter methylation [147, 358]. Moreover, the use of these promoters for xenotransplantation is less promising as they can be downregulated by inflammatory cytokines such as IFNγ [359].

The hybrid promoter CAG, consisting of the viral CMV enhancer element, the chicken β-actin promoter and the rabbit globin intron, is frequently used for transgene expression in xenotransplantation research and seem to be best suited for constitutive, ubiquitous expression at high levels [147, 360-365]. However, especially immunomodulatory proteins such as LEA29Y require more precise gene regulation as excessive protein synthesis causes a severe immune-compromised health status of the animals [194, 195].

In the field of xenotransplantation, human and porcine promoters, with sequence lengths up to 40 kb, were commonly used to drive genomic sequences of the human complement regulatory proteins CD46, CD55 and CD59 [84, 147, 365-367]. Depending on the length of the chosen sequence, these promoters can comprise a maximum of regulatory elements enabling biological expression patterns. The usage of certain mammalian promoters, in contrast to viral

and hybrid ones, is also suitable to provide tissue-specific transgene expression at high levels, reducing side-effects at the same time. Therefore, strategies for tissue-specific expression of CTLA4-Ig/LEA29Y were developed. Driving a hCTLA4-Ig construct by the neuron-specific enolase promoter, for example, limited transgene expression to corneal keratocytes and various areas of the brain, and LEA29Y expression restricted to pancreatic islet-cells was achieved using the core promoter of the porcine insulin gene [196-198, 368]. This reduces systemic effects but requires a new pig line for each organ.

8.1.1.2 Antibiotic-inducible systems

The antibiotic-controlled Tet-On and Tet-Off systems are alternative means to enable transgene expression at the favoured time point(s) [369, 370]. Both systems are based on regulatory elements originally identified for control of the tetracycline resistance cassette in bacteria. The Tet technology requires (A) a synthetic promoter (P_{tet}) with proximal *tetO* operator elements driving the gene-of-interest (GOI) and (B) a transgene encoding a transactivator protein that binds to *tetO* thereby activating P_{tet} and inducing transcription of the GOI. The DNA-binding properties of the transactivator can be altered by binding of tetracycline-derivates, such as doxycycline, in a positive (Tet-On) or negative (Tet-Off) way [371]: The Tet-On system allows antibiotic-controlled activation of gene expression, whereas the Tet-Off approach is used for silencing the transcription of the GOI [372]. Both systems have been used intensively for various applications in mice but also used in pigs to e.g. regulate *EGFP* expression [371, 373]. However, Tet-On and Tet-Off seem to be less suitable to control the expression of immunomodulatory transgenes in the context of xenotransplantation, since in both cases either the human recipient or the donor animal would have to be permanently treated with doxycycline, which is used as a broad-spectrum antibiotic in medicine. This can cause adverse reactions including gastrointestinal disorders, thrombocytopenia, infections of mucous membranes by other bacteria or yeast fungi, irreversible tooth discoloration and toxic injury of liver and kidney [374, 375]. To avoid these undesired side-effects, cytokine-responsive promoters can be used as a feasible alternative for inducible and gradual transgene expression in xenotransplantation.

8.1.1.3 Cytokine-inducible promoters

The rationale to use promoters responding to pro-inflammatory cytokines is based on the fact that (A) enduring expression of immune-modulatory molecules at high levels can have severe side-effects on the porcine health status and (B) expression of these transgenes should actually only be induced upon inflammation as a signal for beginning rejection. As inflammation is triggered by cytokine release, the chosen promoters have to contain cytokine-responsive elements such as NF-κB binding sites. In the best case, the basal promoter activity should be very low, almost close to zero, to prevent immunomodulatory effects for the pigs. After xenotransplantation and initial rejection responses in the human, the promoter has to respond to cytokine release within a short time frame to prevent graft damage and to inhibit further rejection responses. Therefore, the ideal promoter should possess a strong induction potential and mediate a powerful expression of the transgene after cytokine stimulation. The concept of a cytokine-inducible transgene expression within a Smart Graft was initially tested and evaluated in this work.

8.1.2 Selection of candidate promoters to implement the Smart Graft strategy

Promoters of genes known to be involved in inflammatory processes were chosen for initial experiments to determine promoter activity and cytokine-responsiveness *in vitro*. In a native chromatin environment, gene induction by inflammatory stimuli is generally supported by the promoter itself, spanning the transcription initiation site (core promoter) and containing proximal regulatory elements, and distal enhancers that come close to the promoter by looping out interjacent DNA sequences [376, 377]. The promoter sequences selected here were not longer than 3 kb to facilitate cloning, transfection and future gene targeting while still covering an adequate number of regulatory elements [376]. The NF-κB binding sites present in all candidate promoters are the basic requirement for rapid inducibility by TNF and IL-1β, the key pro-inflammatory cytokines also released during emerging xenograft rejection.

8.1.3 *In vitro* characterisation of candidate promoters

Three human, one porcine and one semi-synthetic promoters were considered as candidates to implement the Smart Graft strategy. The ELAM promoter from plasmid pNiFty with three

endogenous and five additional binding sites, the native human CCL2 and porcine A20 promoters showed significant responsiveness to human TNF with medium (ELAM, hCCL2 2.9 kb) and low (pA20) basal activity. It is still unclear which basal expression of T cell regulatory genes will be tolerated without causing immuno-deficiencies and which levels are necessary to inhibit xenograft rejection. A variety of cytokine-inducible promoters, based on hCCL2 and pA20, was thus generated with low to high basal and inducible activity.

CCL2, also known as monocyte chemotactic protein 1 (MCP-1), is a chemokine produced by a variety of cell types in response to viral infection and oxidative stress and plays a role in recruiting monocytes and other immune cells [378, 379]. Regulation of human CCL2 expression has been intensively studied in previous reports and was described to be largely dependent on NF-κB as well as AP-1 [318-321, 380]. The heterodimeric transcription factor AP-1 can be activated upon exposure to TNF and IL-1β either post-translationally via mitogen-activated protein kinase (MAPK) pathways or by NF-κB-mediated expression of AP-1 subunits [381-384]. The importance of the individual transcription factor binding sites on hCCL2 promoter induction, however, varied depending on the stimulating agent (e.g. TNF/IL-1β, LPS, bacteria, protein kinase C stimulators) and the cell type used [318-321, 380]. In this work, the distal NF-κB binding sites, that were shown to be important for cytokine-responsiveness in murine embryonic fibroblasts and human tumor cell lines, were relocated closer to the proximal hCCL2 promoter by deleting 2.4 kb of the interjacent DNA sequence [319, 385]. Although one out of three AP-1 binding sites was removed, promoter activity was dramatically enhanced in pKDNFs after challenge with hTNF and hIL-1β.

The ubiquitin-editing enzyme A20 is an inhibitor of NF-κB activation and expressed upon stimulation by e.g. pro-inflammatory cytokines as well as bacterial and viral products that are mediated by NF-κB [139, 386]. Transcription control of the human A20 gene has been well described previously. Ubiquitous SP-1 transcription factors bound to GC-rich consensus sequences within the promoter enable association of the general transcription apparatus to the TATA-less core promoter, while DRB sensitivity-inducing factor (DSIF) inhibits mRNA elongation [325, 326]. Under basal conditions, DSIF is controlled by the E-box protein upstream stimulatory factor 1 (USF1) that binds closely upstream of two NF-κB recognition sites. After NF-κB induction by cell stimulation, USF1 is displaced from the human A20 promoter, NF-κB and the core promoter gain control over DSIF and gene transcription is

continued [326]. Gene regulation of porcine A20 has not been studied so far. However, high sequence identity between the human and the porcine A20 promoter indicates homologous control of gene expression. SP-1 was reported to modulate basal expression levels of some NF-κB-regulated genes and also to increase promoter activity in response to TNF [317, 319]. In this work, integration of additional clusters of SP-1 recognition sites next to the endogenous one did not influence cytokine-inducibility of the porcine A20 promoter. The addition of NF-κB binding sites several hundred bp upstream the transcription start site and/or adjacent to the existing ones, in contrast, increased responsiveness to TNF and conferred sensitivity to IL-1β. Also, basal expression was increased in some pA20 promoter variants. As expected, inducibility of the pA20 promoter could not be enhanced indefinitely, since the interplay between basal and specific transcription factors with the RNA polymerase is quite complex.

8.1.4 Cell line PK-15 for bioimaging analyses

PK-15 is a spontaneously immortalized cell line that originates from an adult porcine kidney. This cell line was chosen for the *in vivo* promoter analyses because PK-15 cells showed stable engraftment and cell growth after transplantation into NSG mice. Infiltration of the graft by murine immune cells after reconstitution of the immune system was another essential prerequisite for successful evaluation of promoter inducibility *in vivo*. The additionally tested ST cell line, in contrast, did not provide these desired properties.

Despite precise injection of a defined cell number, the PK-15-induced tumors showed morphological variations such as size, shape and structure (see Figure 30). Tumors with larger surface showed deeper penetration by murine immune cells. Consequently, *in vivo* promoter induction might have been stronger in these tumors. The use of several animals per examined promoter was therefore important to minimize the effect of tumor morphology on promoter activation.

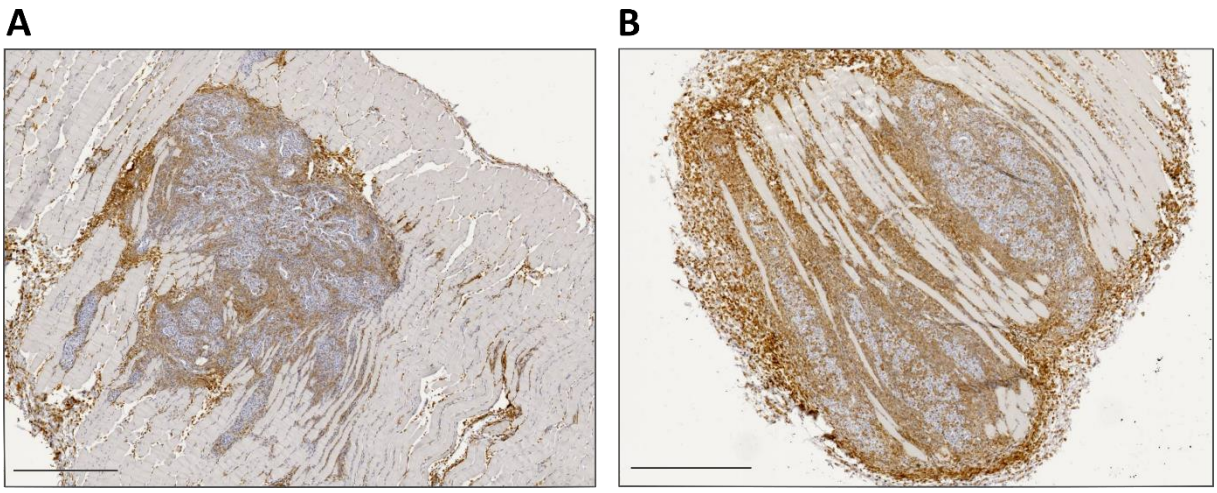

Figure 30 – Section of graft sites after immune cell infiltration
Examples for roundish-compact (A, mouse 839, CCL2 dis/prox) and long-shaped (B, mouse 840, pA20+4SP+10/3NF) appearance of PK-15-induced tumors. Shown in brown: CD45-positive immune cells. Scale bar: 500 µm.

The genetic instability of the PK-15 cell line, previously reported by Fiebig *et al.*, however, might be the reason for missing Fluc signals especially observed in pA20+4SP+10/3NF bearing cells during both runs of bioimaging [342]. It was already noticed during preselection of the clones that an average of 70% (ranging from 34% to 82%) showed damage of the Fluc cDNA. It can only be speculated whether the relatively high GC content (59%) or comparatively large length of Fluc cDNA (1.7 kb) was the reason for the preferred damage within this section of the construct. Since all clones used for *in vivo* promoter evaluation had been checked in advance for integrity and functionality of the dual luciferase cassette, the damage to the Fluc sequence must have occurred either during cell cultivation in preparation for transplantation or directly in the mouse itself.

8.1.5 Mouse xenograft model for *in vivo* promoter analyses

In two independent runs of *in vivo* bioimaging, five out of six selected promoters were shown to be activated by the murine immune system in a mouse xenograft model. Indeed, the *in vivo* induction levels of almost all promoters were similar or even considerably stronger than detected after challenge with human TNF or IL-1β in the *in vitro* cell culture experiments. This observation might be explained by the fact that TNF and IL-1β are both released by the murine immune cells and thus initiate NF-κB-dependent promoter activation simultaneously via two

signalling pathways. It is also known from clinical and experimental research that recipients of allo- or xenografts show expression of IL-17 during acute rejection episodes [173, 387-390]. This cytokine with multiple pro-inflammatory functions is produced by Th17 cells and is another activator of NF-κB that probably has contributed to the induction of the Smart Graft promoters in the mouse [391, 392]. In contrast, other factors that activate NF-κB independently of immune cells, such as potential hypoxia within the PK-15-induced tumors and secreted growth hormones, do not explain the stronger promoter induction *in vivo*, since these are also present in the group of control animals. It can be assumed that inducibility of the tested promoters will be even stronger after transplantation of a Smart Graft into a human recipient than observed in the mouse model, since the effects of murine IL-1β on NF-κB-dependent gene activation *in vitro* was considerably weaker than of the human variant.

8.1.6 Introducing cytokine-responsive transgene cassettes into the porcine *ROSA26* locus

After testing the Smart Graft strategy *in vitro* and in a murine xenograft model, feasibility of dynamic gene expression in organs and tissues must be investigated in a transgenic pig model and the appropriate promoter activity for biological functional concentrations of protective molecules identified in follow-up experiments. In addition to the choice of promoter sequences, however, other factors such as the number of transgene cassettes inserted and the site(s) of DNA integration will affect the expression level in the animal. I thus decided against a random integration approach and opted for targeted introduction of the cytokine-inducible constructs into the porcine *ROSA26* locus.

The *ROSA26* locus has been used in many species as an integration site for exogenous DNA to generate genetically modified animals, including mice, rats, cattle, sheep and pigs [295, 345, 393-397]. Foreign genes placed at this permissive chromatin region are stably expressed without causing gene disruption or alteration through insertional mutagenesis. Besides using the endogenous *ROSA26* promoter for ubiquitous transgene expression at a medium level, this locus also supports tissue-specific or antibiotic-controlled expression when exogenous promoter sequences or transcriptional regulatory elements are used [398-400]. These findings suggest that *ROSA26* may also enable cytokine-inducible transgene expression. Our group demonstrated that independently expressed transgenes can be placed into porcine *ROSA26*

by a serial re-targeting approach [364]. This allows, when required, the exchange of existing sequences and addition of further transgenes at the same integration site to generate an optimal xeno-donor and to predict the inheritance of all transgenes.

However, the re-targeting strategy is a time-consuming procedure. Therefore, one of the two targeting vectors generated here was additionally equipped with a MIN tag, which is a special phage attachment site (attP) recognized by the serine integrase Bxb1. Once integrated into the porcine genome, the MIN site allows precise and highly efficient introduction of further transgene cassettes by Bxb1-mediated recombination between MIN tag and a bacterial attachment (attB) site at the donor-DNA construct [346].

The promoter variant pA20+4SP+10/3NF was used to control the expression of *LEA29Y* as it showed a comparatively low basal activity with a moderate to strong responsiveness to hTNF and hIL-1β in the cell culture experiments. The ELAM promoter, having shown similar properties to pA20+4SP+10/3NF, was chosen to drive hPD-L1 expression. In contrast to LEA29Y, overexpression of hPD-L1 has no impact on the health of the transgenic pig due to absent functional interaction with pPD-1 [203]. Nevertheless, a low basal concentration of hPD-L1 in the human recipient is favourable to minimize the risk of impairing the patient's general immune status.

In this work, cytokine-responsive transgene cassettes were successfully introduced into the porcine *ROSA26* locus. However, the number of transfection experiments and cell clones isolated has to be further increased, since gene targeting through homologous recombination remains a very rare event. A reasonable number of positive cell clones is required to enhance the chance of living transgenic offspring by SCNT.

8.1.7 Subsequent investigations on Smart Graft pigs

After successful generation of Smart Graft piglets using the targeting vectors presented here, some further investigations will be conducted. First, tissues and organs will be screened for basal transgene transcription by RT-PCR. The detailed pattern of basal transgene expression will then be characterized by immunohistochemistry at protein level.

Cytokine-dependent expression of *LEA29Y* and *PD-L1* at the porcine *ROSA26* locus will be investigated in Smart Graft cell isolates, e.g. AECs and fibroblasts. Cell treatment can thereby be conducted with recombinant human TNF and IL-1β or alternatively a cytokine mixture produced by activated human leukocytes to cover a broader spectrum of potentially stimulating molecules. Upregulated transgene expression will then be detected by quantitative PCR (qPCR) or ddPCR on transcript level. Enzyme-linked immunosorbent assays (ELISA) and flow cytometry analyses will be additionally used to determine altered LEA29Y and PD-L1 protein levels after cytokine challenge.

Another question to be clarified is whether the promoter strengths of pA20+4SP+10/3NF and ELAM are suitable to produce biologically functional concentrations of LEA29Y and PD-L1. Therefore, the inhibitory effect of cytokine-triggered transgene expression on human T cell proliferation will be analysed after incubation with stimulated peripheral blood mononuclear cells (PBMCs) of Smart Graft pigs. The susceptibility of cytokine-stimulated Smart Graft fibroblasts to leukocyte-mediated lysis will additionally be investigated by *in vitro* cytotoxicity assays with human PBMCs. For both experiments, the results published by Buermann *et al*. where the CAG promoter was chosen to control h*PD-L1* expression in transgenic pigs could serve as a benchmark [203].

Combined expression of *LEA29Y* and h*PD-L1* may be of special interest for islet xenotransplantation, since T cell-mediated rejection is the major cause of porcine islet loss [180, 181]. Both molecules reduce the activity of xenoreactive T cells: While LEA29Y directly inhibits T cell activation by blocking co-stimulatory interactions, hPD-L1 transmits suppressive signals to already activated T cells and stimulates proliferation of Tregs as well, that were shown to play a role in the induction and maintenance of allogaft tolerance [202, 204]. Pig-to-primate transplantation of LEA29Y or hPD-L1 expressing pancreatic islets have not been reported so far. However, porcine β-cells transgenic for LEA29Y showed long-term survival in humanized mice without immunosuppressive therapy [198]. Also, allotransplantation studies with mice have recently demonstrated that overexpression of PD-L1 prevented immune rejection of murine islets [401]. The different modes of action may provide complementary protection against effector T cell reactivity in LEA29Y and hPD-L1 co-expressing xenografts.

Transplantation of encapsulated porcine islets provides certain protection against the recipient's immune system. However, some membranes and coating materials are permeable

to antibodies or pig-derived carbohydrate antigens [402]. Future combination of the Smart Graft constructs with multiple knockouts, e.g. *GGTA1*, *CMAH* and *B4GALNT2*, is thus advisable to enhance the resistance against antibody-mediated rejection. Additional expression of further molecules, e.g. complement regulatory proteins and coagulation inhibitors, might be beneficial for non-encapsulated islet xenotransplantation.

8.1.8 Other potential applications

Besides driving T cell-regulatory genes, the promoters presented in this thesis can also be used to control expression of potent anti-inflammatory proteins such as TGF-β and IL-10 to reduce upcoming inflammation responses after xenotransplantation. The temporal and spatial restriction of transgene expression as well as expression levels depending on the severity of inflammation may enable minimization of potential negative side effects [403-406].

The strategy underlying the Smart Graft concept can also be employed for other purposes. One example is the usage of NF-κB-controlled promoters in chimeric antigen receptor (CAR)-modified T cell therapy. This type of cancer immunotherapy uses autologous T cells expressing engineered CARs that recognize tumor-associated antigens (TAAs) and initiate T cell activation for target cell elimination. Although CAR T cell therapy has achieved great success in treating haematological malignancies, clinical trials have revealed several side effects including on-target off-tumor toxicity due to weakly expressed TAAs in normal tissues [407-410]. Those undesired T cells responses have also been reported in solid tumors [411]. As the special microenvironment of solid tumors is characterized by hypoxia and inflammation that both activate NF-κB signalling, the usage of Smart Graft promoters may enable local activation of CAR expression at the site of cancer, thereby minimizing the damage to healthy tissues [412, 413].

Inducible promoters of the Smart Graft approach may also be applied for the prevention of bacterial contaminations in bioreactors. Flagellin proteins of both Gram-positive and Gram negative-bacteria are strong activators of NF-κB via Toll-like receptor 5, which is expressed in diverse somatic cells and mammalian cell lines (e.g. HEK293) [414-416]. Using Smart Graft promoters for auto-inducible expression of antibiotic genes by the eukaryotic producing strain itself may substitute the addition of culture media antibiotics. This could save costs and

mitigate adverse effects on protein synthesis and metabolic processes caused by the prophylactic use of antibiotics [417-419].

This is just a small number of examples that illustrate the wide potential applicability of the inducible promoters developed, analyzed and presented in this thesis. Generally, the Smart Graft strategy can be used for all approaches where transgene expression shall be activated via NF-κB signalling by stimuli like inflammation, tissue damage, graft rejection, hypoxia, tumor growth and bacterial components.

8.2 Multiple gene knockouts for xenograft improvement

Since the first *GGTA1*-knockout pig for xenotransplantation was generated in the early 2000s, the list of gene inactivations with beneficial effects on immunogenicity as well as on molecular and anatomical compatibility between xenograft and recipient has steadily increased: Inactivation of *GGTA1*, *CMAH* and *B4GALNT2*, for instance, prevents synthesis of the xenogenic carbohydrate epitopes αGal, Neu5Gc and Sda thereby dramatically reducing antibody-mediated rejection processes. Phagocytosis of human platelets, a major problem in liver xenotransplantation, is reduced by the knockout of *ASGR1*. Inactivation of the ULBP1 provides protection against NK cell-mediated lysis, while removal of functional SLA class I receptors by a knockout of *SLA-1*, *SLA-2*, *SLA-3* or *B2M* helps to inhibit activation of xenoreactive cytotoxic T cells. Moreover, the size of donor organs can be optimized by inactivating GHR.

However, the increasing number of desired gene knockouts raises the question of how they can be combined most efficiently in one animal with the smallest technical effort, the shortest period of time, the lowest number of experimental animals and how potentially adverse off-target mutations can be reliably detected.

8.2.1 Strategies to generate pigs with multiple gene knockouts

One approach to produce pigs with multiple gene knockouts is to crossbreed single-modified animals. Although this is technically simple, necessary breeding to the F2 generation is

comparatively time-consuming and creation of homozygous offspring is highly inefficient. This method becomes quite impracticable when more than two knockouts are required.

Alternatively, serial cloning can also be considered to accumulate multiple gene knockouts. The cycle of genetic manipulation of somatic cells, SCNT, cell isolation of modified fetuses or piglets and further genome editing is thereby repeated until all the GOIs are inactivated. Intensive pre-screening of cell clones is the main advantage of this approach. However, cloning efficiency as well as the number of live cloned offspring was shown to be significantly decreased by repeated SCNT [307]. Reduced developmental potential of porcine embryos generated by serial NT has also been reported which might result from incomplete reprogramming and accumulated epigenetic errors induced by the cloning process [420]. Although it is likely that these negative effects can be mitigated by breeding periods between the individual cloning rounds, this would dramatically prolongate completion of the final knockout combination.

In contrast, simultaneous inactivation of multiple genes, carried out either directly in the fertilized oocyte or in somatic cells, is substantially faster. Cytoplasmic microinjection of CRISPR/Cas components in porcine zygotes can be conducted quickly, but carries the risk of mosaicism which might prevent germline transmission of the genetic modifications. Moreover, since embryos cannot be submitted to antibiotic selection and pre-implantation screening for CRISPR/Cas-induced mutations is impractical for large numbers of embryos, a considerable number of animals without the intended modifications will be produced [421].

The method of choice is therefore CRISPR/Cas-based multiplex gene editing in somatic cells. The usage of multi-knockout vectors, such as those generated and applied in this work, thereby enables editing of a large number of loci by transfecting a minimum number of different genetic constructs. In addition, such vectors facilitate future changes of the genetic background, e.g. for combination with multiple transgenes. This approach was already successfully used by our group to produce viable pigs with inactivated GGTA1, CMAH, B4GALNT2 and SLA class I [110]. Since in this my thesis project up to seven genes/gene clusters should be inactivated simultaneously, two high-efficiency guide sequences per target gene were used to optimize the probability of multiple, functional gene knockouts. With every additional CRISPR/Cas-mediated DSB, however, the risk of lethal off-target mutations and chromosome aberrations, such as chromosomal deletions and rearrangements, increases

[63]. To maximize efficiency of SCNT, it was therefore advisable to use pools of independently modified clones. The enrichment of cells with homozygous *GGTA1*/SLA-I double-knockout further reduced heterozygous mutations in the cell pools that are now available for SCNT.

8.2.2 Detecting off-target mutations

Once animals with multiple gene knockouts will have been generated, an intensive characterisation of off-target mutations will be performed. Basically, off-target events in coding exons are critical as they can impair functionality of the corresponding gene product. Also, intronic off-target sites harbour the risk of altering the gene product when splicing sites are affected by inDel mutations [422, 423]. DNA sequence alterations in 5' and 3' untranslated regions (UTRs), in contrast, can modulate gene regulation and mRNA stability, while off-target effects in intergenic regions are regarded as biologically less relevant [424-426]. *In silico* tools allow prediction of putative off-target sites by aligning each 18-20 bp sgRNA target recognition site against the whole porcine genome tolerating a defined number of mismatches. These computationally predicted sites will then be analysed in the multi-knockout piglets by Sanger sequencing. Since inherent genetic variation can generate novel protospacers and PAM sequences, highly sensitive next generation sequencing (NGS) approaches can be considered to screen for non-predicted CRISPR/Cas-induced off-target editing [427-430]. However, far more important than genome-wide identification of every unintended mutation is to select the multi-knockout founder animals with regard to a healthy phenotype and good breeding characteristics, since off-target events will breed out over time.

9. INDEX OF FIGURES

Index of figures

10. INDEX OF TABLES

Index of tables

11. LIST OF ABBREVIATIONS

A20	TNFα-induced protein 3
ADCC	Antibody-dependent cell-mediated cytotoxicity
AEC	Aortic endothelial cell
αGal	Galα1-3Galβ1-(3)4GlcNAc-R epitope
AMP	Adenosine monophosphate
AP-1	Adaptor protein complex 1
APC	Antigen presenting cell
APR	Acute phase response
ASGR1	Asialoglycoprotein receptor
AttB	Bacterial attachment site
AttP	Phage attachment site
AVXR	Acute vascular xenograft rejection
B2M	Beta-2-microglobulin
B4GALNT2	β1,4 N-acetyl-galactosaminyl transferase 2
bp	Base pair
C/EBP-β	CCAAT/enhancer-binding protein beta
CAG	Semi-synthetic promoter composed of CMV enhancer, chicken β-actin promoter, rabbit globin intron
CAR	Chimeric antigen receptor
Cas	CRISPR-associated
CBH	Chicken β hybrid
CCL2, MCP-1	C-C motif chemokine, also known as monocyte chemotactic protein 1
cDNA	Complementary DNA
CMAH	CMP-N-acetylneuraminic acid hydroxylase
CMP	Cytidine monophosphate
CMV	Cytomegalovirus
Cpf1	Cas12a enzyme
CREB	Cyclic AMP responsive element-binding protein

CRISPR	Clustered regulatory interspaced short palindromic repeats
CRP	C-reactive protein
crRNA	CRISPR RNA
CTL	Cytotoxic T lymphocyte
CTLA4	Cytotoxic T-lymphocyte antigen 4
Ctrl	Control
CXR	Cellular xenograft rejection
DC	Dendritic cell
ddPCR	Droplet digital PCR
Dis	Distal
DSB	Double-strand break
DSIF	DRB sensitivity-inducing factor
E-box	Enhancer box
EC	Endothelial cell
ELAM	E-selectin
ELISA	Enzyme-linked immunosorbent assay
EGFP	Enhanced green fluorescent protein
EPCR	Endothelial protein C receptor
ESC	Embryonic stem cell
Fluc	Firefly luciferase
GalNAc	N-acetylgalactosamine
GAPDH	Glyceraldehyde 3-phosphate dehydrogenase
gDNA	Genomic DNA
GGTA1	α1,3-galactosyltransferase 1
GLR	German landrace
GOI	Gene of interest
HAR	Hyperacute rejection
HDR	Homology directed repair
HE	Haematoxylin and eosin
HEV	Hepatitis E virus
HLA	Human leukocyte antigen

HO-1	Heme oxigenase 1
HSV-TK	Herpes simplex virus thymidine kinase
i.m	Intramuscular
i.p.	Intraperitoneal
IFN	Interferon
Ig	Immune globuline
IGHG1	Immunoglobulin heavy constant gamma 1
IL	Interleukin
IL1R1	Interleukin-1 receptor type 1
InDel	Small insertions or deletions
KO	Knockout
LEA29Y	High-affinity variant of CTLA4-Ig
LMU	Ludwig-Maximilians-Universität München
LPS	Lipopolysaccharide
MHC	Major histocompatibility complex
MIN	Multifunctional integrase
mutCIITA	Dominant-negative variant of class II transactivator
Neu5Ac	CMP-N-acetylneuraminic acid
Neu5Gc	CMP-N-glycolylneuraminic acid
NF-κB	Nuclear factor-κB
NGS	Next generation sequencing
NHEJ	Non-homologous end joining
NHP	Nonhuman primate
NK	Natural killer
NOD	Non-obese diabetic
NSG	NOD scid gamma
nt	Nucleotide
OD	Optical density
OSM	Oncostatin M
p50/p65	Subunits of proteins forming NF-κB
PAM	Protospacer-adjacent motif
PBMC	Peripheral blood mononuclear cells

PCMV	Porcine cytomegalovirus
PCR	Polymerase chain reaction
PD-1	Programmed cell death protein 1
PD-L1	Programmed death 1 ligand 1
PERV	Porcine endogenous retrovirus
PK-15	Porcine kidney 15, cell line
pKDNF	Porcine kidney fibroblasts
Prox	Proximal
RLU	Relative light unit
Rluc	Renilla luciferase
s.c.	Subcutaneous
SCNT	Somatic cell nuclear transfer
SCP1	Human mesenchymal stem cell line
Sda	Sda antigen
SEAP	Secreted embryonic alkaline phosphatase
sgRNA	Single guide RNA
SIRPα	Signal-regulatory protein alpha-1
SLA	Swine leukocyte antigen
SP-1	Transcription factor specificity protein 1
SpCas9	Streptococcus pyogenes derived Cas9 enzyme
SPF	Specific pathogen-free
ST	Swine testis
SV40	Simian virus 40
TAA	Tumor-associated antigens
TALEN	Transcription activator-like effector nucleases
TCR	T cell receptor
Tet-On/Tet-Off	Antigen-dependent systems allowing doxycycline-induced activation (Tet-On) or inhibition (Tet-Off) of transgene transcription
TF	Tissue factor
TFPI	Tissue factor pathway inhibitor
TGF	Transforming growth factor

Th	T helper
TM	Thrombomodulin
TNF	Tumor necrosis factor
TNFAIP1	TNFα-induced protein 1
TNFR1	TNF receptor 1
tracrRNA	Trans-activating crRNA
Treg	Regulatory T cells
TUM	Technische Universität München
U6	RNA polymerase III promoter U6
UDP	Uridine triphosphate
ULBP1	UL16-binding protein 1
USF1	Upstream stimulatory factor 1
UTR	Untranslated regions
VCAM1	Vascular cell adhesion protein 1
wt	Wildtype
ZFN	Zink-finger nuclease
Δx	partial sequence of x

12. REFERENCES

[1] **EUROTRANSPLANT (2009-2018).** Yearly Statistics Overview Eurotransplant, from https://www.eurotransplant.org/cms/index.php?page=yearlystats (retrieved 03 Sep 2019).

[2] **EUROTRANSPLANT (2018).** Eurotransplant International Foundation - Annual Report 2018, from https://www.eurotransplant.org/cms/index.php?page=annual_reports (retrieved 03 Sep 2019).

[3] **THYBO, K.H. & ESKESEN, V. (2013).** The most important reason for lack of organ donation is family refusal. *Danish medical journal* 60, A4585.

[4] **JANSEN, N.E., VAN LEIDEN, H.A., HAASE-KROMWIJK, B.J. *et al.* (2010).** Organ donation performance in the Netherlands 2005-08; medical record review in 64 hospitals. *Nephrology, dialysis, transplantation : official publication of the European Dialysis and Transplant Association - European Renal Association* 25, 1992-1997.

[5] **VAN LEIDEN, H.A., JANSEN, N.E., HAASE-KROMWIJK, B.J. *et al.* (2010).** Higher refusal rates for organ donation among older potential donors in the Netherlands: impact of the donor register and relatives. *Transplantation* 90, 677-682.

[6] **BROWN, C.V., FOULKROD, K.H., DWORACZYK, S. *et al.* (2010).** Barriers to obtaining family consent for potential organ donors. *The Journal of trauma* 68, 447-451.

[7] **WESSLAU, C., GROSSE, K., KRUGER, R. *et al.* (2007).** How large is the organ donor potential in Germany? Results of an analysis of data collected on deceased with primary and secondary brain damage in intensive care unit from 2002 to 2005. *Transplant international : official journal of the European Society for Organ Transplantation* 20, 147-155.

[8] **BAHRAMI, A., KHALEGHI, E., VAKILZADEH, A.K. *et al.* (2017).** Process and barriers to organ donation and causes of brain death in northeast of Iran. *Electronic physician* 9, 3797-3802.

[9] **RADUNZ, S., JUNTERMANNS, B., HEUER, M. *et al.* (2012).** The effect of education on the attitude of medical students towards organ donation. *Ann Transplant* 17, 140-144.

[10] **TERBONSSEN, T., SETTMACHER, U., WURST, C. *et al.* (2015).** Effectiveness of Organ Donation Information Campaigns in Germany: A Facebook Based Online Survey. *Interactive journal of medical research* 4, e16.

[11] **YILMAZ, T.U. (2011).** Importance of education in organ donation. *Exp Clin Transplant* 9, 370-375.

[12] **BLAGG, C.R. (2007).** The early history of dialysis for chronic renal failure in the United States: a view from Seattle. *Am J Kidney Dis* 49, 482-496.

[13] **KRAMER, A., PIPPIAS, M., NOORDZIJ, M. *et al.* (2019).** The European Renal Association - European Dialysis and Transplant Association (ERA-EDTA) Registry Annual Report 2016: a summary. *Clin Kidney J* 12, 702-720.

[14] **LUND, L.H., EDWARDS, L.B., KUCHERYAVAYA, A.Y. *et al.* (2014).** The registry of the International Society for Heart and Lung Transplantation: thirty-first official adult heart transplant report--2014; focus theme: retransplantation. *The Journal of heart and lung transplantation : the official publication of the International Society for Heart Transplantation* 33, 996-1008.

[15] **LAHPOR, J.R. (2009).** State of the art: implantable ventricular assist devices. *Current opinion in organ transplantation* 14, 554-559.

[16] **HAN, J. & TRUMBLE, D.R. (2019).** Cardiac Assist Devices: Early Concepts, Current Technologies, and Future Innovations. *Bioengineering (Basel, Switzerland)* 6.

[17] **MANCINI, D. & COLOMBO, P.C. (2015).** Left Ventricular Assist Devices: A Rapidly Evolving Alternative to Transplant. *J Am Coll Cardiol* 65, 2542-2555.

[18] **DZOBO, K., THOMFORD, N.E., SENTHEBANE, D.A. *et al.* (2018).** Advances in Regenerative Medicine and Tissue Engineering: Innovation and Transformation of Medicine. *Stem cells international* 2018, 2495848.

[19] **MURPHY, S.V. & ATALA, A. (2014).** 3D bioprinting of tissues and organs. *Nature biotechnology* 32, 773-785.

[20] **KOLESKY, D.B., TRUBY, R.L., GLADMAN, A.S. *et al.* (2014).** 3D bioprinting of vascularized, heterogeneous cell-laden tissue constructs. *Adv Mater* 26, 3124-3130.

[21] **MIRONOV, V., VISCONTI, R.P., KASYANOV, V. *et al.* (2009).** Organ printing: tissue spheroids as building blocks. *Biomaterials* 30, 2164-2174.

[22] **NAKAMURA, M., IWANAGA, S., HENMI, C. *et al.* (2010).** Biomatrices and biomaterials for future developments of bioprinting and biofabrication. *Biofabrication* 2, 014110.

[23] **LIU, J. & YAN, C. (2018).** 3D Printing of Scaffolds for Tissue Engineering**,** 3D Printing. D. Cvetković, IntechOpen.

[24] **MIN, S., KO, I.K. & YOO, J.J. (2019).** State-of-the-Art Strategies for the Vascularization of Three-Dimensional Engineered Organs. *Vascular specialist international* 35, 77-89.

[25] **RODRIGUEZ UMANA, H. (1995).** Grafting of bone from a dog into the human skull: an historical note. *Plast Reconstr Surg* 96, 1481.

[26] **GIBSON, T. (1955).** Zoografting: a curious chapter in the history of plastic surgery. *Br J Plast Surg* 8, 234-242.

[27] **COOPER, D.K. (2012).** A brief history of cross-species organ transplantation. *Proceedings (Baylor University. Medical Center)* 25, 49-57.

[28] **DESCHAMPS, J.Y., ROUX, F.A., SAI, P. *et al.* (2005).** History of xenotransplantation. *Xenotransplantation* 12, 91-109.

[29] **REEMTSMA, K., MCCRACKEN, B.H., SCHLEGEL, J.U. *et al.* (1964).** Renal Heterotransplantation in Man. *Ann Surg* 160, 384-410.

[30] **STARZL, T.E., MARCHIORO, T.L., PETERS, G.N. *et al.* (1964).** Renal Heterotransplantation from Baboon to Man: Experience with 6 Cases. *Transplantation* 2, 752-776.

[31] **DENNER, J. & TONJES, R.R. (2012).** Infection barriers to successful xenotransplantation focusing on porcine endogenous retroviruses. *Clin Microbiol Rev* 25, 318-343.

[32] **DENNER, J. & MUELLER, N.J. (2015).** Preventing transfer of infectious agents. *Int J Surg* 23, 306-311.

[33] **DENNER, J. (2018).** Reduction of the survival time of pig xenotransplants by porcine cytomegalovirus. *Virology journal* 15, 171.

[34] **DENNER, J. (2015).** Xenotransplantation and Hepatitis E virus. *Xenotransplantation* 22, 167-173.

[35] **BUSBY, S.A., CROSSAN, C., GODWIN, J. *et al.* (2013).** Suggestions for the diagnosis and elimination of hepatitis E virus in pigs used for xenotransplantation. *Xenotransplantation* 20, 188-192.

[36] **DENNER, J. (2015).** Xenotransplantation and porcine cytomegalovirus. *Xenotransplantation* 22, 329-335.

[37] **MUELLER, N.J., BARTH, R.N., YAMAMOTO, S. *et al.* (2002).** Activation of cytomegalovirus in pig-to-primate organ xenotransplantation. *Journal of virology* 76, 4734-4740.

[38] **DENNER, J. (2003).** Porcine endogenous retroviruses (PERVs) and xenotransplantation: screening for transmission in several clinical trials and in experimental models using non-human primates. *Ann Transplant* 8, 39-48.

[39] **KASORNDORKBUA, C., GUENETTE, D.K., HUANG, F.F. *et al.* (2004).** Routes of transmission of swine hepatitis E virus in pigs. *Journal of clinical microbiology* 42, 5047-5052.

[40] **GEROLAMI, R., MOAL, V. & COLSON, P. (2008).** Chronic hepatitis E with cirrhosis in a kidney-transplant recipient. *The New England journal of medicine* 358, 859-860.

[41] **KAMAR, N., SELVES, J., MANSUY, J.M. *et al.* (2008).** Hepatitis E virus and chronic hepatitis in organ-transplant recipients. *The New England journal of medicine* 358, 811-817.

[42] **SALINES, M., ANDRAUD, M. & ROSE, N. (2017).** From the epidemiology of hepatitis E virus (HEV) within the swine reservoir to public health risk mitigation strategies: a comprehensive review. *Veterinary research* 48, 31.

[43] **MATSUDA, H., OKADA, K., TAKAHASHI, K. *et al.* (2003).** Severe hepatitis E virus infection after ingestion of uncooked liver from a wild boar. *The Journal of infectious diseases* 188, 944.

[44] **COLSON, P., BORENTAIN, P., QUEYRIAUX, B. *et al.* (2010).** Pig liver sausage as a source of hepatitis E virus transmission to humans. *The Journal of infectious diseases* 202, 825-834.

[45] **KASORNDORKBUA, C., OPRIESSNIG, T., HUANG, F.F. *et al.* (2005).** Infectious swine hepatitis E virus is present in pig manure storage facilities on United States farms, but evidence of water contamination is lacking. *Applied and environmental microbiology* 71, 7831-7837.

[46] **MOROZOV, V.A., MOROZOV, A.V., ROTEM, A. *et al.* (2015).** Extended Microbiological Characterization of Gottingen Minipigs in the Context of Xenotransplantation: Detection and Vertical Transmission of Hepatitis E Virus. *PLoS One* 10, e0139893.

[47] **DENNER, J. (2019).** Hepatitis E virus (HEV)-The Future. *Viruses* 11.

[48] **WHITTEKER, J.L., DUDANI, A.K. & TACKABERRY, E.S. (2008).** Human fibroblasts are permissive for porcine cytomegalovirus in vitro. *Transplantation* 86, 155-162.

[49] **EDINGTON, N. (1986).** Porcine cytomegalovirus**,** Diseases of Swine. Edn. 6, Iowa State University Press, Ames, Iowa, 330-336.

[50] **YAMADA, K., TASAKI, M., SEKIJIMA, M. *et al.* (2014).** Porcine cytomegalovirus infection is associated with early rejection of kidney grafts in a pig to baboon xenotransplantation model. *Transplantation* 98, 411-418.

[51] **MUELLER, N.J., LIVINGSTON, C., KNOSALLA, C. *et al.* (2004).** Activation of porcine cytomegalovirus, but not porcine lymphotropic herpesvirus, in pig-to-baboon xenotransplantation. *The Journal of infectious diseases* 189, 1628-1633.

[52] **EGERER, S., FIEBIG, U., KESSLER, B. *et al.* (2018).** Early weaning completely eliminates porcine cytomegalovirus from a newly established pig donor facility for xenotransplantation. *Xenotransplantation* 25, e12449.

[53] **TAKEUCHI, Y., PATIENCE, C., MAGRE, S. *et al.* (1998).** Host range and interference studies of three classes of pig endogenous retrovirus. *Journal of virology* 72, 9986-9991.

[54] **HARRISON, I., TAKEUCHI, Y., BARTOSCH, B. *et al.* (2004).** Determinants of high titer in recombinant porcine endogenous retroviruses. *Journal of virology* 78, 13871-13879.

[55] **LE TISSIER, P., STOYE, J.P., TAKEUCHI, Y. *et al.* (1997).** Two sets of human-tropic pig retrovirus. *Nature* 389, 681-682.

[56] **MARTIN, U., WINKLER, M.E., ID, M. *et al.* (2000).** Productive infection of primary human endothelial cells by pig endogenous retrovirus (PERV). *Xenotransplantation* 7, 138-142.

[57] **DENNER, J. (2018).** Why was PERV not transmitted during preclinical and clinical xenotransplantation trials and after inoculation of animals? *Retrovirology* 15, 28.

[58] **TACKE, S.J., KURTH, R. & DENNER, J. (2000).** Porcine endogenous retroviruses inhibit human immune cell function: risk for xenotransplantation? *Virology* 268, 87-93.

[59] **DIECKHOFF, B., PETERSEN, B., KUES, W.A. *et al.* (2008).** Knockdown of porcine endogenous retrovirus (PERV) expression by PERV-specific shRNA in transgenic pigs. *Xenotransplantation* 15, 36-45.

[60] **RAMSOONDAR, J., VAUGHT, T., BALL, S. *et al.* (2009).** Production of transgenic pigs that express porcine endogenous retrovirus small interfering RNAs. *Xenotransplantation* 16, 164-180.

[61] **SEMAAN, M., KAULITZ, D., PETERSEN, B. *et al.* (2012).** Long-term effects of PERV-specific RNA interference in transgenic pigs. *Xenotransplantation* 19, 112-121.

[62] **YANG, L., GUELL, M., NIU, D. *et al.* (2015).** Genome-wide inactivation of porcine endogenous retroviruses (PERVs). *Science* 350, 1101-1104.

[63] **NIU, D., WEI, H.J., LIN, L. *et al.* (2017).** Inactivation of porcine endogenous retrovirus in pigs using CRISPR-Cas9. *Science* 357, 1303-1307.

[64] **ROSE, A.G. & COOPER, D.K. (2000).** Venular thrombosis is the key event in the pathogenesis of antibody-mediated cardiac rejection. *Xenotransplantation* 7, 31-41.

[65] **YANG, Y.G. & SYKES, M. (2007).** Xenotransplantation: current status and a perspective on the future. *Nat Rev Immunol* 7, 519-531.

[66] **SCHUURMAN, H.J., CHENG, J. & LAM, T. (2003).** Pathology of xenograft rejection: a commentary. *Xenotransplantation* 10, 293-299.

[67] **COOPER, D.K., GOLLACKNER, B. & SACHS, D.H. (2002).** Will the pig solve the transplantation backlog? *Annual review of medicine* 53, 133-147.

[68] **SACKS, S.H. & ZHOU, W. (2012).** The role of complement in the early immune response to transplantation. *Nat Rev Immunol* 12, 431-442.

[69] **GALILI, U. (2005).** The alpha-gal epitope and the anti-Gal antibody in xenotransplantation and in cancer immunotherapy. *Immunol Cell Biol* 83, 674-686.

[70] **GALILI, U., SHOHET, S.B., KOBRIN, E. *et al.* (1988).** Man, apes, and Old World monkeys differ from other mammals in the expression of alpha-galactosyl epitopes on nucleated cells. *J Biol Chem* 263, 17755-17762.

[71] **LUDERITZ, O., SIMMONS, D.A. & WESTPHAL, G. (1965).** The immunochemistry of Salmonella chemotype VI O-antigens. The structure of oligosaccharides from Salmonella group U (o 43) lipopolysaccharides. *The Biochemical journal* 97, 820-826.

[72] **CURVALL, M., LINDBERG, B., LONNGREN, J. *et al.* (1973).** Structural studies of the Klebsiella O group 8 lipopolysaccharide. *Acta chemica Scandinavica* 27, 4019-4021.

[73] **GALILI, U., MANDRELL, R.E., HAMADEH, R.M. *et al.* (1988).** Interaction between human natural anti-alpha-galactosyl immunoglobulin G and bacteria of the human flora. *Infection and immunity* 56, 1730-1737.

[74] **GALILI, U. (2015).** Significance of the evolutionary alpha1,3-galactosyltransferase (GGTA1) gene inactivation in preventing extinction of apes and old world monkeys. *Journal of molecular evolution* 80, 1-9.

[75] **DAHL, K., KIRKEBY, S., D'APICE, A.F. *et al.* (2005).** The bacterial flora of alpha-Gal knockout mice express the alpha-Gal epitope comparable to wild type mice. *Transpl Immunol* 14, 9-16.

[76] **LAI, L., KOLBER-SIMONDS, D., PARK, K.W. *et al.* (2002).** Production of alpha-1,3-galactosyltransferase knockout pigs by nuclear transfer cloning. *Science* 295, 1089-1092.

[77] **PHELPS, C.J., KOIKE, C., VAUGHT, T.D. *et al.* (2003).** Production of alpha 1,3-galactosyltransferase-deficient pigs. *Science* 299, 411-414.

[78] **DAI, Y., VAUGHT, T.D., BOONE, J. *et al.* (2002).** Targeted disruption of the alpha1,3-galactosyltransferase gene in cloned pigs. *Nature biotechnology* 20, 251-255.

[79] **KUWAKI, K., TSENG, Y.L., DOR, F.J. *et al.* (2005).** Heart transplantation in baboons using alpha1,3-galactosyltransferase gene-knockout pigs as donors: initial experience. *Nature medicine* 11, 29-31.

[80] **TSENG, Y.L., KUWAKI, K., DOR, F.J. *et al.* (2005).** alpha1,3-Galactosyltransferase gene-knockout pig heart transplantation in baboons with survival approaching 6 months. *Transplantation* 80, 1493-1500.

[81] **MCGREGOR, C.G., DAVIES, W.R., OI, K. *et al.* (2005).** Cardiac xenotransplantation: recent preclinical progress with 3-month median survival. *The Journal of thoracic and cardiovascular surgery* 130, 844-851.

[82] **LOVELAND, B.E., MILLAND, J., KYRIAKOU, P. *et al.* (2004).** Characterization of a CD46 transgenic pig and protection of transgenic kidneys against hyperacute rejection in non-immunosuppressed baboons. *Xenotransplantation* 11, 171-183.

[83] **MENORET, S., PLAT, M., BLANCHO, G. *et al.* (2004).** Characterization of human CD55 and CD59 transgenic pigs and kidney xenotransplantation in the pig-to-baboon combination. *Transplantation* 77, 1468-1471.

[84] **CHEN, R.H., NAFICY, S., LOGAN, J.S. *et al.* (1999).** Hearts from transgenic pigs constructed with CD59/DAF genomic clones demonstrate improved survival in primates. *Xenotransplantation* 6, 194-200.

[85] **ZAIDI, A., SCHMOECKEL, M., BHATTI, F. *et al.* (1998).** Life-supporting pig-to-primate renal xenotransplantation using genetically modified donors. *Transplantation* 65, 1584-1590.

[86] **BACH, F.H., WINKLER, H., FERRAN, C. *et al.* (1996).** Delayed xenograft rejection. *Immunology today* 17, 379-384.

[87] **LOSS, M., VANGEROW, B., SCHMIDTKO, J. *et al.* (2000).** Acute vascular rejection is associated with systemic complement activation in a pig-to-primate kidney xenograft model. *Xenotransplantation* 7, 186-196.

[88] **GRENZ, A., SCHENK, M., ZIPFEL, A. *et al.* (2000).** TNF-alpha and its receptors mediate graft rejection and loss after liver transplantation. *Clin Chem Lab Med* 38, 1183-1185.

[89] **HOLZKNECHT, Z.E., KUYPERS, K.L., PLUMMER, T.B. *et al.* (2002).** Apoptosis and cellular activation in the pathogenesis of acute vascular rejection. *Circ Res* 91, 1135-1141.

[90] **HANCOCK, W.W. (1997).** Delayed xenograft rejection. *World journal of surgery* 21, 917-923.

[91] **LIN, S.S., WEIDNER, B.C., BYRNE, G.W. *et al.* (1998).** The role of antibodies in acute vascular rejection of pig-to-baboon cardiac transplants. *The Journal of clinical investigation* 101, 1745-1756.

[92] **BOUHOURS, D., POURCEL, C. & BOUHOURS, J.E. (1996).** Simultaneous expression by porcine aorta endothelial cells of glycosphingolipids bearing the major epitope for human xenoreactive antibodies (Gal alpha 1-3Gal), blood group H determinant and N-glycolylneuraminic acid. *Glycoconj J* 13, 947-953.

[93] **MUCHMORE, E.A., DIAZ, S. & VARKI, A. (1998).** A structural difference between the cell surfaces of humans and the great apes. *American journal of physical anthropology* 107, 187-198.

[94] **MIWA, Y., KOBAYASHI, T., NAGASAKA, T. *et al.* (2004).** Are N-glycolylneuraminic acid (Hanganutziu-Deicher) antigens important in pig-to-human xenotransplantation? *Xenotransplantation* 11, 247-253.

[95] **BYRNE, G.W., MCGREGOR, C.G.A. & BREIMER, M.E. (2015).** Recent investigations into pig antigen and anti-pig antibody expression. *Int J Surg* 23, 223-228.

[96] **VARKI, A. (2001).** Loss of N-glycolylneuraminic acid in humans: Mechanisms, consequences, and implications for hominid evolution. *American journal of physical anthropology* Suppl 33, 54-69.

[97] **LUTZ, A.J., LI, P., ESTRADA, J.L. *et al.* (2013).** Double knockout pigs deficient in N-glycolylneuraminic acid and galactose alpha-1,3-galactose reduce the humoral barrier to xenotransplantation. *Xenotransplantation* 20, 27-35.

[98] **BYRNE, G.W., DU, Z., STALBOERGER, P. *et al.* (2014).** Cloning and expression of porcine beta1,4 N-acetylgalactosaminyl transferase encoding a new xenoreactive antigen. *Xenotransplantation* 21, 543-554.

[99] **ZHAO, C., COOPER, D.K.C., DAI, Y. *et al.* (2018).** The Sda and Cad glycan antigens and their glycosyltransferase, beta1,4GalNAcT-II, in xenotransplantation. *Xenotransplantation* 25, e12386.

[100] **ESTRADA, J.L., MARTENS, G., LI, P. *et al.* (2015).** Evaluation of human and non-human primate antibody binding to pig cells lacking GGTA1/CMAH/beta4GalNT2 genes. *Xenotransplantation* 22, 194-202.

[101] **WANG, R.G., RUAN, M., ZHANG, R.J. *et al.* (2018).** Antigenicity of tissues and organs from GGTA1/CMAH/beta4GalNT2 triple gene knockout pigs. *Journal of biomedical research* 33, 235-243.

[102] **VALENZUELA, N.M. & REED, E.F. (2013).** Antibodies in transplantation: the effects of HLA and non-HLA antibody binding and mechanisms of injury. *Methods Mol Biol* 1034, 41-70.

[103] **WIECZOREK, M., ABUALROUS, E.T., STICHT, J. *et al.* (2017).** Major Histocompatibility Complex (MHC) Class I and MHC Class II Proteins: Conformational Plasticity in Antigen Presentation. *Front Immunol* 8, 292.

[104] **RAVAL, A., PURI, N., RATH, P.C. *et al.* (1998).** Cytokine regulation of expression of class I MHC antigens. *Experimental & molecular medicine* 30, 1-13.

[105] **PAUL, S. & LAL, G. (2017).** The Molecular Mechanism of Natural Killer Cells Function and Its Importance in Cancer Immunotherapy. *Front Immunol* 8, 1124.

[106] **MARTENS, G.R., REYES, L.M., LI, P. *et al.* (2017).** Humoral Reactivity of Renal Transplant-Waitlisted Patients to Cells From GGTA1/CMAH/B4GalNT2, and SLA Class I Knockout Pigs. *Transplantation* 101, e86-e92.

[107] **TANAKA-MATSUDA, M., ANDO, A., ROGEL-GAILLARD, C. *et al.* (2009).** Difference in number of loci of swine leukocyte antigen classical class I genes among haplotypes. *Genomics* 93, 261-273.

[108] **REYES, L.M., ESTRADA, J.L., WANG, Z.Y. *et al.* (2014).** Creating class I MHC-null pigs using guide RNA and the Cas9 endonuclease. *J Immunol* 193, 5751-5757.

[109] **WANG, Y., DU, Y., ZHOU, X. *et al.* (2016).** Efficient generation of B2m-null pigs via injection of zygote with TALENs. *Sci Rep* 6, 38854.

[110] **FISCHER, K., RIEBLINGER, B., HEIN, R. *et al.* (2020).** Viable pigs after simultaneous inactivation of porcine MHC class I and three xenoreactive antigen genes GGTA1, CMAH and B4GALNT2. *Xenotransplantation* 27, e12560.

[111] **EDGINGTON, T.S., MACKMAN, N., BRAND, K. *et al.* (1991).** The structural biology of expression and function of tissue factor. *Thrombosis and haemostasis* 66, 67-79.

[112] **MARTIN, F.A., MURPHY, R.P. & CUMMINS, P.M. (2013).** Thrombomodulin and the vascular endothelium: insights into functional, regulatory, and therapeutic aspects. *Am J Physiol Heart Circ Physiol* 304, H1585-1597.

[113] **LAWSON, J.H., DANIELS, L.J. & PLATT, J.L. (1997).** The evaluation of thrombomodulin activity in porcine to human xenotransplantation. *Transplantation proceedings* 29, 884-885.

[114] **ROUSSEL, J.C., MORAN, C.J., SALVARIS, E.J. *et al.* (2008).** Pig thrombomodulin binds human thrombin but is a poor cofactor for activation of human protein C and TAFI. *Am J Transplant* 8, 1101-1112.

[115] **MIWA, Y., YAMAMOTO, K., ONISHI, A. *et al.* (2010).** Potential value of human thrombomodulin and DAF expression for coagulation control in pig-to-human xenotransplantation. *Xenotransplantation* 17, 26-37.

[116] **IWASE, H., EKSER, B., SATYANANDA, V. *et al.* (2015).** Pig-to-baboon heterotopic heart transplantation--exploratory preliminary experience with pigs transgenic for human thrombomodulin and comparison of three costimulation blockade-based regimens. *Xenotransplantation* 22, 211-220.

[117] **KOPP, C.W., SIEGEL, J.B., HANCOCK, W.W. *et al.* (1997).** Effect of porcine endothelial tissue factor pathway inhibitor on human coagulation factors. *Transplantation* 63, 749-758.

[118] **JI, H., LI, X., YUE, S. *et al.* (2015).** Pig BMSCs Transfected with Human TFPI Combat Species Incompatibility and Regulate the Human TF Pathway in Vitro and in a Rodent Model. *Cell Physiol Biochem* 36, 233-249.

[119] **BAJAJ, M.S., BIRKTOFT, J.J., STEER, S.A. *et al.* (2001).** Structure and biology of tissue factor pathway inhibitor. *Thrombosis and haemostasis* 86, 959-972.

[120] **IWASE, H., EKSER, B., HARA, H. *et al.* (2014).** Regulation of human platelet aggregation by genetically modified pig endothelial cells and thrombin inhibition. *Xenotransplantation* 21, 72-83.

[121] **ROBSON, S.C., KACZMAREK, E., SIEGEL, J.B. *et al.* (1997).** Loss of ATP diphosphohydrolase activity with endothelial cell activation. *The Journal of experimental medicine* 185, 153-163.

[122] **ROBSON, S.C., DAOUD, S., BEGIN, M. *et al.* (1997).** Modulation of vascular ATP diphosphohydrolase by fatty acids. *Blood Coagul Fibrinolysis* 8, 21-27.

[123] **MARCUS, A.J., BROEKMAN, M.J., DROSOPOULOS, J.H. *et al.* (1997).** The endothelial cell ecto-ADPase responsible for inhibition of platelet function is CD39. *The Journal of clinical investigation* 99, 1351-1360.

[124] **MARCUS, A.J., BROEKMAN, M.J., DROSOPOULOS, J.H. *et al.* (2005).** Role of CD39 (NTPDase-1) in thromboregulation, cerebroprotection, and cardioprotection. *Semin Thromb Hemost* 31, 234-246.

[125] **ALLARD, B., LONGHI, M.S., ROBSON, S.C. *et al.* (2017).** The ectonucleotidases CD39 and CD73: Novel checkpoint inhibitor targets. *Immunol Rev* 276, 121-144.

[126] **DWYER, K.M., ROBSON, S.C., NANDURKAR, H.H. *et al.* (2004).** Thromboregulatory manifestations in human CD39 transgenic mice and the implications for thrombotic disease and transplantation. *The Journal of clinical investigation* 113, 1440-1446.

[127] **DWYER, K.M., MYSORE, T.B., CRIKIS, S. *et al.* (2006).** The transgenic expression of human CD39 on murine islets inhibits clotting of human blood. *Transplantation* 82, 428-432.

[128] **TAYLOR, F.B., JR., PEER, G.T., LOCKHART, M.S. *et al.* (2001).** Endothelial cell protein C receptor plays an important role in protein C activation in vivo. *Blood* 97, 1685-1688.

[129] **ESMON, C.T. (2003).** The protein C pathway. *Chest* 124, 26S-32S.

[130] **BUDORF, L., RYBAK, E., ZHANG, T. (2013).** Human EPCR Expression in GalTKO.hCD46 Lungs Extends Survival Time and Lowers PVR in a Xenogenic Lung Perfusion Model. *The Journal of Heart and Lung Transplantation* 32.

[131] **LU, T., YANG, B., WANG, R. *et al.* (2019).** Xenotransplantation: Current Status in Preclinical Research. *Front Immunol* 10, 3060.

[132] **SHU, S., REN, J. & SONG, J. (2020).** Cardiac xenotransplantation: a promising way to treat advanced heart failure. *Heart Failure Reviews*.

[133] **EKSER, B., LONG, C., ECHEVERRI, G.J. *et al.* (2010).** Impact of thrombocytopenia on survival of baboons with genetically modified pig liver transplants: clinical relevance. *Am J Transplant* 10, 273-285.

[134] **SPIESS, M. & LODISH, H.F. (1985).** Sequence of a second human asialoglycoprotein receptor: conservation of two receptor genes during evolution. *Proceedings of the National Academy of Sciences of the United States of America* 82, 6465-6469.

[135] **PARIS, L.L., CHIHARA, R.K., SIDNER, R.A. *et al.* (2012).** Differences in human and porcine platelet oligosaccharides may influence phagocytosis by liver sinusoidal cells in vitro. *Xenotransplantation* 19, 31-39.

[136] **CHIHARA, R.K., PARIS, L.L., REYES, L.M. *et al.* (2011).** Primary porcine Kupffer cell phagocytosis of human platelets involves the CD18 receptor. *Transplantation* 92, 739-744.

[137] **PARIS, L.L., CHIHARA, R.K., REYES, L.M. *et al.* (2011).** ASGR1 expressed by porcine enriched liver sinusoidal endothelial cells mediates human platelet phagocytosis in vitro. *Xenotransplantation* 18, 245-251.

[138] **PARIS, L.L., ESTRADA, J.L., LI, P. *et al.* (2015).** Reduced human platelet uptake by pig livers deficient in the asialoglycoprotein receptor 1 protein. *Xenotransplantation* 22, 203-210.

[139] **VEREECKE, L., BEYAERT, R. & VAN LOO, G. (2009).** The ubiquitin-editing enzyme A20 (TNFAIP3) is a central regulator of immunopathology. *Trends Immunol* 30, 383-391.

[140] **TENHUNEN, R., MARVER, H.S. & SCHMID, R. (1968).** The enzymatic conversion of heme to bilirubin by microsomal heme oxygenase. *Proceedings of the National Academy of Sciences of the United States of America* 61, 748-755.

[141] **GOZZELINO, R., JENEY, V. & SOARES, M.P. (2010).** Mechanisms of cell protection by heme oxygenase-1. *Annu Rev Pharmacol Toxicol* 50, 323-354.

[142] **LARSEN, R., GOUVEIA, Z., SOARES, M.P. *et al.* (2012).** Heme cytotoxicity and the pathogenesis of immune-mediated inflammatory diseases. *Front Pharmacol* 3, 77.

[143] **WAGENER, F.A., EGGERT, A., BOERMAN, O.C. *et al.* (2001).** Heme is a potent inducer of inflammation in mice and is counteracted by heme oxygenase. *Blood* 98, 1802-1811.

[144] **SOARES, M.P., USHEVA, A., BROUARD, S. *et al.* (2002).** Modulation of endothelial cell apoptosis by heme oxygenase-1-derived carbon monoxide. *Antioxidants & redox signaling* 4, 321-329.

[145] **OROPEZA, M., PETERSEN, B., CARNWATH, J.W. *et al.* (2009).** Transgenic expression of the human A20 gene in cloned pigs provides protection against apoptotic and inflammatory stimuli. *Xenotransplantation* 16, 522-534.

[146] **PETERSEN, B., RAMACKERS, W., LUCAS-HAHN, A. *et al.* (2011).** Transgenic expression of human heme oxygenase-1 in pigs confers resistance against xenograft rejection during ex vivo perfusion of porcine kidneys. *Xenotransplantation* 18, 355-368.

[147] **FISCHER, K., KRANER-SCHEIBER, S., PETERSEN, B. *et al.* (2016).** Efficient production of multi-modified pigs for xenotransplantation by 'combineering', gene stacking and gene editing. *Sci Rep* 6, 29081.

[148] **LANGIN, M., MAYR, T., REICHART, B. *et al.* (2018).** Consistent success in life-supporting porcine cardiac xenotransplantation. *Nature* 564, 430-433.

[149] **KIM, S.C., MATHEWS, D.V., BREEDEN, C.P. *et al.* (2019).** Long-term survival of pig-to-rhesus macaque renal xenografts is dependent on CD4 T cell depletion. *Am J Transplant* 19, 2174-2185.

[150] **PINO-CHAVEZ, G. (2001).** Differentiating Acute Humoral from Acute Cellular Rejection Histopathologically. *Graft* 4, 60-62.

[151] **BENZIMRA, M., CALLIGARO, G.L. & GLANVILLE, A.R. (2017).** Acute rejection. *Journal of thoracic disease* 9, 5440-5457.

[152] **COZZI, E., BHATTI, F., SCHMOECKEL, M. *et al.* (2000).** Long-term survival of nonhuman primates receiving life-supporting transgenic porcine kidney xenografts. *Transplantation* 70, 15-21.

[153] **COZZI, E., VIAL, C., OSTLIE, D. *et al.* (2003).** Maintenance triple immunosuppression with cyclosporin A, mycophenolate sodium and steroids allows prolonged survival of primate recipients of hDAF porcine renal xenografts. *Xenotransplantation* 10, 300-310.

[154] **LANIER, L.L. (2005).** NK cell recognition. *Annu Rev Immunol* 23, 225-274.

[155] **FAURIAT, C., LONG, E.O., LJUNGGREN, H.G. *et al.* (2010).** Regulation of human NK-cell cytokine and chemokine production by target cell recognition. *Blood* 115, 2167-2176.

[156] **BAUMANN, B.C., STUSSI, G., HUGGEL, K. *et al.* (2007).** Reactivity of human natural antibodies to endothelial cells from Galalpha(1,3)Gal-deficient pigs. *Transplantation* 83, 193-201.

[157] **SCHAAPHERDER, A.F., DAHA, M.R., TE BULTE, M.T. *et al.* (1994).** Antibody-dependent cell-mediated cytotoxicity against porcine endothelium induced by a majority of human sera. *Transplantation* 57, 1376-1382.

[158] **SULLIVAN, J.A., OETTINGER, H.F., SACHS, D.H. *et al.* (1997).** Analysis of polymorphism in porcine MHC class I genes: alterations in signals recognized by human cytotoxic lymphocytes. *J Immunol* 159, 2318-2326.

[159] **LILIENFELD, B.G., CREW, M.D., FORTE, P. *et al.* (2007).** Transgenic expression of HLA-E single chain trimer protects porcine endothelial cells against human natural killer cell-mediated cytotoxicity. *Xenotransplantation* 14, 126-134.

[160] **STRONG, R.K., HOLMES, M.A., LI, P. *et al.* (2003).** HLA-E allelic variants. Correlating differential expression, peptide affinities, crystal structures, and thermal stabilities. *J Biol Chem* 278, 5082-5090.

[161] **BONGONI, A., KIERMEIR, D., CONSTANTINESCU, M. *et al.* (2014).** Functional Evaluation of hCD46 and HLA-E Transgenes in an Ex Vivo Pig-to-Human Xenoperfusion Model.: Abstract# D2843. *Transplantation* 98, 414-415.

[162] **SFRISO, R., ABICHT, J., MAYR, T. *et al.* (2017).** Evaluation of innate immune activation after ex vivo xenoperfusion of GTKO/hCD46/HLA-E transgenic pig hearts with human blood. *Xenotransplantation* 24.

[163] **PUGA YUNG, G., BONGONI, A.K., PRADIER, A. *et al.* (2018).** Release of pig leukocytes and reduced human NK cell recruitment during ex vivo perfusion of HLA-E/human CD46 double-transgenic pig limbs with human blood. *Xenotransplantation* 25.

[164] **LILIENFELD, B.G., GARCIA-BORGES, C., CREW, M.D. *et al.* (2006).** Porcine UL16-binding protein 1 expressed on the surface of endothelial cells triggers human NK cytotoxicity through NKG2D. *J Immunol* 177, 2146-2152.

[165] **JOANNA, Z., MAGDALENA, H., AGNIESZKA, N.T. *et al.* (2018).** The production of UL16-binding protein 1 targeted pigs using CRISPR technology. *3 Biotech* 8, 70.

[166] **NOWAK-TERPIŁOWSKA, A., LIPIŃSKI, D., HRYHOROWICZ, M. *et al.* (2020).** Production of ULBP1-KO pigs with human CD55 expression using CRISPR technology. *Journal of Applied Animal Research* 48, 93-101.

[167] **CANDINAS, D., BELLIVEAU, S., KOYAMADA, N. *et al.* (1996).** T cell independence of macrophage and natural killer cell infiltration, cytokine production, and endothelial activation during delayed xenograft rejection. *Transplantation* 62, 1920-1927.

[168] **LIN, Y., VANDEPUTTE, M. & WAER, M. (1997).** Contribution of activated macrophages to the process of delayed xenograft rejection. *Transplantation* 64, 1677-1683.

[169] **WALLGREN, A.C., KARLSSON-PARRA, A. & KORSGREN, O. (1995).** The main infiltrating cell in xenograft rejection is a CD4+ macrophage and not a T lymphocyte. *Transplantation* 60, 594-601.

[170] **LIN, Y., VANDEPUTTE, M. & WAER, M. (1997).** Natural killer cell- and macrophage-mediated rejection of concordant xenografts in the absence of T and B cell responses. *J Immunol* 158, 5658-5667.

[171] **JIN, R., GREENWALD, A., PETERSON, M.D. *et al.* (2006).** Human monocytes recognize porcine endothelium via the interaction of galectin 3 and alpha-GAL. *J Immunol* 177, 1289-1295.

[172] **EL-OUAGHLIDI, A., JAHR, H., PFEIFFER, G. *et al.* (1999).** Cytokine mRNA expression in peripheral blood cells of immunosuppressed human islet transplant recipients. *J Mol Med (Berl)* 77, 115-117.

[173] **ZHAO, Y., COOPER, D.K.C., WANG, H. *et al.* (2019).** Potential pathological role of pro-inflammatory cytokines (IL-6, TNF-alpha, and IL-17) in xenotransplantation. *Xenotransplantation* 26, e12502.

[174] **GREENWALD, A.G., JIN, R. & WADDELL, T.K. (2009).** Galectin-3-mediated xenoactivation of human monocytes. *Transplantation* 87, 44-51.

[175] **CADILI, A. & KNETEMAN, N. (2008).** The role of macrophages in xenograft rejection. *Transplantation proceedings* 40, 3289-3293.

[176] **LONG, C., HARA, H., PAWLIKOWSKI, Z. *et al.* (2009).** Genetically engineered pig red blood cells for clinical transfusion: initial in vitro studies. *Transfusion* 49, 2418-2429.

[177] **IDE, K., WANG, H., TAHARA, H. *et al.* (2007).** Role for CD47-SIRPalpha signaling in xenograft rejection by macrophages. *Proceedings of the National Academy of Sciences of the United States of America* 104, 5062-5066.

[178] **WANG, Z.Y., PARIS, L.L., CHIHARA, R.K. *et al.* (2012).** Immortalized porcine liver sinusoidal endothelial cells: an in vitro model of xenotransplantation-induced thrombocytopenia. *Xenotransplantation* 19, 249-255.

[179] **TENA, A., KURTZ, J., LEONARD, D.A. *et al.* (2014).** Transgenic expression of human CD47 markedly increases engraftment in a murine model of pig-to-human hematopoietic cell transplantation. *Am J Transplant* 14, 2713-2722.

[180] **OLACK, B.J., JARAMILLO, A., BENSHOFF, N.D. *et al.* (2002).** Rejection of porcine islet xenografts mediated by CD4+ T cells activated through the indirect antigen recognition pathway. *Xenotransplantation* 9, 393-401.

[181] **SCALEA, J., HANECAMP, I., ROBSON, S.C. *et al.* (2012).** T-cell-mediated immunological barriers to xenotransplantation. *Xenotransplantation* 19, 23-30.

[182] **YAMADA, K., SACHS, D.H. & DERSIMONIAN, H. (1995).** Direct and indirect recognition of pig class II antigens by human T cells. *Transplantation proceedings* 27, 258-259.

[183] **DORLING, A., LOMBARDI, G., BINNS, R. *et al.* (1996).** Detection of primary direct and indirect human anti-porcine T cell responses using a porcine dendritic cell population. *Eur J Immunol* 26, 1378-1387.

[184] **DORLING, A., BINNS, R. & LECHLER, R.I. (1996).** Direct human T-cell anti-pig xenoresponses are vigorous but significantly weaker than direct alloresponses. *Transplantation proceedings* 28, 653.

[185] **ROLLINS, S.A., KENNEDY, S.P., CHODERA, A.J. *et al.* (1994).** Evidence that activation of human T cells by porcine endothelium involves direct recognition of porcine SLA and costimulation by porcine ligands for LFA-1 and CD2. *Transplantation* 57, 1709-1716.

[186] **HARA, H., WITT, W., CROSSLEY, T. *et al.* (2013).** Human dominant-negative class II transactivator transgenic pigs - effect on the human anti-pig T-cell immune response and immune status. *Immunology* 140, 39-46.

[187] **SAMY, K.P., BUTLER, J.R., LI, P. *et al.* (2017).** The Role of Costimulation Blockade in Solid Organ and Islet Xenotransplantation. *Journal of immunology research* 2017, 8415205.

[188] **SHARPE, A.H. (2009).** Mechanisms of costimulation. *Immunol Rev* 229, 5-11.

[189] **LENSCHOW, D.J., ZENG, Y., THISTLETHWAITE, J.R. *et al.* (1992).** Long-term survival of xenogeneic pancreatic islet grafts induced by CTLA4lg. *Science* 257, 789-792.

[190] **LARSEN, C.P., PEARSON, T.C., ADAMS, A.B. *et al.* (2005).** Rational development of LEA29Y (belatacept), a high-affinity variant of CTLA4-Ig with potent immunosuppressive properties. *Am J Transplant* 5, 443-453.

[191] **NOBLE, J., JOUVE, T., JANBON, B. *et al.* (2019).** Belatacept in kidney transplantation and its limitations. *Expert Rev Clin Immunol* 15, 359-367.

[192] **BLUESTONE, J.A., ST CLAIR, E.W. & TURKA, L.A. (2006).** CTLA4Ig: bridging the basic immunology with clinical application. *Immunity* 24, 233-238.

[193] **BADELL, I.R., KARADKHELE, G.M., VASANTH, P. *et al.* (2019).** Abatacept as rescue immunosuppression after calcineurin inhibitor treatment failure in renal transplantation. *Am J Transplant* 19, 2342-2349.

[194] **PHELPS, C.J., BALL, S.F., VAUGHT, T.D. *et al.* (2009).** Production and characterization of transgenic pigs expressing porcine CTLA4-Ig. *Xenotransplantation* 16, 477-485.

[195] **BAHR, A., KASER, T., KEMTER, E. *et al.* (2016).** Ubiquitous LEA29Y Expression Blocks T Cell Co-Stimulation but Permits Sexual Reproduction in Genetically Modified Pigs. *PLoS One* 11, e0155676.

[196] **MARTIN, C., PLAT, M., NERRIERE-DAGUIN, V. *et al.* (2005).** Transgenic expression of CTLA4-Ig by fetal pig neurons for xenotransplantation. *Transgenic Res* 14, 373-384.

[197] **VABRES, B., LE BAS-BERNARDET, S., RIOCHET, D. *et al.* (2014).** hCTLA4-Ig transgene expression in keratocytes modulates rejection of corneal xenografts in a pig to non-human primate anterior lamellar keratoplasty model. *Xenotransplantation* 21, 431-443.

[198] **BUERCK, L.W., SCHUSTER, M., ODUNCU, F.S. *et al.* (2017).** LEA29Y expression in transgenic neonatal porcine islet-like cluster promotes long-lasting xenograft survival in humanized mice without immunosuppressive therapy. *Sci Rep* 7, 3572.

[199] **FISCHER, A., MANSKE, K., SEISSLER, J. *et al.* (2020).** Cytokine-inducible promoters to drive dynamic transgene expression: The "Smart Graft" strategy. *Xenotransplantation* 27, e12634.

[200] **FREEMAN, G.J., LONG, A.J., IWAI, Y. *et al.* (2000).** Engagement of the PD-1 immunoinhibitory receptor by a novel B7 family member leads to negative regulation of lymphocyte activation. *The Journal of experimental medicine* 192, 1027-1034.

[201] **NISHIMURA, H. & HONJO, T. (2001).** PD-1: an inhibitory immunoreceptor involved in peripheral tolerance. *Trends Immunol* 22, 265-268.

[202] **PLEGE, A., BORNS, K., BAARS, W. *et al.* (2009).** Suppression of human T-cell activation and expansion of regulatory T cells by pig cells overexpressing PD-ligands. *Transplantation* 87, 975-982.

[203] **BUERMANN, A., PETKOV, S., PETERSEN, B. *et al.* (2018).** Pigs expressing the human inhibitory ligand PD-L1 (CD 274) provide a new source of xenogeneic cells and tissues with low immunogenic properties. *Xenotransplantation* 25, e12387.

[204] **WOOD, K.J. & SAKAGUCHI, S. (2003).** Regulatory T cells in transplantation tolerance. *Nat Rev Immunol* 3, 199-210.

[205] **BANCROFT, G.J., SCHREIBER, R.D., BOSMA, G.C. *et al.* (1987).** A T cell-independent mechanism of macrophage activation by interferon-gamma. *J Immunol* 139, 1104-1107.

[206] **STEIMLE, V., SIEGRIST, C.A., MOTTET, A. *et al.* (1994).** Regulation of MHC class II expression by interferon-gamma mediated by the transactivator gene CIITA. *Science* 265, 106-109.

[207] **FRUH, K. & YANG, Y. (1999).** Antigen presentation by MHC class I and its regulation by interferon gamma. *Current opinion in immunology* 11, 76-81.

[208] **KESKINEN, P., RONNI, T., MATIKAINEN, S. *et al.* (1997).** Regulation of HLA class I and II expression by interferons and influenza A virus in human peripheral blood mononuclear cells. *Immunology* 91, 421-429.

[209] **KANG, S., BROWN, H.M. & HWANG, S. (2018).** Direct Antiviral Mechanisms of Interferon-Gamma. *Immune Netw* 18, e33.

[210] **DINARELLO, C.A. (1996).** Biologic basis for interleukin-1 in disease. *Blood* 87, 2095-2147.

[211] **KRAMER, F., TORZEWSKI, J., KAMENZ, J. *et al.* (2008).** Interleukin-1beta stimulates acute phase response and C-reactive protein synthesis by inducing an NFkappaB- and C/EBPbeta-dependent autocrine interleukin-6 loop. *Molecular immunology* 45, 2678-2689.

[212] **BEN-SASSON, S.Z., HU-LI, J., QUIEL, J. *et al.* (2009).** IL-1 acts directly on CD4 T cells to enhance their antigen-driven expansion and differentiation. *Proceedings of the National Academy of Sciences of the United States of America* 106, 7119-7124.

[213] **FALKOFF, R.J., MURAGUCHI, A., HONG, J.X. *et al.* (1983).** The effects of interleukin 1 on human B cell activation and proliferation. *J Immunol* 131, 801-805.

[214] **LIAO, W., LIN, J.X. & LEONARD, W.J. (2011).** IL-2 family cytokines: new insights into the complex roles of IL-2 as a broad regulator of T helper cell differentiation. *Current opinion in immunology* 23, 598-604.

[215] **KOURO, T. & TAKATSU, K. (2009).** IL-5- and eosinophil-mediated inflammation: from discovery to therapy. *International immunology* 21, 1303-1309.

[216] **TAKATSU, K. (1998).** Interleukin 5 and B cell differentiation. *Cytokine Growth Factor Rev* 9, 25-35.

[217] **HEINRICH, P.C., CASTELL, J.V. & ANDUS, T. (1990).** Interleukin-6 and the acute phase response. *The Biochemical journal* 265, 621-636.

[218] **DE VRIES, J.E. (1995).** Immunosuppressive and anti-inflammatory properties of interleukin 10. *Ann Med* 27, 537-541.

[219] **O'FARRELL, A.M., LIU, Y., MOORE, K.W. *et al.* (1998).** IL-10 inhibits macrophage activation and proliferation by distinct signaling mechanisms: evidence for Stat3-dependent and -independent pathways. *The EMBO journal* 17, 1006-1018.

[220] **MITTAL, S.K. & ROCHE, P.A. (2015).** Suppression of antigen presentation by IL-10. *Current opinion in immunology* 34, 22-27.

[221] **D'ORAZIO, T.J. & NIEDERKORN, J.Y. (1998).** A Novel Role for TGF-β and IL-10 in the Induction of Immune Privilege. *The Journal of Immunology* 160, 2089-2098.

[222] **BROUCKAERT, P. & FIERS, W. (1996).** Tumor necrosis factor and the systemic inflammatory response syndrome. *Current topics in microbiology and immunology* 216, 167-187.

[223] **MADGE, L.A. & POBER, J.S. (2001).** TNF signaling in vascular endothelial cells. *Experimental and molecular pathology* 70, 317-325.

[224] **PARAMESWARAN, N. & PATIAL, S. (2010).** Tumor necrosis factor-alpha signaling in macrophages. *Critical reviews in eukaryotic gene expression* 20, 87-103.

[225] **SANJABI, S., ZENEWICZ, L.A., KAMANAKA, M. *et al.* (2009).** Anti-inflammatory and pro-inflammatory roles of TGF-beta, IL-10, and IL-22 in immunity and autoimmunity. *Current opinion in pharmacology* 9, 447-453.

[226] **HARA, M., KINGSLEY, C.I., NIIMI, M. *et al.* (2001).** IL-10 is required for regulatory T cells to mediate tolerance to alloantigens in vivo. *J Immunol* 166, 3789-3796.

[227] **JOHNSTON, C.J., SMYTH, D.J., DRESSER, D.W. *et al.* (2016).** TGF-beta in tolerance, development and regulation of immunity. *Cellular immunology* 299, 14-22.

[228] **AKDIS, C.A. & BLASER, K. (2001).** Mechanisms of interleukin-10-mediated immune suppression. *Immunology* 103, 131-136.

[229] **FIORENTINO, D.F., BOND, M.W. & MOSMANN, T.R. (1989).** Two types of mouse T helper cell. IV. Th2 clones secrete a factor that inhibits cytokine production by Th1 clones. *The Journal of experimental medicine* 170, 2081-2095.

[230] **LAIDLAW, B.J., CUI, W., AMEZQUITA, R.A. *et al.* (2015).** Production of IL-10 by CD4(+) regulatory T cells during the resolution of infection promotes the maturation of memory CD8(+) T cells. *Nat Immunol* 16, 871-879.

[231] **KUMAR, A., ANGEL, J.B., DAFTARIAN, M.P. *et al.* (1998).** Differential production of IL-10 by T cells and monocytes of HIV-infected individuals: association of IL-10 production with CD28-mediated immune responsiveness. *Clinical and experimental immunology* 114, 78-86.

[232] **TAGA, K. & TOSATO, G. (1992).** IL-10 inhibits human T cell proliferation and IL-2 production. *J Immunol* 148, 1143-1148.

[233] **MURPHY, K.M., TRAVERS, P. & WALPORT, M. (2009).** Janeway Immunologie. Vol. 7, Spektrum Akademischer Verlag, Heidelberg, 448-449.

[234] **LEE, K.S., BAEK, D.W., KIM, K.H. *et al.* (2005).** IL-10-dependent down-regulation of MHC class II expression level on monocytes by peritoneal fluid from endometriosis patients. *International immunopharmacology* 5, 1699-1712.

[235] **DE LA BARRERA, S., ALEMAN, M., MUSELLA, R. *et al.* (2004).** IL-10 down-regulates costimulatory molecules on Mycobacterium tuberculosis-pulsed macrophages and impairs the lytic activity of CD4 and CD8 CTL in tuberculosis patients. *Clinical and experimental immunology* 138, 128-138.

[236] **WORTHINGTON, J.J., FENTON, T.M., CZAJKOWSKA, B.I. *et al.* (2012).** Regulation of TGFbeta in the immune system: an emerging role for integrins and dendritic cells. *Immunobiology* 217, 1259-1265.

[237] **BRANTON, M.H. & KOPP, J.B. (1999).** TGF-beta and fibrosis. *Microbes Infect* 1, 1349-1365.

[238] **CHEN, W., JIN, W., HARDEGEN, N. *et al.* (2003).** Conversion of peripheral CD4+CD25- naive T cells to CD4+CD25+ regulatory T cells by TGF-beta induction of transcription factor Foxp3. *The Journal of experimental medicine* 198, 1875-1886.

[239] **ZIEGLER, S.F. & BUCKNER, J.H. (2009).** FOXP3 and the regulation of Treg/Th17 differentiation. *Microbes Infect* 11, 594-598.

[240] **SANJABI, S., OH, S.A. & LI, M.O. (2017).** Regulation of the Immune Response by TGF-beta: From Conception to Autoimmunity and Infection. *Cold Spring Harb Perspect Biol* 9, a022236.

[241] **WERNER, F., JAIN, M.K., FEINBERG, M.W. *et al.* (2000).** Transforming growth factor-beta 1 inhibition of macrophage activation is mediated via Smad3. *J Biol Chem* 275, 36653-36658.

[242] **LI, M.O., WAN, Y.Y., SANJABI, S. *et al.* (2006).** Transforming growth factor-beta regulation of immune responses. *Annu Rev Immunol* 24, 99-146.

[243] **VARFOLOMEEV, E.E. & ASHKENAZI, A. (2004).** Tumor necrosis factor: an apoptosis JuNKie? *Cell* 116, 491-497.

[244] **GRIVENNIKOV, S.I., TUMANOV, A.V., LIEPINSH, D.J. *et al.* (2005).** Distinct and nonredundant in vivo functions of TNF produced by t cells and macrophages/neutrophils: protective and deleterious effects. *Immunity* 22, 93-104.

[245] **CUI, W., MORRISON, D.C. & SILVERSTEIN, R. (2000).** Differential tumor necrosis factor alpha expression and release from peritoneal mouse macrophages in vitro in response to proliferating gram-positive versus gram-negative bacteria. *Infection and immunity* 68, 4422-4429.

[246] **BLANCO, P., PALUCKA, A.K., PASCUAL, V. *et al.* (2008).** Dendritic cells and cytokines in human inflammatory and autoimmune diseases. *Cytokine Growth Factor Rev* 19, 41-52.

[247] **WANG, R., JAW, J.J., STUTZMAN, N.C. *et al.* (2012).** Natural killer cell-produced IFN-gamma and TNF-alpha induce target cell cytolysis through up-regulation of ICAM-1. *J Leukoc Biol* 91, 299-309.

[248] **RANTA, V., ORPANA, A., CARPEN, O. *et al.* (1999).** Human vascular endothelial cells produce tumor necrosis factor-alpha in response to proinflammatory cytokine stimulation. *Critical care medicine* 27, 2184-2187.

[249] **SAKAGUCHI, M., KATO, H., NISHIYORI, A. *et al.* (1995).** Characterization of CD4+ T helper cells in patients with Kawasaki disease (KD): preferential production of tumour necrosis factor-alpha (TNF-alpha) by V beta 2- or V beta 8- CD4+ T helper cells. *Clinical and experimental immunology* 99, 276-282.

[250] **BISTRIAN, B.R. (1999).** Acute phase proteins and the systemic inflammatory response. *Critical care medicine* 27, 452-453.

[251] **GEWURZ, H., MOLD, C., SIEGEL, J. *et al.* (1982).** C-reactive protein and the acute phase response. *Advances in internal medicine* 27, 345-372.

[252] **JAIN, S., GAUTAM, V. & NASEEM, S. (2011).** Acute-phase proteins: As diagnostic tool. *Journal of pharmacy & bioallied sciences* 3, 118-127.

[253] **CUMBERBATCH, M. & KIMBER, I. (1992).** Dermal tumour necrosis factor-alpha induces dendritic cell migration to draining lymph nodes, and possibly provides one stimulus for Langerhans' cell migration. *Immunology* 75, 257-263.

[254] **SUTO, H., NAKAE, S., KAKURAI, M. *et al.* (2006).** Mast cell-associated TNF promotes dendritic cell migration. *J Immunol* 176, 4102-4112.

[255] **LOPEZ-CASTEJON, G. & BROUGH, D. (2011).** Understanding the mechanism of IL-1beta secretion. *Cytokine Growth Factor Rev* 22, 189-195.

[256] **SCHENK, M., FABRI, M., KRUTZIK, S.R. *et al.* (2014).** Interleukin-1beta triggers the differentiation of macrophages with enhanced capacity to present mycobacterial antigen to T cells. *Immunology* 141, 174-180.

[257] **JAIN, A., SONG, R., WAKELAND, E.K. *et al.* (2018).** T cell-intrinsic IL-1R signaling licenses effector cytokine production by memory CD4 T cells. *Nat Commun* 9, 3185.

[258] **SANTARLASCI, V., COSMI, L., MAGGI, L. *et al.* (2013).** IL-1 and T Helper Immune Responses. *Front Immunol* 4, 182.

[259] **YAMASHITA, U. (1987).** Role of interleukin-1 in B-cell activation. *Ann Inst Pasteur Immunol* 138, 496-500.

[260] **NAKAE, S., ASANO, M., HORAI, R. *et al.* (2001).** Interleukin-1 beta, but not interleukin-1 alpha, is required for T-cell-dependent antibody production. *Immunology* 104, 402-409.

[261] **MURPHY, K.M., TRAVERS, P. & WALPORT, M. (2009).** Janeway Immunologie. Vol. 7, Spektrum Akademischer Verlag, Heidelberg, 121.

[262] **ARASE, H., ARASE, N. & SAITO, T. (1996).** Interferon gamma production by natural killer (NK) cells and NK1.1+ T cells upon NKR-P1 cross-linking. *The Journal of experimental medicine* 183, 2391-2396.

[263] **OHTEKI, T., FUKAO, T., SUZUE, K. *et al.* (1999).** Interleukin 12-dependent interferon gamma production by CD8alpha+ lymphoid dendritic cells. *The Journal of experimental medicine* 189, 1981-1986.

[264] **DARWICH, L., COMA, G., PENA, R. *et al.* (2009).** Secretion of interferon-gamma by human macrophages demonstrated at the single-cell level after costimulation with interleukin (IL)-12 plus IL-18. *Immunology* 126, 386-393.

[265] **MANETTI, R., GEROSA, F., GIUDIZI, M.G. *et al.* (1994).** Interleukin 12 induces stable priming for interferon gamma (IFN-gamma) production during differentiation of human T helper (Th) cells and transient IFN-gamma production in established Th2 cell clones. *The Journal of experimental medicine* 179, 1273-1283.

[266] **BHAT, P., LEGGATT, G., WATERHOUSE, N. *et al.* (2017).** Interferon-gamma derived from cytotoxic lymphocytes directly enhances their motility and cytotoxicity. *Cell Death Dis* 8, e2836.

[267] **LAWRENCE, T. (2009).** The nuclear factor NF-kappaB pathway in inflammation. *Cold Spring Harb Perspect Biol* 1, a001651.

[268] **CHEN, G. & GOEDDEL, D.V. (2002).** TNF-R1 signaling: a beautiful pathway. *Science* 296, 1634-1635.

[269] **WOJDASIEWICZ, P., PONIATOWSKI, L.A. & SZUKIEWICZ, D. (2014).** The role of inflammatory and anti-inflammatory cytokines in the pathogenesis of osteoarthritis. *Mediators Inflamm* 2014, 561459.

[270] **LIU, T., ZHANG, L., JOO, D. *et al.* (2017).** NF-kappaB signaling in inflammation. *Signal Transduct Target Ther* 2, 17023.

[271] **GREENLUND, A.C., MORALES, M.O., VIVIANO, B.L. *et al.* (1995).** Stat recruitment by tyrosine-phosphorylated cytokine receptors: an ordered reversible affinity-driven process. *Immunity* 2, 677-687.

[272] **SCHRODER, K., HERTZOG, P.J., RAVASI, T. *et al.* (2004).** Interferon-gamma: an overview of signals, mechanisms and functions. *J Leukoc Biol* 75, 163-189.

[273] **SCHNEIDER, W.M., CHEVILLOTTE, M.D. & RICE, C.M. (2014).** Interferon-stimulated genes: a complex web of host defenses. *Annu Rev Immunol* 32, 513-545.

[274] **EVANS, M.J. & KAUFMAN, M.H. (1981).** Establishment in culture of pluripotential cells from mouse embryos. *Nature* 292, 154-156.

[275] **THOMAS, K.R. & CAPECCHI, M.R. (1987).** Site-directed mutagenesis by gene targeting in mouse embryo-derived stem cells. *Cell* 51, 503-512.

[276] **VASSILIEV, I. & NOTTLE, M.B. (2013).** Isolation and culture of porcine embryonic stem cells. *Methods Mol Biol* 1074, 85-95.

[277] **DENNING, C., DICKINSON, P., BURL, S. *et al.* (2001).** Gene targeting in primary fetal fibroblasts from sheep and pig. *Cloning Stem Cells* 3, 221-231.

[278] **LEUCHS, S., SAALFRANK, A., MERKL, C. *et al.* (2012).** Inactivation and inducible oncogenic mutation of p53 in gene targeted pigs. *PLoS One* 7, e43323.

[279] **DENNING, C., BURL, S., AINSLIE, A. *et al.* (2001).** Deletion of the alpha(1,3)galactosyl transferase (GGTA1) gene and the prion protein (PrP) gene in sheep. *Nature biotechnology* 19, 559-562.

[280] **MOEHLE, E.A., ROCK, J.M., LEE, Y.L. *et al.* (2007).** Targeted gene addition into a specified location in the human genome using designed zinc finger nucleases. *Proceedings of the National Academy of Sciences of the United States of America* 104, 3055-3060.

[281] **CUI, C., SONG, Y., LIU, J. *et al.* (2015).** Gene targeting by TALEN-induced homologous recombination in goats directs production of beta-lactoglobulin-free, high-human lactoferrin milk. *Sci Rep* 5, 10482.

[282] **CHANG, N., SUN, C., GAO, L. *et al.* (2013).** Genome editing with RNA-guided Cas9 nuclease in zebrafish embryos. *Cell Res* 23, 465-472.

[283] **SANSBURY, B.M., HEWES, A.M. & KMIEC, E.B. (2019).** Understanding the diversity of genetic outcomes from CRISPR-Cas generated homology-directed repair. *Communications biology* 2, 458.

[284] **FISHMAN-LOBELL, J., RUDIN, N. & HABER, J.E. (1992).** Two alternative pathways of double-strand break repair that are kinetically separable and independently modulated. *Mol Cell Biol* 12, 1292-1303.

[285] **MOORE, J.K. & HABER, J.E. (1996).** Cell cycle and genetic requirements of two pathways of nonhomologous end-joining repair of double-strand breaks in Saccharomyces cerevisiae. *Mol Cell Biol* 16, 2164-2173.

[286] **RANJHA, L., HOWARD, S.M. & CEJKA, P. (2018).** Main steps in DNA double-strand break repair: an introduction to homologous recombination and related processes. *Chromosoma* 127, 187-214.

[287] **KIM, Y.G., CHA, J. & CHANDRASEGARAN, S. (1996).** Hybrid restriction enzymes: zinc finger fusions to Fok I cleavage domain. *Proceedings of the National Academy of Sciences of the United States of America* 93, 1156-1160.

[288] **BIBIKOVA, M., CARROLL, D., SEGAL, D.J. *et al.* (2001).** Stimulation of homologous recombination through targeted cleavage by chimeric nucleases. *Mol Cell Biol* 21, 289-297.

[289] **LI, T., HUANG, S., JIANG, W.Z. *et al.* (2011).** TAL nucleases (TALNs): hybrid proteins composed of TAL effectors and FokI DNA-cleavage domain. *Nucleic acids research* 39, 359-372.

[290] **MILLER, J.C., TAN, S., QIAO, G. *et al.* (2011).** A TALE nuclease architecture for efficient genome editing. *Nature biotechnology* 29, 143-148.

[291] **JINEK, M., CHYLINSKI, K., FONFARA, I. *et al.* (2012).** A programmable dual-RNA-guided DNA endonuclease in adaptive bacterial immunity. *Science* 337, 816-821.

[292] **WIEDENHEFT, B., STERNBERG, S.H. & DOUDNA, J.A. (2012).** RNA-guided genetic silencing systems in bacteria and archaea. *Nature* 482, 331-338.

[293] **CONG, L., RAN, F.A., COX, D. *et al.* (2013).** Multiplex genome engineering using CRISPR/Cas systems. *Science* 339, 819-823.

[294] **MALI, P., YANG, L., ESVELT, K.M. *et al.* (2013).** RNA-guided human genome engineering via Cas9. *Science* 339, 823-826.

[295] **WU, M., WEI, C., LIAN, Z. *et al.* (2016).** Rosa26-targeted sheep gene knock-in via CRISPR-Cas9 system. *Sci Rep* 6, 24360.

[296] **ZETSCHE, B., GOOTENBERG, J.S., ABUDAYYEH, O.O. *et al.* (2015).** Cpf1 is a single RNA-guided endonuclease of a class 2 CRISPR-Cas system. *Cell* 163, 759-771.

[297] **KOMOR, A.C., KIM, Y.B., PACKER, M.S. *et al.* (2016).** Programmable editing of a target base in genomic DNA without double-stranded DNA cleavage. *Nature* 533, 420-424.

[298] **GAUDELLI, N.M., KOMOR, A.C., REES, H.A. *et al.* (2017).** Programmable base editing of A*T to G*C in genomic DNA without DNA cleavage. *Nature* 551, 464-471.

[299] **GILBERT, L.A., HORLBECK, M.A., ADAMSON, B. *et al.* (2014).** Genome-Scale CRISPR-Mediated Control of Gene Repression and Activation. *Cell* 159, 647-661.

[300] **McDonald, J.I., Celik, H., Rois, L.E. *et al.* (2016).** Reprogrammable CRISPR/Cas9-based system for inducing site-specific DNA methylation. *Biol Open* 5, 866-874.

[301] **Choudhury, S.R., Cui, Y., Lubecka, K. *et al.* (2016).** CRISPR-dCas9 mediated TET1 targeting for selective DNA demethylation at BRCA1 promoter. *Oncotarget* 7, 46545-46556.

[302] **Wilmut, I., Schnieke, A.E., McWhir, J. *et al.* (1997).** Viable offspring derived from fetal and adult mammalian cells. *Nature* 385, 810-813.

[303] **Schnieke, A.E., Kind, A.J., Ritchie, W.A. *et al.* (1997).** Human factor IX transgenic sheep produced by transfer of nuclei from transfected fetal fibroblasts. *Science* 278, 2130-2133.

[304] **Niemann, H. (2016).** Epigenetic reprogramming in mammalian species after SCNT-based cloning. *Theriogenology* 86, 80-90.

[305] **Lai, L. & Prather, R.S. (2003).** Production of cloned pigs by using somatic cells as donors. *Cloning Stem Cells* 5, 233-241.

[306] **Young, L.E., Schnieke, A.E., McCreath, K.J. *et al.* (2003).** Conservation of IGF2-H19 and IGF2R imprinting in sheep: effects of somatic cell nuclear transfer. *Mech Dev* 120, 1433-1442.

[307] **Kurome, M., Geistlinger, L., Kessler, B. *et al.* (2013).** Factors influencing the efficiency of generating genetically engineered pigs by nuclear transfer: multi-factorial analysis of a large data set. *BMC Biotechnol* 13, 43.

[308] **Cho, S.K., Kim, J.H., Park, J.Y. *et al.* (2007).** Serial cloning of pigs by somatic cell nuclear transfer: restoration of phenotypic normality during serial cloning. *Developmental dynamics : an official publication of the American Association of Anatomists* 236, 3369-3382.

[309] **Hammer, R.E., Pursel, V.G., Rexroad, C.E., Jr. *et al.* (1985).** Production of transgenic rabbits, sheep and pigs by microinjection. *Nature* 315, 680-683.

[310] **Li, Z., Zeng, F., Meng, F. *et al.* (2014).** Generation of transgenic pigs by cytoplasmic injection of piggyBac transposase-based pmGENIE-3 plasmids. *Biol Reprod* 90, 93.

[311] **Hai, T., Teng, F., Guo, R. *et al.* (2014).** One-step generation of knockout pigs by zygote injection of CRISPR/Cas system. *Cell Res* 24, 372-375.

[312] **Petersen, B., Frenzel, A., Lucas-Hahn, A. *et al.* (2016).** Efficient production of biallelic GGTA1 knockout pigs by cytoplasmic microinjection of CRISPR/Cas9 into zygotes. *Xenotransplantation* 23, 338-346.

[313] **Kurome, M., Kessler, B., Wuensch, A. *et al.* (2015).** Nuclear transfer and transgenesis in the pig. *Methods Mol Biol* 1222, 37-59.

[314] **Schindler, U. & Baichwal, V.R. (1994).** Three NF-kappa B binding sites in the human E-selectin gene required for maximal tumor necrosis factor alpha-induced expression. *Mol Cell Biol* 14, 5820-5831.

[315] **JENSEN, L.E. & WHITEHEAD, A.S. (2003).** ELAM-1/E-selectin promoter contains an inducible AP-1/CREB site and is not NF-kappa B-specific. *Biotechniques* 35, 54-56, 58.

[316] **IADEMARCO, M.F., MCQUILLAN, J.J., ROSEN, G.D. *et al.* (1992).** Characterization of the promoter for vascular cell adhesion molecule-1 (VCAM-1). *J Biol Chem* 267, 16323-16329.

[317] **LIU, M., SUN, Z., ZHOU, A. *et al.* (2010).** Functional characterization of the promoter region of human TNFAIP1 gene. *Mol Biol Rep* 37, 1699-1705.

[318] **SHYY, Y.J., LI, Y.S. & KOLATTUKUDY, P.E. (1990).** Structure of human monocyte chemotactic protein gene and its regulation by TPA. *Biochemical and biophysical research communications* 169, 346-351.

[319] **UEDA, A., OKUDA, K., OHNO, S. *et al.* (1994).** NF-kappa B and Sp1 regulate transcription of the human monocyte chemoattractant protein-1 gene. *J Immunol* 153, 2052-2063.

[320] **UEDA, A., ISHIGATSUBO, Y., OKUBO, T. *et al.* (1997).** Transcriptional regulation of the human monocyte chemoattractant protein-1 gene. Cooperation of two NF-kappaB sites and NF-kappaB/Rel subunit specificity. *J Biol Chem* 272, 31092-31099.

[321] **MARTIN, T., CARDARELLI, P.M., PARRY, G.C. *et al.* (1997).** Cytokine induction of monocyte chemoattractant protein-1 gene expression in human endothelial cells depends on the cooperative action of NF-kappa B and AP-1. *Eur J Immunol* 27, 1091-1097.

[322] **FINZER, P., SOTO, U., DELIUS, H. *et al.* (2000).** Differential transcriptional regulation of the monocyte-chemoattractant protein-1 (MCP-1) gene in tumorigenic and non-tumorigenic HPV 18 positive cells: the role of the chromatin structure and AP-1 composition. *Oncogene* 19, 3235-3244.

[323] **DENG, X., XU, M., YUAN, C. *et al.* (2013).** Transcriptional regulation of increased CCL2 expression in pulmonary fibrosis involves nuclear factor-kappaB and activator protein-1. *Int J Biochem Cell Biol* 45, 1366-1376.

[324] **KRIKOS, A., LAHERTY, C.D. & DIXIT, V.M. (1992).** Transcriptional activation of the tumor necrosis factor alpha-inducible zinc finger protein, A20, is mediated by kappa B elements. *J Biol Chem* 267, 17971-17976.

[325] **AINBINDER, E., REVACH, M., WOLSTEIN, O. *et al.* (2002).** Mechanism of rapid transcriptional induction of tumor necrosis factor alpha-responsive genes by NF-kappaB. *Mol Cell Biol* 22, 6354-6362.

[326] **AMIR-ZILBERSTEIN, L. & DIKSTEIN, R. (2008).** Interplay between E-box and NF-kappaB in regulation of A20 gene by DRB sensitivity-inducing factor (DSIF). *J Biol Chem* 283, 1317-1323.

[327] **GHERSA, P., HOOFT VAN HUIJSDUIJNEN, R., WHELAN, J. *et al.* (1994).** Inhibition of E-selectin gene transcription through a cAMP-dependent protein kinase pathway. *J Biol Chem* 269, 29129-29137.

[328] **DE LUCA, L.G., JOHNSON, D.R., WHITLEY, M.Z. *et al.* (1994).** cAMP and tumor necrosis factor competitively regulate transcriptional activation through and nuclear factor binding to the cAMP-responsive element/activating transcription factor element of the endothelial leukocyte adhesion molecule-1 (E-selectin) promoter. *J Biol Chem* 269, 19193-19196.

[329] **SINGH, R., SHARMA, M.C., SARKAR, C. *et al.* (2014).** Transcription factor C/EBP-beta mediates downregulation of dipeptidyl-peptidase III expression by interleukin-6 in human glioblastoma cells. *The FEBS journal* 281, 1629-1641.

[330] **GREENWEL, P., TANAKA, S., PENKOV, D. *et al.* (2000).** Tumor necrosis factor alpha inhibits type I collagen synthesis through repressive CCAAT/enhancer-binding proteins. *Mol Cell Biol* 20, 912-918.

[331] **DINARELLO, C.A. & VAN DER MEER, J.W. (2013).** Treating inflammation by blocking interleukin-1 in humans. *Semin Immunol* 25, 469-484.

[332] **SIMM, N. (2016).** Identification and characterization of inducible promoter elements for the expression of T-cell regulatory genes in transgenic pigs for xenotransplantation. Master's thesis, TUM School of Life Sciences, Technische Universität München, Freising.

[333] **MURRAY, A.G., KHODADOUST, M.M., POBER, J.S. *et al.* (1994).** Porcine aortic endothelial cells activate human T cells: direct presentation of MHC antigens and costimulation by ligands for human CD2 and CD28. *Immunity* 1, 57-63.

[334] **BATTEN, P., YACOUB, M.H. & ROSE, M.L. (1996).** Effect of human cytokines (IFN-gamma, TNF-alpha, IL-1 beta, IL-4) on porcine endothelial cells: induction of MHC and adhesion molecules and functional significance of these changes. *Immunology* 87, 127-133.

[335] **MAUERER, A. (2019).** In vitro analysis of various promoters for xenotransplantation. Bachelor's Thesis, TUM School of Lifesciences, Technische Universität München, Freising.

[336] **SHULTZ, L.D., LYONS, B.L., BURZENSKI, L.M. *et al.* (2005).** Human lymphoid and myeloid cell development in NOD/LtSz-scid IL2R gamma null mice engrafted with mobilized human hemopoietic stem cells. *J Immunol* 174, 6477-6489.

[337] **MCCLURKIN, A.W. & NORMAN, J.O. (1966).** Studies on transmissible gastroenteritis of swine. II. Selected characteristics of a cytopathogenic virus common to five isolates from transmissible gastroenteritis. *Can J Comp Med Vet Sci* 30, 190-198.

[338] **ATCC (2018).** American Type Culture Collection. Product sheet, ST (ATCC CRL-1746), from https://www.lgcstandards-atcc.org/Products/All/CRL-1746?geo_country=de#documentation (retrieved 10.07. 2019).

[339] **DSMZ (2019).** Deutsche Sammlung für Mikroorganismen und Zellkulturen. Product sheet, ST (ACC 641), from https://www.dsmz.de/collection/catalogue/details/culture/ACC-641 (retrieved 10.07. 2019).

[340] **LI, S., RAN, X.Q., XU, L. *et al.* (2011).** microRNA and mRNA expression profiling analysis of dichlorvos cytotoxicity in porcine kidney epithelial PK15 cells. *DNA Cell Biol* 30, 1073-1083.

[341] **PIRTLE, E.C. (1966).** Variation in the modal chromosome number of two PK-15 porcine kidney cell lines. *American journal of veterinary research* 27, 747-749.

[342] **FIEBIG, U., FISCHER, K., BAHR, A. *et al.* (2018).** Porcine endogenous retroviruses: Quantification of the copy number in cell lines, pig breeds, and organs. *Xenotransplantation* 25, e12445.

[343] **ZHU, Y., LAU, A., LAU, J. *et al.* (2007).** Enhanced replication of porcine circovirus type 2 (PCV2) in a homogeneous subpopulation of PK15 cell line. *Virology* 369, 423-430.

[344] **TODARO, G.J., BENVENISTE, R.E., LIEBER, M.M. *et al.* (1974).** Characterization of a type C virus released from the porcine cell line PK(15). *Virology* 58, 65-74.

[345] **LI, S., FLISIKOWSKA, T., KUROME, M. *et al.* (2014).** Dual fluorescent reporter pig for Cre recombination: transgene placement at the ROSA26 locus. *PLoS One* 9, e102455.

[346] **MULHOLLAND, C.B., SMETS, M., SCHMIDTMANN, E. *et al.* (2015).** A modular open platform for systematic functional studies under physiological conditions. *Nucleic acids research* 43, e112.

[347] **RINKE, K. (2019).** CRISPR/Cas9 mediated knockout of the UL16-binding protein 1 in porcine cells for the purpose of xenotransplantation. Bachelor's Thesis, TUM School of Life Sciences, Technischne Universität München, Freising.

[348] **BAO, L., CHEN, H., JONG, U. *et al.* (2014).** Generation of GGTA1 biallelic knockout pigs via zinc-finger nucleases and somatic cell nuclear transfer. *Sci China Life Sci* 57, 263-268.

[349] **MOHIUDDIN, M.M., SINGH, A.K., CORCORAN, P.C. *et al.* (2016).** Chimeric 2C10R4 anti-CD40 antibody therapy is critical for long-term survival of GTKO.hCD46.hTBM pig-to-primate cardiac xenograft. *Nat Commun* 7, 11138.

[350] **CHOI, H.J., LEE, J.J., KIM, D.H. *et al.* (2015).** Blockade of CD40-CD154 costimulatory pathway promotes long-term survival of full-thickness porcine corneal grafts in nonhuman primates: clinically applicable xenocorneal transplantation. *Am J Transplant* 15, 628-641.

[351] **LINSLEY, P.S. & GOLSTEIN, P. (1996).** Lymphocyte activation: T-cell regulation by CTLA-4. *Current biology : CB* 6, 398-400.

[352] **SCHEIPERS, P. & REISER, H. (1998).** Role of the CTLA-4 receptor in T cell activation and immunity. Physiologic function of the CTLA-4 receptor. *Immunologic research* 18, 103-115.

[353] **WECLAWIAK, H., KAMAR, N., OULD-MOHAMED, A. *et al.* (2010).** Biological agents in kidney transplantation: belatacept is entering the field. *Expert opinion on biological therapy* 10, 1501-1508.

[354] **VAUGHAN, A.N., MALDE, P., ROGERS, N.J. *et al.* (2000).** Porcine CTLA4-Ig lacks a MYPPPY motif, binds inefficiently to human B7 and specifically suppresses human CD4+ T cell responses costimulated by pig but not human B7. *J Immunol* 165, 3175-3181.

[355] **KOSHIKA, T., PHELPS, C., FANG, J. *et al.* (2011).** Relative efficiency of porcine and human cytotoxic T-lymphocyte antigen 4 immunoglobulin in inhibiting human CD4+ T-cell responses co-stimulated by porcine and human B7 molecules. *Immunology* 134, 386-397.

[356] **BARROW, K.M., PEREZ-CAMPO, F.M. & WARD, C.M. (2006).** Use of the cytomegalovirus promoter for transient and stable transgene expression in mouse embryonic stem cells. *Methods Mol Biol* 329, 283-294.

[357] **XU, Q., CHEN, W., WANG, Z. *et al.* (2009).** Mice transgenic with SV40-late-promoter-driven Polyomavirus Middle T oncogene exclusively develop hemangiomas. *Transgenic Res* 18, 399-406.

[358] **BROOKS, A.R., HARKINS, R.N., WANG, P. *et al.* (2004).** Transcriptional silencing is associated with extensive methylation of the CMV promoter following adenoviral gene delivery to muscle. *J Gene Med* 6, 395-404.

[359] **HARMS, J.S., OLIVEIRA, S.C. & SPLITTER, G.A. (1999).** Regulation of transgene expression in genetic immunization. *Braz J Med Biol Res* 32, 155-162.

[360] **HALBERT, C.L., LAM, S.L. & MILLER, A.D. (2007).** High-efficiency promoter-dependent transduction by adeno-associated virus type 6 vectors in mouse lung. *Human gene therapy* 18, 344-354.

[361] **ABE, H., NAKAZAWA, M., KASUGA, K. *et al.* (2014).** The CAG Promoter is More Active than the CEF Promoter for the Expression of Transgenes in a Mouse ES Cell Line E14-Derived EB3 Cells. *Biotechnology & Biotechnological Equipment* 25, 2301-2304.

[362] **ALEXOPOULOU, A.N., COUCHMAN, J.R. & WHITEFORD, J.R. (2008).** The CMV early enhancer/chicken beta actin (CAG) promoter can be used to drive transgene expression during the differentiation of murine embryonic stem cells into vascular progenitors. *BMC Cell Biol* 9, 2.

[363] **DENG, W., YANG, D., ZHAO, B. *et al.* (2011).** Use of the 2A peptide for generation of multi-transgenic pigs through a single round of nuclear transfer. *PLoS One* 6, e19986.

[364] **RIEBLINGER, B., FISCHER, K., KIND, A. *et al.* (2018).** Strong xenoprotective function by single-copy transgenes placed sequentially at a permissive locus. *Xenotransplantation* 25, e12382.

[365] **AIGNER, B., KLYMIUK, N. & WOLF, E. (2010).** Transgenic pigs for xenotransplantation: selection of promoter sequences for reliable transgene expression. *Current opinion in organ transplantation* 15, 201-206.

[366] **DIAMOND, L.E., QUINN, C.M., MARTIN, M.J. *et al.* (2001).** A human CD46 transgenic pig model system for the study of discordant xenotransplantation. *Transplantation* 71, 132-142.

[367] **ZHOU, C.Y., MCINNES, E., COPEMAN, L. *et al.* (2005).** Transgenic pigs expressing human CD59, in combination with human membrane cofactor protein and human decay-accelerating factor. *Xenotransplantation* 12, 142-148.

[368] **KLYMIUK, N., VAN BUERCK, L., BAHR, A. *et al.* (2012).** Xenografted islet cell clusters from INSLEA29Y transgenic pigs rescue diabetes and prevent immune rejection in humanized mice. *Diabetes* 61, 1527-1532.

[369] **GOSSEN, M. & BUJARD, H. (1992).** Tight control of gene expression in mammalian cells by tetracycline-responsive promoters. *Proceedings of the National Academy of Sciences of the United States of America* 89, 5547-5551.

[370] **GOSSEN, M., FREUNDLIEB, S., BENDER, G. *et al.* (1995).** Transcriptional activation by tetracyclines in mammalian cells. *Science* 268, 1766-1769.

[371] **SCHONIG, K., FREUNDLIEB, S. & GOSSEN, M. (2013).** Tet-Transgenic Rodents: a comprehensive, up-to date database. *Transgenic Res* 22, 251-254.

[372] **DAS, A.T., TENENBAUM, L. & BERKHOUT, B. (2016).** Tet-On Systems For Doxycycline-inducible Gene Expression. *Current gene therapy* 16, 156-167.

[373] **JIN, Y.X., JEON, Y., LEE, S.H. *et al.* (2014).** Production of pigs expressing a transgene under the control of a tetracycline-inducible system. *PLoS One* 9, e86146.

[374] **PHARMAINDEX (2019).** Doxycyclin, from https://www.gelbe-liste.de/wirkstoffe/Doxycyclin_30 (retrieved 15 Mar 2021).

[375] **(2019).** LiverTox: Clinical and Research Information on Drug-Induced Liver Injury. Doxycycline, from https://www.ncbi.nlm.nih.gov/books/NBK548353/ (retrieved 15 Mar 2021).

[376] **SMALE, S.T. (2010).** Selective transcription in response to an inflammatory stimulus. *Cell* 140, 833-844.

[377] **MASTON, G.A., EVANS, S.K. & GREEN, M.R. (2006).** Transcriptional regulatory elements in the human genome. *Annu Rev Genomics Hum Genet* 7, 29-59.

[378] **DESHMANE, S.L., KREMLEV, S., AMINI, S. *et al.* (2009).** Monocyte chemoattractant protein-1 (MCP-1): an overview. *Journal of interferon & cytokine research : the official journal of the International Society for Interferon and Cytokine Research* 29, 313-326.

[379] **FANTUZZI, L., SPADARO, F., PURIFICATO, C. *et al.* (2008).** Phosphatidylcholine-specific phospholipase C activation is required for CCR5-dependent, NF-kB-driven CCL2 secretion elicited in response to HIV-1 gp120 in human primary macrophages. *Blood* 111, 3355-3363.

[380] **CHO, N.H., SEONG, S.Y., HUH, M.S. *et al.* (2002).** Induction of the gene encoding macrophage chemoattractant protein 1 by Orientia tsutsugamushi in human endothelial cells involves activation of transcription factor activator protein 1. *Infection and immunity* 70, 4841-4850.

[381] **EFERL, R. & WAGNER, E.F. (2003).** AP-1: a double-edged sword in tumorigenesis. *Nat Rev Cancer* 3, 859-868.

[382] **FUJIOKA, S., NIU, J., SCHMIDT, C. *et al.* (2004).** NF-kappaB and AP-1 connection: mechanism of NF-kappaB-dependent regulation of AP-1 activity. *Mol Cell Biol* 24, 7806-7819.

[383] **WHITMARSH, A.J. & DAVIS, R.J. (1996).** Transcription factor AP-1 regulation by mitogen-activated protein kinase signal transduction pathways. *J Mol Med (Berl)* 74, 589-607.

[384] **KYRIAKIS, J.M. (1999).** Activation of the AP-1 transcription factor by inflammatory cytokines of the TNF family. *Gene Expr* 7, 217-231.

[385] **PING, D., JONES, P.L. & BOSS, J.M. (1996).** TNF regulates the in vivo occupancy of both distal and proximal regulatory regions of the MCP-1/JE gene. *Immunity* 4, 455-469.

[386] **BEYAERT, R., HEYNINCK, K. & VAN HUFFEL, S. (2000).** A20 and A20-binding proteins as cellular inhibitors of nuclear factor-kappa B-dependent gene expression and apoptosis. *Biochemical pharmacology* 60, 1143-1151.

[387] **KANG, H.K., WANG, S., DANGI, A. *et al.* (2017).** Differential Role of B Cells and IL-17 Versus IFN-gamma During Early and Late Rejection of Pig Islet Xenografts in Mice. *Transplantation* 101, 1801-1810.

[388] **GORBACHEVA, V., FAN, R., LI, X. *et al.* (2010).** Interleukin-17 promotes early allograft inflammation. *The American journal of pathology* 177, 1265-1273.

[389] **LOONG, C.C., HSIEH, H.G., LUI, W.Y. *et al.* (2002).** Evidence for the early involvement of interleukin 17 in human and experimental renal allograft rejection. *J Pathol* 197, 322-332.

[390] **VANAUDENAERDE, B.M., DUPONT, L.J., WUYTS, W.A. *et al.* (2006).** The role of interleukin-17 during acute rejection after lung transplantation. *Eur Respir J* 27, 779-787.

[391] **JIN, W. & DONG, C. (2013).** IL-17 cytokines in immunity and inflammation. *Emerg Microbes Infect* 2, e60.

[392] **ZENOBIA, C. & HAJISHENGALLIS, G. (2015).** Basic biology and role of interleukin-17 in immunity and inflammation. *Periodontol 2000* 69, 142-159.

[393] **SRINIVAS, S., WATANABE, T., LIN, C.S. *et al.* (2001).** Cre reporter strains produced by targeted insertion of EYFP and ECFP into the ROSA26 locus. *BMC Dev Biol* 1, 4.

[394] **KOBAYASHI, T., KATO-ITOH, M., YAMAGUCHI, T. *et al.* (2012).** Identification of rat Rosa26 locus enables generation of knock-in rat lines ubiquitously expressing tdTomato. *Stem Cells Dev* 21, 2981-2986.

[395] **WANG, M., SUN, Z., ZOU, Z. *et al.* (2018).** Efficient targeted integration into the bovine Rosa26 locus using TALENs. *Sci Rep* 8, 10385.

[396] **LI, P., BURLAK, C., ESTRADA, J. *et al.* (2014).** Identification and cloning of the porcine ROSA26 promoter and its role in transgenesis. *Transplantation Technology* 2.

[397] **LI, X., YANG, Y., BU, L. *et al.* (2014).** Rosa26-targeted swine models for stable gene over-expression and Cre-mediated lineage tracing. *Cell Res* 24, 501-504.

[398] **KONG, Q., HAI, T., MA, J. *et al.* (2014).** Rosa26 locus supports tissue-specific promoter driving transgene expression specifically in pig. *PLoS One* 9, e107945.

[399] **WORTGE, S., ESHKIND, L., CABEZAS-WALLSCHEID, N. *et al.* (2010).** Tetracycline-controlled transgene activation using the ROSA26-iM2-GFP knock-in mouse strain permits GFP monitoring of DOX-regulated transgene-expression. *BMC Dev Biol* 10, 95.

[400] **HAENEBALCKE, L., GOOSSENS, S., NAESSENS, M. *et al.* (2013).** Efficient ROSA26-based conditional and/or inducible transgenesis using RMCE-compatible F1 hybrid mouse embryonic stem cells. *Stem Cell Rev Rep* 9, 774-785.

[401] **BATRA, L., SHRESTHA, P., ZHAO, H. *et al.* (2020).** Localized Immunomodulation with PD-L1 Results in Sustained Survival and Function of Allogeneic Islets without Chronic Immunosuppression. *J Immunol* 204, 2840-2851.

[402] **KUMAGAI-BRAESCH, M., JACOBSON, S., MORI, H. *et al.* (2013).** The TheraCyte device protects against islet allograft rejection in immunized hosts. *Cell Transplant* 22, 1137-1146.

[403] **ZHANG, Y., DAI, Y., RAMAN, A. *et al.* (2020).** Overexpression of TGF-beta1 induces renal fibrosis and accelerates the decline in kidney function in polycystic kidney disease. *Am J Physiol Renal Physiol* 319, F1135-F1148.

[404] **SURESHBABU, A., SYED, M.A., BODDUPALLI, C.S. *et al.* (2015).** Conditional overexpression of TGFbeta1 promotes pulmonary inflammation, apoptosis and mortality via TGFbetaR2 in the developing mouse lung. *Respir Res* 16, 4.

[405] **DACE, D.S., KHAN, A.A., STARK, J.L. *et al.* (2009).** Interleukin-10 overexpression promotes Fas-ligand-dependent chronic macrophage-mediated demyelinating polyneuropathy. *PLoS One* 4, e7121.

[406] **PENG, H., WANG, W., ZHOU, M. *et al.* (2013).** Role of interleukin-10 and interleukin-10 receptor in systemic lupus erythematosus. *Clin Rheumatol* 32, 1255-1266.

[407] **PORTER, D.L., LEVINE, B.L., KALOS, M. *et al.* (2011).** Chimeric antigen receptor-modified T cells in chronic lymphoid leukemia. *The New England journal of medicine* 365, 725-733.

[408] **GRUPP, S.A., KALOS, M., BARRETT, D. *et al.* (2013).** Chimeric antigen receptor-modified T cells for acute lymphoid leukemia. *The New England journal of medicine* 368, 1509-1518.

[409] **MAUDE, S.L., FREY, N., SHAW, P.A. *et al.* (2014).** Chimeric antigen receptor T cells for sustained remissions in leukemia. *The New England journal of medicine* 371, 1507-1517.

[410] **BONIFANT, C.L., JACKSON, H.J., BRENTJENS, R.J. *et al.* (2016).** Toxicity and management in CAR T-cell therapy. *Mol Ther Oncolytics* 3, 16011.

[411] **MORGAN, R.A., YANG, J.C., KITANO, M. *et al.* (2010).** Case report of a serious adverse event following the administration of T cells transduced with a chimeric antigen receptor recognizing ERBB2. *Mol Ther* 18, 843-851.

[412] **OLIVER, K.M., GARVEY, J.F., NG, C.T. *et al.* (2009).** Hypoxia activates NF-kappaB-dependent gene expression through the canonical signaling pathway. *Antioxidants & redox signaling* 11, 2057-2064.

[413] **TRINER, D. & SHAH, Y.M. (2016).** Hypoxia-inducible factors: a central link between inflammation and cancer. *The Journal of clinical investigation* 126, 3689-3698.

[414] **HAYASHI, F., SMITH, K.D., OZINSKY, A. *et al.* (2001).** The innate immune response to bacterial flagellin is mediated by Toll-like receptor 5. *Nature* 410, 1099-1103.

[415] **GEWIRTZ, A.T., NAVAS, T.A., LYONS, S. *et al.* (2001).** Cutting edge: bacterial flagellin activates basolaterally expressed TLR5 to induce epithelial proinflammatory gene expression. *J Immunol* 167, 1882-1885.

[416] **SIMON, R. & SAMUEL, C.E. (2007).** Activation of NF-kappaB-dependent gene expression by Salmonella flagellins FliC and FljB. *Biochemical and biophysical research communications* 355, 280-285.

[417] **KUHLMANN, I. (1995).** The prophylactic use of antibiotics in cell culture. *Cytotechnology* 19, 95-105.

[418] **RYU, A.H., ECKALBAR, W.L., KREIMER, A. *et al.* (2017).** Use antibiotics in cell culture with caution: genome-wide identification of antibiotic-induced changes in gene expression and regulation. *Sci Rep* 7, 7533.

[419] **ELLIOTT, R.L. & JIANG, X.P. (2019).** The adverse effect of gentamicin on cell metabolism in three cultured mammary cell lines: "Are cell culture data skewed?". *PLoS One* 14, e0214586.

[420] **XING, X., MAGNANI, L., LEE, K. *et al.* (2009).** Gene expression and development of early pig embryos produced by serial nuclear transfer. *Mol Reprod Dev* 76, 555-563.

[421] **KLINGER, B.J. (2020).** Genetic engineering of the pig embryo. PhD thesis, TUM School of Life Sciences, Technische Universität München, Freising.

[422] **GARCIA-TUNON, I., ALONSO-PEREZ, V., VUELTA, E. *et al.* (2019).** Splice donor site sgRNAs enhance CRISPR/Cas9-mediated knockout efficiency. *PLoS One* 14, e0216674.

[423] **KRAWCZAK, M., REISS, J. & COOPER, D.N. (1992).** The mutational spectrum of single base-pair substitutions in mRNA splice junctions of human genes: causes and consequences. *Human genetics* 90, 41-54.

[424] **LAKSHMI JAYARAJ, K., THULASIDHARAN, N., ANTONY, A. *et al.* (2021).** Targeted editing of tomato carotenoid isomerase reveals the role of 5' UTR region in gene expression regulation. *Plant cell reports* 40, 621-635.

[425] **ZHAO, W., SIEGEL, D., BITON, A. *et al.* (2017).** CRISPR-Cas9-mediated functional dissection of 3'-UTRs. *Nucleic acids research* 45, 10800-10810.

[426] **ZHANG, Q., FU, Y., THAKUR, C. *et al.* (2020).** CRISPR-Cas9 gene editing causes alternative splicing of the targeting mRNA. *Biochemical and biophysical research communications* 528, 54-61.

[427] **FROCK, R.L., HU, J., MEYERS, R.M. *et al.* (2015).** Genome-wide detection of DNA double-stranded breaks induced by engineered nucleases. *Nature biotechnology* 33, 179-186.

[428] **FUJIKI, R., IKEDA, M., YOSHIDA, A. *et al.* (2018).** Assessing the Accuracy of Variant Detection in Cost-Effective Gene Panel Testing by Next-Generation Sequencing. *J Mol Diagn* 20, 572-582.

[429] **TSAI, S.Q., NGUYEN, N.T., MALAGON-LOPEZ, J. *et al.* (2017).** CIRCLE-seq: a highly sensitive in vitro screen for genome-wide CRISPR-Cas9 nuclease off-targets. *Nat Methods* 14, 607-614.

[430] **TSAI, S.Q., ZHENG, Z., NGUYEN, N.T. *et al.* (2015).** GUIDE-seq enables genome-wide profiling of off-target cleavage by CRISPR-Cas nucleases. *Nature biotechnology* 33, 187-197.

[431] **BAUMGART, M. (2016).** Analysis and further improvement of multi-transgenic pigs for an efficient inhibition of the vascular and cellular rejection. Master's thesis, TUM School of Life Sciences, Technische Universität München, Freising.

13. APPENDIX

13.1 Cloning of reporter constructs and targeting vectors

13.1.1 Cloning of SEAP reporter plasmids

SEAP reporter plasmids containing the promoters CAG (A021), pA20 (A006), ELAM (A022) and hVCAM1 (A020) have been generated in advance by Mona Baumgart and Nina Simm (Master's students) at the Chair of Livestock Biotechnology, TUM, GER [332, 431]. Cloning of further SEAP constructs is described in this section.

The promoter hTNFAIP1 was first amplified by PCR using hSCP1 gDNA as template (hTNFAIP1 prom F1/R1), subcloned into pJET1.2 and inserted into XbaI-digested pcDNA-CAG-SEAP (A021) using NEBuilder HiFi Assembly (hTNFAIP1 NEB F1/R1), thereby replacing the CAG promoter and generating pcDNA-hTNFAIP1-SEAP (A036). Amplification of the individual hCCL2 promoter elements was carried out using hSCP1 gDNA as template and the primer combinations listed in Table 31. Human CCL2 fragments were subcloned into pJET1.2 and introduced into XbaI-linearized pcDNA-CAG-SEAP (A021) by NEBuilder HiFi Assembly (Table 31). The generated plasmids were called pcDNA-hCCL2-2.9kb-SEAP (A062), pcDNA-hCCL2-prox-SEAP (A039) and pcDNA-hCCL2-dis/prox-SEAP (A059).

Table 31 – Primer combinations for promoter subcloning and subsequent generation of SEAP reporter plasmids using NEBuilder HiFi Assembly

Plasmid	Plasmid No.	Plasmid generation	
		Primers	Template
Subcloning			
pJET-hCCL2-2.9kb	A061	hCCL2 prom F8/R7	hSPC1
pJET-hCCL2-prox (A)	A032	hCCL2 prom F5/R4	hSPC1
pJET-hCCL2-prox (B)	A057	hCCL2 prom XbaI/ R7	hSCP1
pJET-hCCL2-dis	A056	hCCL2 Prom F8/R6	hSCP1
pJET-hCCL2-dis/prox	A058	Ligation of hCCL2-prox (B) (A057, XbaI) into XbaI-linearized plasmid A056	
SEAP constructs			
pcDNA-hCCL2-2.9kb-SEAP	A062	hCCL2 NEB F2/R2	A061
pcDNA-hCCL2-prox-SEAP	A039	hCCL2F5s NEB F1/ R1	A032
pcDNA-hCCL2-dis/prox	A059	hCCL2 NEB F2/R2	A058

Modification of the endogenous porcine A20 promoter was conducted by successively introducing transcription factor binding sites into plasmid pcDNA-pA20-SEAP (A006). Cloning into defined promoter regions was performed by conventional cloning of oligonucleotides or by NEBuilder HiFi Assembly and is summarized in Table 32.

Table 32 – Primer combinations and oligonucleotides used for generation of pA20 promoter variants
NEB: NEBuilder HiFi Assembly; CC: conventional cloning.

Plasmid	Plasmid No.	Plasmid generation			
		Cloning method	Backbone, linearis.	Primers/ Oligonulceotides	Temp-late
pcDNA-pA20+3NFkB-SEAP	A043	NEB	A006, AfeI	1. pA20 prom F4, SEAP R3 2. A20 3xNFkB F1/ R1	A006
pcDNA-pA20+5NFkB-SEAP	A044	CC	A043, XhoI	2xNFkB XhoI F/R	x
pcDNA-pA20+2SP1-SEAP	A049	NEB	A006, HindIII	1. pA20 prom F5/ R2 2. pA20 2xSP1 F/R	A006 x
pcDNA-pA20+7NFkB-SEAP	A050	CC	A006, XhoI	2xNFkB XhoI F/R	x
pcDNA-pA20+9NFkB-SEAP	A051	CC	A006, XhoI	2xNFkB XhoI F/R	x
pcDNA-pA20+8SP1-SEAP	A052	CC	A049, NheI	pA20 NheI SP1 F/R	x
pcDNA-pA20+6SP1-SEAP	A053	CC	A049, NheI	pA20 NheI SP1 F/R	x
pcDNA-pA20+4SP1-SEAP	A054	CC	A049, NheI	pA20 NheI SP1 F/R	x
pcDNA-pA20+4SP1+3NFkB -SEAP	A055	NEB	A054, AfeI	1. pA20 prom F4, SEAP R3 2. A20 3xNFkB F1/ R1	A054
pcDNA-pA20+5NFkB-4SP1 -3NFkB-SEAP	A063	CC	A055	pA20 5xNFkB F1/ R1	x
pcDNA-pA20+4SP1+9NFkB -SEAP	A066	NEB	A054, AfeI	pA20 prom F7/ SEAP R3	A051
pcDNA-pA20+5NFkB +4SP1+9NFkB-SEAP	A067	CC	A066, HindIII	pA20 5xNFkB F1/ R1	x
pcDNA-pA20+10NFkB +4SP1+3NFkB-SEAP	A068	CC	A055, HindIII	pA20 5xNFkB F1/ R1	x

13.1.2 Cloning of dual-luciferase constructs

Generation of the dual-luciferase constructs used for *in vivo* promoter induction experiments is described in this section. Each candidate promoter was first inserted into a SnaBI-linearized

pSL1180+psiCHECK (A069) vector and a hygromycin resistance cassette was then introduced by NEBuilder HiFi Assembly. The final plasmids were called psL1180+psiCHECK-CAG-Hygro (A080), pSL1180+psiCHECK-ELAM-Hygro (A081), pSL1180+psiCHECK-hCCL2-dis/prox-Hygro (A082), pSL1180+psiCHECK-pA20+3NFkB-Hygro (A084) and pSL1180+psiCHECK-pA20+10NFkB+4SP1+3NFkB-Hygro (A085). The dual-luciferase plasmid carrying the pA20 promoter (pSL1180+psiCHECK-pA20-Hygro, A083) was generated by modifying plasmid A084. Detailed cloning information is given in Table 33.

Table 33 – Primer combinations used for generation of dual-luciferase constructs
NEB: NEBuilder HiFi Assembly; CC: conventional cloning.

Plasmid	Plasmid No.	Plasmid generation			
		Cloning method	Backbone, linearis.	Primers	Temp-late
Dual-luciferase constructs (no hygro^R)					
pSL1180+psiCHECK-CAG	A072	CC	Ligation of CAG (A021, BglII) into SnaBI-linearized plasmid A069		
pSL1180+psiCHECK-ELAM	A073	NEB	A069, SnaBI	ELAM NEB F1/R1	A022
pSL1180+psiCHECK-hCCL2 -dis/prox	A074	NEB	A069, SnaBI	hCCL2 NEB F3/R3	A058
pSL1180+psiCHECK-pA20 +3NFkB	A076	NEB	A069, SnaBI	pA20 NEB F1/R1	A043
pSL1180+psiCHECK-pA20 +10NFkB+4SP1+3NFKB	A077	NEB	A069, SnaBI	pA20 NEB F1/R1	A068
Dual-luciferase constructs (+ hygro^R)					
pSL1180+psiCHECK-CAG -Hygro	A080	NEB	A072, XhoI	pX-Hygro-NEB XhoI F1/R1	A078
pSL1180+psiCHECK-ELAM -Hygro	A081	NEB	A073, XhoI	pX-Hygro-NEB XhoI F1/R1	A078
pSL1180+psiCHECK-hCCL2 -dis/prox-Hygro	A082	NEB	A074, XhoI	pX-Hygro-NEB XhoI F1/R1	A078
pSL1180+psiCHECK-pA20 -Hygro	A083	NEB	A085, NotI	pA20 NEB F1/R1	A006
pSL1180+psiCHECK-pA20 +3NFkB-Hygro	A084	NEB	A076, NdeI	Hygro psi NEB XhoI F1/R1	A078
pSL1180+psiCHECK-pA20 +10NFkB+4SP1+3NFKB -Hygro	A085	NEB	A077, NdeI	pX-Hygro-NEB XhoI F1/R1	A078

13.1.3 Cloning of gene-targeting vectors

Cloning of vectors targeting the porcine ROSA26-locus is subject of this section. To generate plasmid ROSA26-BS-pA20multi-LEA29Y (A133), the *LEA29Y* sequence, bGHpA and the promoter pA20+4SP+10/3NF was successively subcloned into the plasmid pJET1.2. The transgene cassette was then inserted between the homology arms of the AgeI/AvrII-digested vector ROSA26-SA-BS-LA (A118). Cloning was performed by conventional cloning and NEBuilder HiFi Assembly and is described in detail in Table 34. Generation of the gene-targeting vector ROSA26-BS-pA20multi-LEA29Y-ELAM-PDL1-MIN (A166) was performed by inserting the ELAM-hPDL1-bGHpA-MIN cassette of the AvrII-digested plasmid A164 into the AvrII-linearized plasmid A133 and modifying the DNA sequence between the start codon of *LEA29Y* and its promoter: the BspI-digested plasmid was assembled with the DNA fragment derived from PCR using the primers NEB LEA F1/Lea hEx2 R1 and A133 as template.

Table 34 – Details for cloning the gene-targeting vector A133
NEB: NEBuilder HiFi Assembly; CC: conventional cloning.

Plasmid	**Plasmid No.**	**Plasmid generation**			
		Cloning method	**Backbone, linearis.**	**Primers**	**Template**
pJET1.2-LEA29Y	A120	CC	Ligation of *LEA29Y* sequence (A117, HindIII/NotI) into pJET1.2		
pJET1.2-LEA29Y-bGHpA	A131	NEB	A120, EcoRI	bGHpA NEB F2/R4	A115
pJET1.2-pA20multi-LEA29Y-bGHpA	A132	NEB	A131, NotI	pA20 NEB F4/R4	A068
ROSA26-BS-pA20multi-LEA29Y	A133	CC	Ligation of pA20 +4 SP-1 +10/3 NF-κB (A131, AvrII/PmeI/AgeI) into A118 (AgeI/AvrII)		

13.2 Sequences of transgene constructs

13.2.1 *LEA29Y* sequence present on targeting vectors A133 and A166

Composition of the *LEA29Y* sequence used for gene placement into the *ROSA26* locus is shown in Table 35. It includes the signal peptide sequence of the human *OCM* gene, almost the entire sequence of human *CTLA4* exon 2 and the first nucleotides of exon 3 (Transcript-ID: ENST00000302823.8, Ensembl Release 95). The 3' terminal part of the *LEA29Y* sequence

encodes the hinge region and the CH2 and CH3 domains of human *IGHG1* (UniProtKB: P01857).

Table 35 – Sequence and annotation of the LEA29Y construct used in A133 and A166

Reference DNA sequences refer to Ensembl Genome Browser (Ensembl Release 95; https://www.ensembl.org/). Protein domains were identified using UniProt Knowledgebase (https://www.uniprot.org/).

Sequence

```
   1 atgggggtac tgctcacaca gaggacgctg ctcagtctgg tccttgcact cctgtttcca
  61 agcatggcga gcatggcgat gcacgtggcc cagcctgctg tggtactggc cagcagccga
 121 ggcatcgcca gctttgtgtg tgagtatgca tctccaggca aatatactga ggtccgggtg
 181 acagtgcttc ggcaggctga cagccaggtg actgaagtct gtgcggcaac ctacatgatg
 241 gggaatgagt tgaccttcct agatgattcc atctgcacgg gcacctccag tggaaatcaa
 301 gtgaacctca ctatccaagg actgagggcc atggacacgg gactctacat ctgcaaggtg
 361 gagctcatgt acccaccgcc atactacgag ggcataggca acggaaccca gatttatgta
 421 attgatccag aaccgtgccc agattctgat caggagccca aatcttctga caaaactcac
 481 acatccccac cgtccccagc acctgaactc ctggggggat cgtcagtctt cctcttcccc
 541 ccaaaaccca aggacaccct catgatctcc cggacccctg aggtcacatg cgtggtggtg
 601 gacgtgagcc acgaagaccc tgaggtcaag ttcaactggt acgtggacgg cgtggaggtg
 661 cataatgcca agacaaagcc gcgggaggag cagtacaaca gcacgtaccg ggtggtcagc
 721 gtcctcaccg tcctgcacca ggactggctg aatggcaagg agtacaagtg caaggtctcc
 781 aacaaagccc tcccagcccc catcgagaaa accatctcca aagccaaagg gcagccccga
 841 gaaccacagg tgtacaccct gcccccatcc cgggatgagc tgaccaagaa ccaggtcagc
 901 ctgacctgcc tggtcaaagg cttctatccc agcgacatcg ccgtggagtg ggagagcaat
 961 gggcagccgg agaacaacta caagaccacg cctcccgtgc tggactccga cggctccttc
1021 ttcctctaca gcaagctcac cgtggacaag agcaggtggc agcaggggaa cgtcttctca
1081 tgctccgtga tgcatgaggc tctgcacaac cactacacgc agaagagcct ctccctgtct
1141 ccgggtaaat ga
```

Annotation

Position, nt	Gene, specification	Reference
1-78	human *OSM*	1. Transcript-ID:
*1-75	*signal peptide	ENST00000215781.2
		2. UniProtKB: P13725
79-449	human *CTLA4*	Transcript-ID:
*79-424	*Δexon 2	ENST00000302823.8
*425-449	*Δexon 3	
454-1152	human *IGHG1*	1. Transcript-ID:
*454-489	*hinge region	ENST00000390549.6
*490-828	*CH2 region	2. UniProtKB: P01857
*829-1149	*CH3 region	

Nucleotides varying from the reference sequences given above			
Position, nt	**nt exchange**	**aa change**	
163-165	gcc→tat	A→Y	reported in [190]
388-390	ct→ga	L→E	reported in [190]
467	g→c	C→S	
485	g→c	C→S	
494	g→c	C→S	
520	c→t	P→S	
711	t→g	T→R	
1119	a→g	R→T	

13.2.2 Human *PD-L1* sequence present on targeting vector A166

The DNA sequence and detailed annotation information of human *PD-L1* used in targeting vector A166 is given in Table 36. It includes the non-coding exon 1, exon 2 to 6, the coding-part of exon 7 and the first 37 bp of the 3' UTR (Transcript-ID: ENST00000215781.2, Ensembl Release 95).

Table 36 – Sequence and annotation of the hPD-L1 construct used in A166

Annotation refers to h*PD-L1* Transcript-ID ENST00000215781.2 (Ensembl Release 95; https://www.ensembl.org).

Sequence
1 gcgtcccgcg cggccccagt tctgcgcagc ttcccgaggc tccgcaccag ccgcgcttct
61 gtccgcctgc agggcattcc agaaagatga ggatatttgc tgtctttata ttcatgacct
121 actggcattt gctgaacgca tttactgtca cggttcccaa ggacctatat gtggtagagt
181 atggtagcaa tatgacaatt gaatgcaaat tcccagtaga aaaacaatta gacctggctg
241 cactaattgt ctattgggaa atggaggata agaacattat tcaatttgtg catggagagg
301 aagacctgaa ggttcagcat agtagctaca gacagagggc ccggctgttg aaggaccagc
361 tctccctggg aaatgctgca cttcagatca cagatgtgaa attgcaggat gcaggggtgt
421 accgctgcat gatcagctat ggtggtgccg actacaagcg aattactgtg aaagtcaatg
481 ccccatacaa caaaatcaac caaagaattt tggttgtgga tccagtcacc tctgaacatg
541 aactgacatg tcaggctgag ggctacccca aggccgaagt catctggaca agcagtgacc
601 atcaagtcct gagtggtaag accaccacca ccaattccaa gagagaggag aagcttttca
661 atgtgaccag cacactgaga atcaacacaa caactaatga gattttctac tgcactttta
721 ggagattaga tcctgaggaa aaccatacag ctgaattggt catcccagaa ctacctctgg
781 cacatcctcc aaatgaaagg actcacttgg taattctggg agccatctta ttatgccttg
841 gtgtagcact gacattcatc ttccgtttaa gaaaagggag aatgatggat gtgaaaaaat
901 gtggcatcca agatacaaac tcaaagaagc aaagtgatac acatttggag gagacgtaat
961 ccagcattgg aacttctgat cttcaagcag ggattc

Annotation	
Position, nt	**Feature**
1-72	exon 1
*1-72	*Δ5' UTR
73-138	exon 2
*73-86	*Δ5' UTR
*87-89	*start codon
139-480	exon 3
481-768	exon 4
769-876	exon 5
877-936	exon 6
937-996	Δexon 7
*965-967	*stop codon
*968-996	*Δ3' UTR

13.3 Knockout analyses

13.3.1 Determination of guide efficiency and knockout screening

Guide efficiencies to introduce InDel-mutations were evaluated in the puromycin-selected using the webtool TIDE (chapter 7.2.1). Gene editing frequency after transfection of three multi-knockout vectors (A190, A191, A192) was analysed after puromycin selection and enrichment of GGTA1/SLA-I negative cells in two pools. (chapter 7.2.3). The primers used for pool analyses and subsequent sanger sequencing are listed in Table 37.

Table 37 – Primers used to analyse CRISPR/Cas9 modified cells

[a] used in chapter 7.2.1, [b] used in chapter 7.2.3.

Target site	Screening primers			Sequencing primer
ASGR1 E1 T1	ASGR1 E2 F1	ASGR1 I2 R1	634 bp	ASGR1 E2 F1
ASGR1 E4 T1	ASGR1 E3 F1[a]	ASGR1 E6 R1[a]	723 bp	ASGR1 E6 R1
	ASGR1 I2 F2[b]	ASGR1 Ex4 R1[b]	505 bp	ASGR1 Ex4 R1
B2M E1 T1	pB2M Scr 5'UTR F1	pB2M Scr I1 R1	377 bp	pB2M Scr I1 R1
B4GNT2 E2 T3	B4G I1 F1	B4G I2 R1	837 bp	B4G I1 F1
B4GNT2 E3 T3	B4Gal Scr I2 F1	B4Gal Scr I3 R1	330 bp	B4Gal Scr I3 R1
CMAH E9 T1	CMAH I8 F1	CMAH I9 R	738 bp	CMAH I8 F1
CMAH E7 T1	CMAH I6 F1	CMAH E8 R1	751 bp	CMAH I6 F1
CMAH E10 T2	CMAH Scr E10 F2	CMAH Scr E10 R2	357 bp	CMAH Scr E10 F2
GGTA1 E7 T6	Gal Scr E7 T56 F	Gal Scr E7 T56 R	362 bp	Gal Scr E7 T56 F
GGTA1 E8 T3	GGTA1 E11 F1	Gal Scr E8 T3 R	378 bp	GGTA1 E11 F1

GGTA1 E8 T4	Gal I7 F1	Gal Scr E8 T3 R	900 bp	Gal I7 F1
GHR E10 T1	GHR I8 F1	GHR I10 R1	482 bp	GHR I8 F1
GHR E14 T1	GHR I13 F1	GHR I14 R1	489 bp	GHR I13 F1
MHC-I E4 T1	MHCI Antigen F1	MHCI Antigen R1	362 bp	MHCI Antigen F1
MHC-I E4 T2	MHCI Antigen F1	MHCI Antigen R1	362 bp	MHCI Antigen F1
ULBP1 E1 T1	ULBP1 Ex1 F1	ULBP1 I1 R1	254 bp	ULBP1 Ex1 F1
ULBP1 E1 T2	ULBP1 Ex1 F1	ULBP1 I1 R1	254 bp	ULBP1 Ex1 F1
ULBP1 E2 T3	ULBP1 Ex2 F1	ULBP1 I2 R1	350 bp	ULBP1 Ex2 F1
ULBP1 E2 T4	ULBP1 Ex2 F1	ULBP1 I2 R1	350 bp	ULBP1 Ex2 F1

13.3.2 Cloning of multi-knockout vectors

Double-stranded sgRNA oligonucleotides, 18 to 20 bp in length, with additional BbsI restriction sites were subcloned into the BbsI-linearized plasmid pSL1180-U6-MCS-tracRNA-756 (A142) between U6 promoter and sgRNA scaffold sequence. Restriction fragments were then integrated successively into plasmid px330-U6-MCS-tracRNA-705 (A174) as described in Table 38 to generate two multi-knockout vectors called px330-GGTA1E8T3-CMAHE9T1-ASGR1E1T1-ASGR1E4T1 (A191) and px330-B2ME1T1-ULBP1E1T2-ULBP1E2T4-B4GALNT2E2T3 (A192). Cloning was conducted by Katharina Rinke (Bachelor's student) [347].

Table 38 – Details for cloning the multi-knockout vectors A191 and A192

Step	**Plasmid No.**	**Plasmid generation**	
		Backbone, linearisation	**Insert**
1a	A175	A174, BbsI	PX-GGTA1-E8-T3-F18/R18
2a	A177	A175, NheI/NsiI	A153, NheI/NsiI
3a	A179	A177, AfeI/MluI	A147, AfeI/MluI
4a	A191	A179, BamHI/BsrGI	A158, BamHI/BsrGI
1b	A176	A174, BbsI	PX-pB2M-E1-F1/R1
2b	A178	A176, NheI/NsiI	A168, NheI/NsiI
3b	A180	A178, AfeI/MluI	A170, AfeI/MluI
4b	A192	A180, BamHI/BsrGI	A173, BamHI/BsrGI

14. ACKNOWLEDGMENTS

Zuallererst möchte ich mich herzlich bei Prof. Dr. Angelika Schnieke bedanken. Sie hat es mir ermöglicht, meine Promotion über ein solch spannendes Thema an ihrem Lehrstuhl durchzuführen. Ich danke ihr für ihre Unterstützung, für die konstruktiven Gespräche und die Möglichkeit, an zahlreichen Meetings und Kongressen teilzunehmen und unsere Arbeit einem größeren Publikum zu präsentieren.

Prof. Dr. Percy Knolle danke ich für seine Ideen und Ratschläge zu Beginn meiner Promotion. Ganz besonders möchte ich mich bei Prof. Dr. Jochen Seißler, Dr. Dirk Wohlleber und Dr. Katrin Manske für die Behandlung der Mäuse und Durchführung der Bioimaging-Versuche bedanken. Außerdem danke ich Nico Gebhardt für die Einbettung der Gewebeproben.

Besonders bedanken möchte ich mich bei meinem Betreuer Konrad Fischer. Lieber Konrad, danke, dass du dein Wissen und deine Erfahrung stets mit mir geteilt und mir jederzeit mit Rat und Tat zu Seite gestanden hast, wenn ich sie benötigt habe. Meiner Xeno-Kollegin Beate Rieblinger danke ich auch herzlich für ihre grenzenlose Hilfsbereitschaft und viele Unternehmungen außerhalb des Labors. Auch Alexander Kind möchte ich danken, der mir durch die Korrektur von Abstracts, Poster und Manuskripten eine große Hilfe war. Tatiana Flisikowska danke ich für die freundliche Zusammenarbeit und die gute Bewirtung – ganz egal zu welchem Anlass. Danke auch an Krzystof Flisikowski für den kurzen Ausflug in die Welt der Epigenetik und so manche interessante Diskussion.

Außerdem bedanke ich mich bei allen TAs, die für jedes Problem eine Lösung hatten und für einen reibungslosen Ablauf im Labor gesorgt haben: Sulith Christan, unsere gute (Bestell-)Fee und Labor-Kompass, die immer wusste, wo die Dinge zu finden sind, die ich gerade brauchte. Peggy Müller-Fliedner, Alexander Carrapeiro, Nina Simm und Johanna Tebbing danke ich besonders für die Unterstützung während meiner Labor-Pause. Auch danke ich Marlene Stumbaum, Kristina Mosandl, Lea Radomsky und Sarah Robin für die angenehme Zusammenarbeit.

Bei Viola und Steffen Löbnitz möchte ich mich für die Pflege unserer Tiere bedanken. Danke auch an Barbara Bauer für die Regelung aller organisatorischen Angelegenheiten am Lehrstuhl und die Hilfe bei verwaltungstechnischen Fragen.

Ein großes Dankeschön gilt auch allen Doktoranden-KollegInnen, die mich auf meinem Weg begleitet haben und die meine Zeit am Lehrstuhl so besonders gemacht haben: Daniela Huber, Carolin Perleberg und Beate Rieblinger, meine Weggefährtinnen der ersten Stunde, die gerne Ihre Erfahrungen mit mir geteilt haben. Meinen Lieblings-Bürokumpanen Bernhard Klinger, Alessandro Grodziecki und Liang Wei für die angenehme Atmosphäre am Arbeitsplatz. Auch Melanie Nusselt, Guanglin Niu, Daniela Kalla, Thomas Winogrodzki, Ying Wang, David Preisinger, Yue Zhang, Theresa Göring, Laura Beltran Sangüesa und Agniezka Bak möchte ich danken und wünsche ihnen alles Gute für ihre Zukunft.

Außerdem möchte ich mich herzlich bei meinen ForschungspraktikantInnen Julia Zuber, Katharina Jentsch, Jonathan Ostertag, Ludwig Kübelsbeck, Matthias Lenz, Anna-Maria Pedde, Minji Hu sowie meinen BachelorstudentInnen Roger Suau Regordosa, Armin Maurer und Katharina Rinke für ihren tatkräftigen Beitrag zur Xenotransplantations-Forschung bedanken.

Mein größter Dank gilt meiner Familie: Meinen Eltern, meinem Ehemann und meiner Tochter. Danke, dass ihr immer an mich geglaubt habt, für eure bedingungslose Liebe und Unterstützung. Euch widme ich diese Arbeit.